



Contents lists available at SciVerse ScienceDirect

Ore Geology Reviews

journal homepage: www.elsevier.com/locate/oregeorev

A prospective sector in the Tethyan Metallogenic Belt: Geology and geochronology of mineral deposits in the Biga Peninsula, NW Turkey

Ozcan Yigit *

Department of Geological Engineering, Canakkale Onsekiz Mart University, Canakkale 17020, Turkey

ARTICLE INFO

Article history:

Received 18 December 2010

Received in revised form 2 June 2011

Accepted 29 September 2011

Available online xxxx

Keywords:

Turkey

Biga Peninsula

Geochronology

Tethyan metallogeny

Porphyry Au–Cu–Mo

Epithermal

Skarn

Mineral exploration

ABSTRACT

The Tethyan Metallogenic Belt (TMB), extending from Europe through Anatolia to Iran, is one of the world's major metal producing belts, and consists of many sectors. Mineral deposits of the Biga Peninsula in northwestern Turkey exhibit, in many ways, the characteristics of mineral deposits found throughout the belt. Biga Peninsula tectonically forms the westernmost part of the Sakarya Zone and easternmost part of the Rhodope Zone at the intersection of Gondwana and Laurasia.

The Biga Peninsula metallogeny research and exploration project created a GIS inventory of mineral deposits and prospects, and classified them genetically to evaluate the mineral deposit potential using genetic models based on descriptive data. The GIS database, consisting of 128 deposits or prospects, helped to generate new prospects and potential prospects. This field-based study indicated that the Biga Peninsula forms a prime target for gold–copper exploration not only in Turkey but in the world.

The current economically significant mineral deposits of the Biga Peninsula were shaped by Cenozoic calc-alkaline magmatism, ranging between 52 and 18 Ma, and related to mainly collisional and post-collisional tectonic regime. Epithermal Au–Ag deposits including high-(HS), low-(LS) and intermediate-sulfidation (IS) styles, porphyry Au–Cu–Mo and base-metal skarn systems are economically the most important. Though there are no currently economic examples of some of them in the Biga Peninsula, other deposit types include Carlin-like distal disseminated Au–Ag, orogenic Au, especially listwanite hosted, volcanogenic Mn and U, lateritic (ferricrete) Fe deposits, carbonate replacement (CR) and placers.

Several active metal mines, such as Balya, Arapucandere and Koru, are operating in the Biga Peninsula. Kucukdere Au–Ag deposit in Balikesir is the only gold mine in the Biga Peninsula, except for by-product gold produced from base-metal deposits. Results of the study show current total gold endowment of the Biga Peninsula including reserves and/or resources is 9.18 Moz gold [284.2 t] contained in twelve different deposits. Of these only 6 contain significant gold [>0.3 Moz or 10 t]. Halilaga porphyry and Agi Dagi and Kirazli HS epithermal systems have an ongoing resource estimate, and Halilaga is a candidate to be one of the largest Cu–Au deposits not only in the Biga Peninsula, but in Turkey. Currently newly discovered Tepeoba is the largest porphyry Cu–Mo–Au deposit with known resources in the Biga Peninsula.

Here, the first $^{40}\text{Ar}/^{39}\text{Ar}$ step-heating age data conducted on some of the major HS epithermal gold deposits and causative intrusives in the Biga Peninsula are reported. Geochronological results from this project, evaluated with previous studies, indicate at least 3 phases of porphyry and 2 phases of high-sulfidation epithermal gold mineralization in the Biga Peninsula. The most important mineralizing phases and related host rocks for gold mineralization range from 38 to 22 Ma. The Oligocene is especially important for economic epithermal and porphyry systems in the Biga Peninsula, which is comparable to deposits in the Oligo-Miocene Serbomacedonian-Rhodope metallogenic belt of the Balkan Peninsula in SE Europe.

© 2012 Elsevier B.V. All rights reserved.

1. Introduction

“...In the Troad, above the territory of Abydos is Astyra, which now belongs to the Abydeni, a city in ruins, but it was formerly an independent place, and had gold-mines, which are now nearly exhausted, like those in Mount Tmolus near the Pactolus.”

Strabo, Geography Book XIII

Turkey is an emerging mining country within the Tethyan Metallogenic Belt (TMB) on the doorstep of Europe. Though the country is long known for its industrial minerals and dimension stones, the precious- and base-metal endowment of the country is now appreciated; gold is the new paradigm. Recently Turkey has become a world-class gold mining and exploration country. Commercial production

* Corresponding author. Tel. +90 5362683182.

E-mail address: ozcanyigit@hotmail.com.

started in the Ovacik gold mine in 2001, in Kisladag gold mine in 2006, as well as other new gold mines including Kucukdere, Mastra, Copler, Cukuralan, Efemcukuru, Kaymaz and Gicik. Annual gold production in the country has now reached 0.5 Moz and will continue to increase from new mines and increasing production from the existing mines.

The Biga Peninsula, historically known as Troas or the Troad after the ancient city of Troy, is located in the farthest NW of the Turkish Peninsula, also known as Anatolia or Asia Minor. Mining in the Biga Peninsula goes back to ancient times. Present day Havran in Balikesir was known as Aureline or Aureliane, land of gold, in ancient times. According to Frank Calvert, initial discoverer of the site of Troy, the surface and underground gold mines in present day Kartaldag and Madendag, worked before Strabo's time, are the site of the ancient city Astyra, and they were the source of the gold for Priam's Treasure (Allen, 1999). Gold mines in the Kartaldag and Madendag area were operated by a British company, Astyra Gold Mining Co., during WWI years (Molly, 1958). Balya, with ancient and historical mining between 1839–1849 and 1892–1940 by a French company, was the first large scale underground mine in the district.

Though industrial minerals, dimension stones and energy raw materials, such as clays, silex, marbles, limestone, and lignite deposits of the Can Basin in the Biga Peninsula are long-time appreciated commodities, base- and precious metal potential of the district is newly recognized, especially in terms of Au–Cu. Modern mineral exploration in the last decades revealed the true metal potential of the district with the discovery of gold–copper systems, e.g., Agi Dagı, Kirazlı, Halilaga and Kucukdere. Most of the mining operations have been small scale in the Biga Peninsula, with the exception of Balya mine, and they have mainly concentrated on base-metals, mostly Pb–Zn with by product Ag–Au, and some Sb workings. Currently several active metal mines are operating in the Biga Peninsula, though some of them have intermittent production, e.g., Balya, Kucukdere, Arapucandere, Koru, Yenice district, Cataltepe, Kocayayla, and Egmir deposits. Biga Peninsula is one of the focal points of current mineral exploration in Turkey.

This paper is an outgrowth of a field-based study evaluating gold–copper metallogeny of the Biga Peninsula using a GIS database compilation to determine exploration potential as well as metal endowment, which is a part of the authors Turkish Mineral Deposit Database (TMDD) containing more than 11,000 deposits and prospects. Majority of the deposits and prospects presented in this study were personally visited by the author and were sampled during the course of the study. In the course of the project, a total of 393 rock chip and grab samples were taken for geochemical analyses, and a total of 441 rock samples were taken for ore petrography, alteration, and radiometric age dating studies. Rock slabs from all of these samples were prepared for detailed lithologic and ore petrography studies. Furthermore, from these, 131 thin sections and 79 thick polished-sections were made and studied. All geochemical samples were analyzed for Au using AA, and for 50 major and minor elements using ICP-MS, and for whole-rock composition using XRF. All of the geochemical analyses were conducted by ALS Chemex Laboratories in Canada. Furthermore, 208 rock slabs and 227 geochemically analyzed rock-chip samples were analyzed for clay minerals using a portable infrared mineral analyzer, TerraSpec. Radiometric dating of selected samples of mineralization, alteration and host-rock were carried out in Actlabs in Canada. Results were incorporated with available age dates and evaluated for geochronological studies.

The purpose of this paper is to evaluate metal endowment and exploration potential of the mainly metallic mineral deposits of the prolific Biga Peninsula within the metallogenic framework of Turkey as well as TMB. Many new prospects and potential prospects were generated using a combination of geology, structure, geochemistry, and satellite imagery, mainly LandsAT 7ETM+ and ASTER. Geochronological studies were employed to determine spatial and temporal

relations between magmatic activity and mineralization–hydrothermal alteration events. Some of the deposits are dated for the first time in this study using $^{40}\text{Ar}/^{39}\text{Ar}$ age dating. This paper also addresses some metallogenic correlations of the mineral deposits and prospects in the Biga Peninsula with mineral deposits in SE Europe based on the geochronological studies. Finally, implications for future mineral exploration are given based on recent discoveries and exploration trends. In spite of many published inventories and local deposit based studies, with the exception of Yigit (2006, 2009), no paper has yet presented mineral deposits and prospects of the Biga Peninsula, let alone Turkey, in a detailed genetic framework. This field based geological, GIS and geochemical study aims to fill that gap.

2. Geologic and tectonic setting

Biga Peninsula constitutes the northwestern tip of the Turkish Peninsula (Fig. 1), tectonically forming the westernmost part of the Sakarya Zone of the Pontides at the intersection of Gondwana and Laurasia. Thus it illustrates much of the complicated geologic and tectonic history of Turkey in a small area.

Convergence between Gondwana and Laurasia, especially in Paleozoic and Mesozoic times, resulted in collision of continental fragments and amalgamation. East-trending orogenic belts in Turkey were first recognized by Ketin (1966); from north to south, there are Pontides (Laurasian realm), Anatolides, Taurides and Border Folds (Gondwana realm; Fig. 1, small inset). These fourfold tectonic units of Turkey have been modified by many later workers (Gorur, 1998; Okay and Tuysuz, 1999; Sengor, 1984; Sengor and Yilmaz, 1981; Sengor et al., 1980, 1984; Stampfli, 2000) and have been subdivided into many different tectonic zones or micro terranes in later studies (i.e., Moix et al., 2008) (Fig. 1). However, age, stratigraphic relations, tectonic positions and regional correlation of these terranes remains ambiguous. These inherited geological problems emerge in Biga Peninsula as well; for example origin of some of the orogenic rocks within Sakarya zone, i.e., Karakaya Complex (Okay and Goncuoglu, 2004) and Cetmi Ophiolitic Melange (Beccaletto, 2004) is unclear. Izmir–Ankara–Erzincan suture, separating the Pontides in the north from the Anatolide–Tauride platform to the south, and the Bitlis suture, marking the northern edge of the Arabian plate in south-eastern Turkey, are the most prominent tectonic features of Turkey. In other words, these two sutures divide Turkey into three geologically distinct domains (Fig. 1).

Biga Peninsula is tectonically subdivided into two zones that are Rhodope–Strandja in the west and Sakarya in the east (Fig. 1). Though four northeast-trending Pre-Cenozoic tectonic zones were defined in some studies (i.e., Okay et al., 1990), relationships between these zones, as well as origin and boundaries, could not be clarified, i.e., relationship between the Cetmi Ophiolitic Melange or the Denizoren Ophiolite and the Intra-Pontide suture and Neotethyan Izmir–Ankara–Erzincan suture. Nor is the relationship between Cetmi Ophiolitic Melange and the melanges in eastern Rhodope clear, though recent studies indicate that Cetmi Ophiolitic Melange shows some similarities to melanges in the Rhodope Massif (Beccaletto et al., 2005). By the same token determination of age relationships of orogenic rocks within Karakaya Complex as well as corresponding oceanic basins and suture zones, and distribution and origin of these zones in relation to Paleotethys are not fully understood (Okay and Goncuoglu, 2004).

Metamorphic rocks of the Kazdag Group in the Sakarya Zone and rocks in Camlica Metamorphics in Rhodope Zone form the crystalline basement in the Biga Peninsula (Figs. 2 and 3). Permo-Triassic Karakaya Complex in Sakarya Zone and rocks of the Ezine Group in Rhodope Zone, Cetmi Ophiolitic Melange and Denizoren Ophiolite of Cretaceous age form the other prominent Pre-Cenozoic geological features in the Biga Peninsula. Cenozoic volcano-plutonic rocks, covering extensive areas, dominate the geology of the Biga Peninsula (Aldanmaz et al.,

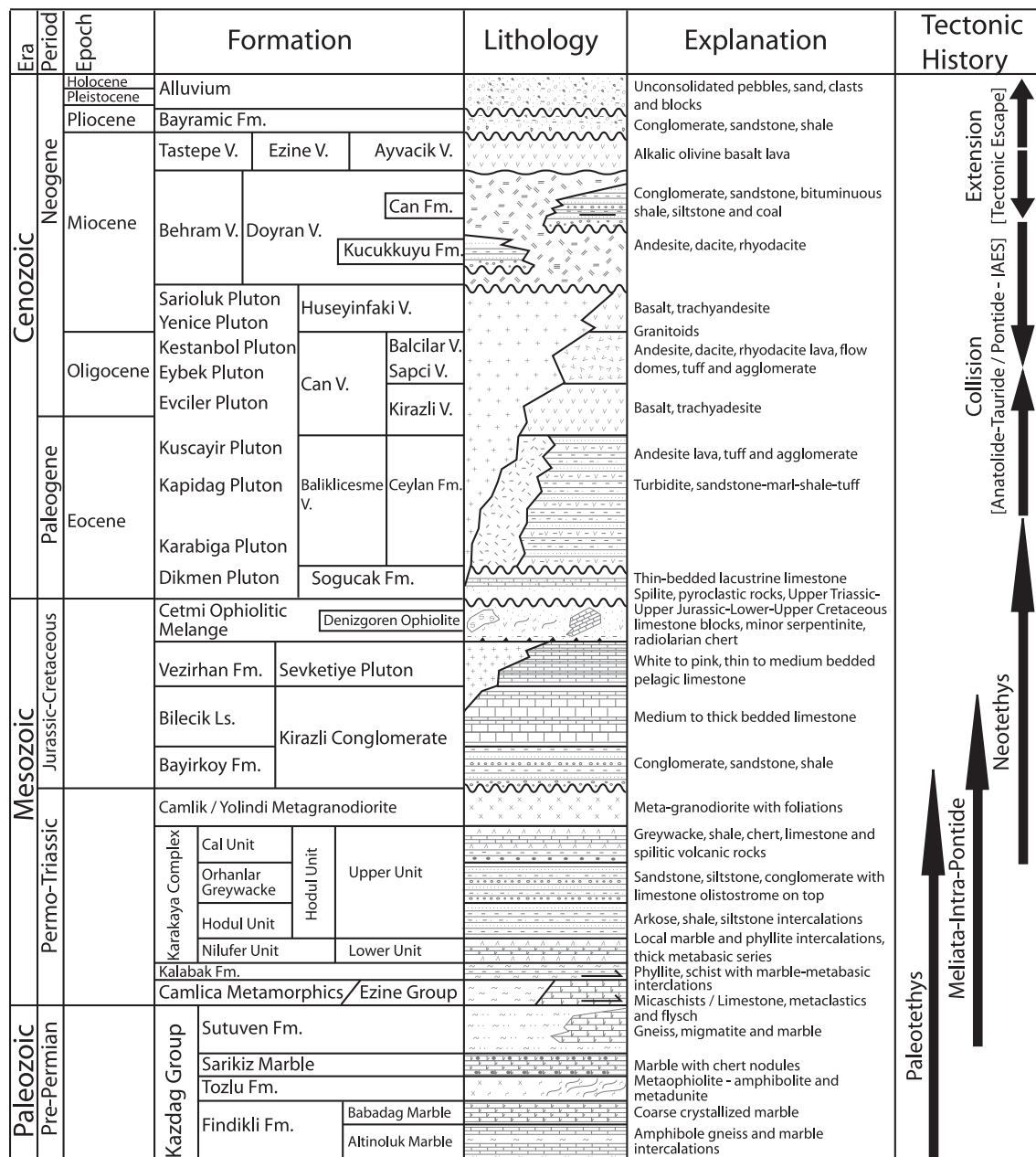


Fig. 2. Generalized stratigraphic section of the Biga Peninsula. Compiled from Akyurek and Soysal (1980), Duru et al. (2004), Ercan et al. (1995), Okay et al. (1990), Siyako et al. (1989), and other sources.

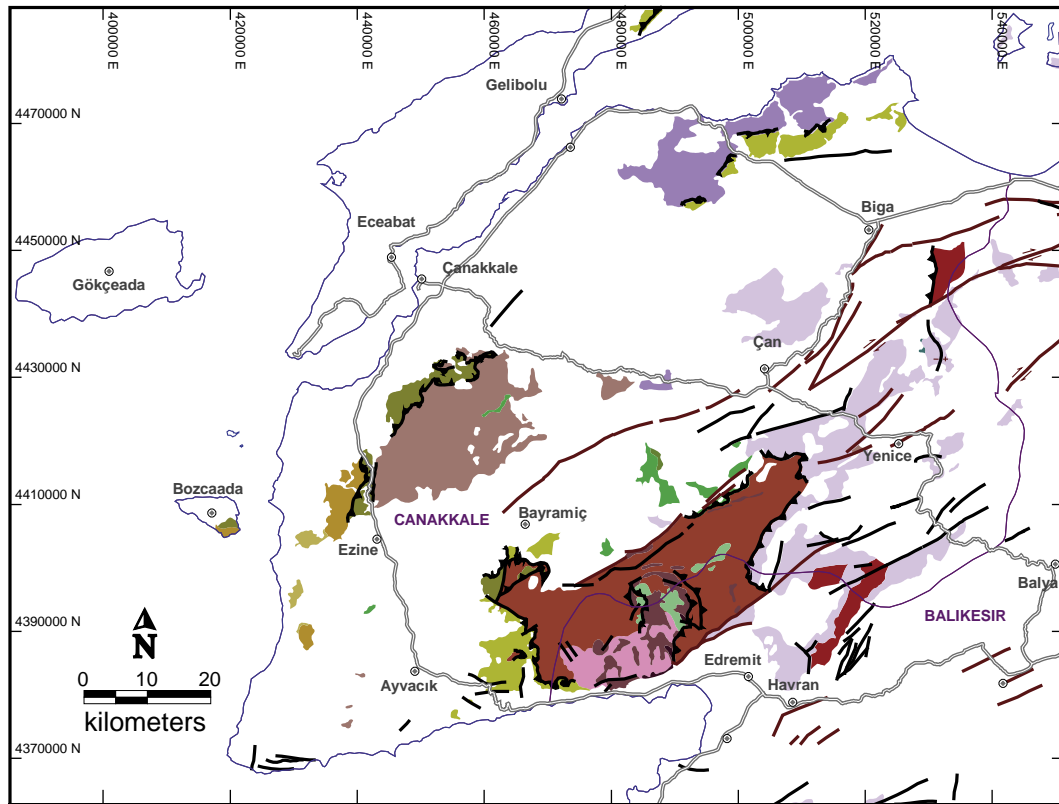
Oligocene times causing formation of the Kazdag Metamorphic Core Complex (Okay and Satir, 2000a). However, current studies using apatite fission-track ages suggest that Kazdag Massif was exhumed between 20 and 10 Ma (Early-Middle Miocene), ages clustering between 17 and 14 Ma (Cavazza et al., 2009).

Extensive metasedimentary rock exposures in the northeast of Ezine and west of Karabiga are called the Camlica Metamorphics (Okay et al., 1990) and form the basement of the Rhodope Zone (Fig. 3). Relics of eclogites in the Camlica Metamorphics indicate a HP-LT metamorphism and three muscovite samples from quartz-mica schists give 69 to 65 Ma Rb/Sr age intervals (Okay and Satir, 2000b). These radiometric ages indicate a regional metamorphism of Maastrichtian age. Though these metamorphic rocks were interpreted as cover rocks of the Kazdag Massif (Kalafatcioglu, 1963), it is thought that the origin as well as evolution of the Camlica

Metamorphics are related to Rhodope-SerboMacedonian Massif (Okay and Satir, 2000b; Okay et al., 2001).

North-trending green-schist facies metamorphic rocks, outcropping northwest and east of Ezine, are called the Ezine Group, and consist of Permo-Triassic epicontinental sedimentary rocks, mainly carbonates (Fig. 3) (Beccaletto and Jenny, 2004) (Karadag Units of Okay et al., 1990). Ezine Group is subdivided into three formations, which are, from bottom to top, Geyikli, Karadag, and Camkoy Formations. It is suggested that Ezine Group rocks are a product of Permo-Triassic rifting in the north of Maliac/Meliata Ocean and they represent Rhodopian passive margin (Beccaletto and Jenny, 2004).

The other important Permo-Triassic age orogenic rocks, consisting of partly metamorphosed, strongly deformed, clastic and volcanic rocks, in the Biga Peninsula are called Karakaya Complex (Tekeli, 1981) (Karakaya Formation of Bingol et al., 1975). Rocks



EXPLANATION

Metamorphic Rocks		Ophiolitic Rocks	
Upper Cretaceous	Metabasic rocks, amphibolite etc.	Mesozoic	Peridotite [Denizgoren Ophiolite]
Upper Paleozoic-Mesozoic	Schist, quartzite, marble, metabasic etc.	Upper Paleocene-Eocene	Metaflysch
Permian	Marble	Upper Cretaceous	Ophiolitic Melange
Upper Paleozoic	Schist	Mesozoic	Undifferentiated basic and ultrabasic rocks
Carboniferous	Metagranodiorite	Unknown	Metaultrabasic rocks [Kazdag Group]
Paleozoic	Schist		
Paleozoic	Gneiss		
Paleozoic	Marble		
Paleozoic	Undifferentiated gneiss, metagranite, schist, amphibolite, marble etc.		
Paleozoic	Amphibolite		
Paleozoic	Undifferentiated gneiss, schist, metagranite, migmatite, amphibolite etc.		
			Active faults
			Faults
			Thrust faults
			Roads
			Major towns

Fig. 3. Distribution of the metamorphic and ophiolitic rocks including ophiolitic melanges in the Biga Peninsula (modified from MTA, 2001). This and all subsequent figures use Universal Transverse Mercator (UTM) projection, Zone +35 with European Datum 1950 (ED 50).

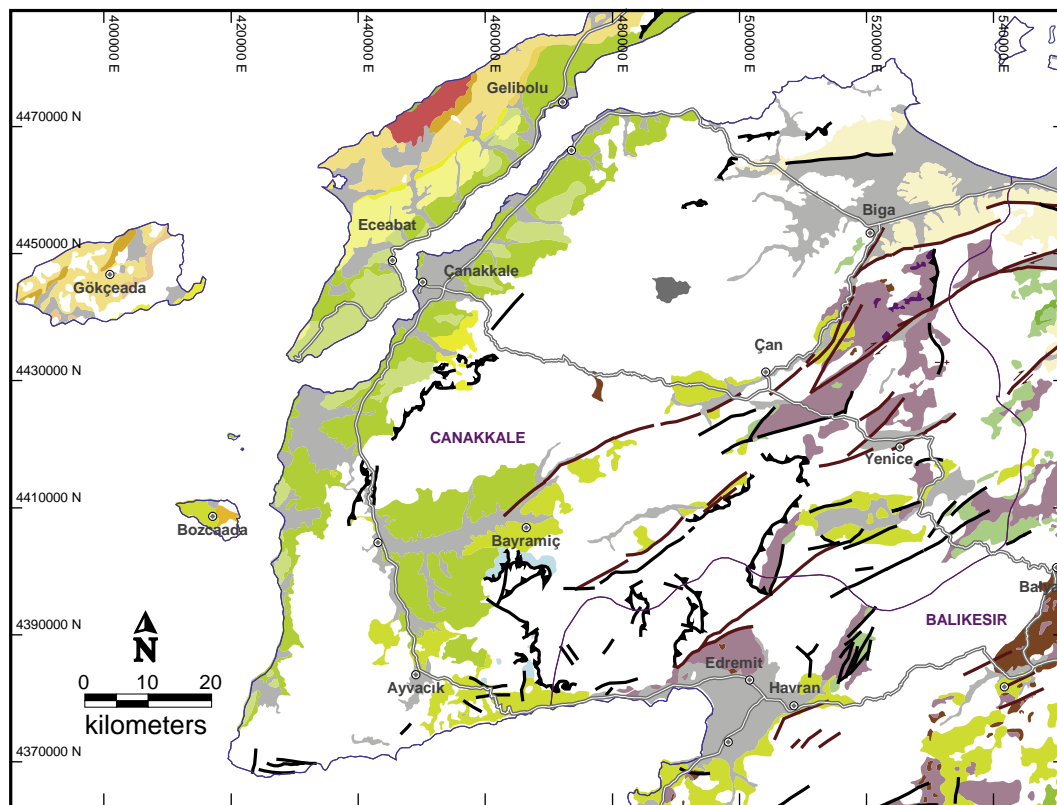
of the Karakaya Complex are exposed in the Kazdag Mountains and extend northeast (Figs. 3 and 4), crosscutting the Biga Peninsula. Karakaya Complex rocks represent a subduction–accretion process.

Karakaya Complex in Biga Peninsula consists of four tectono-stratigraphic units, reflecting a formation of similar age but different depositional basin environments, which are Nilufer Unit, Hodul Unit, Orhanlar Graywacke and Cal Unit (Fig. 2) (Okay et al., 1990). Though some of the most studied rocks in Turkey, origin of the Karakaya Complex is the least understood and differentiation of the units within the complex and their correlation within the Sakarya Zone remain inadequate (Okay and Goncuoglu, 2004). Karakaya Complex is subdivided into only Lower and Upper Units in recent studies (Okay and Altiner, 2004; Okay and Goncuoglu, 2004).

Camlik Metagranodiorite, outcropping north of the town of Havran, intruded into quartz–feldspar schists and phyllites of the Kalabak Formation. Two zircon grains from Camlik Metagranodiorite, one of a few radiometrically dated Pre-Cenozoic intrusives, were dated as 397.5 ± 1.4 Ma, Early Devonian (Okay et al., 2006) using stepwise $^{207}\text{Pb}/^{206}\text{Pb}$ evaporation method, confirming the earlier less precise age of 399 ± 13 Ma (Okay et al., 1996). Yolindi Metagranodiorite in the southeast of the Biga Peninsula is the other Pre-Cenozoic granitoid in the Biga Peninsula (Fig. 3) (Okay et al., 1990).

2.2. Ophiolitic rocks

Ophiolitic rocks of the Biga Peninsula, except metaophiolites in the Kazdag Group and melanges in Hodul unit of the Karakaya Complex,



EXPLANATION

Sedimentary Rocks

Quaternary	Undifferentiated	Upper Senonian	Clastic and carbonate rocks	
Quaternary	Alluvial fan, slope debris etc.	Upper Senonian	Pelagic limestone	
Pliocene	Undifferentiated continental clastic rocks	Upper Jurassic-Lower Cretaceous	Neritic limestone	
Upper Miocene-Pliocene	Undifferentiated continental rocks	Middle Triassic-Jurassic	Neritic limestone [(Cetmi Melange)]	
Upper Miocene	Continental clastic rocks	Middle-Upper Triassic	Carbonate and clastic rocks	[Karakaya Complex - Upper Unit/Hodul]
Upper Miocene	Neritic limestone	Permo-Triassic	Clastic and carbonate rocks (blocks and volcanic rocks in places)	
Middle-Upper Miocene	Continental clastic rocks	Permian	Carbonate rocks with partly clastic rocks	
Miocene	Continental clastic rocks [Can Fm. / Kucukkuyu Fm.]			
Oligocene-Lower Miocene	Clastic rocks			
Upper Eocene	Clastic rocks			
Middle-Upper Eocene	Clastic and carbonate rocks			
Middle-Upper Eocene	Neritic limestone			
Lower-Middle Eocene	Clastic and carbonate rocks			
Lower-Middle Eocene	Clastic rocks (continental in places)			
				Active faults
				Faults
				Thrust faults
				Roads
				Major towns

Fig. 4. Distribution of the sedimentary rocks in the Biga Peninsula. Modified from MTA (2001).

are represented by two major tectono-stratigraphic units; Cetmi Ophiolitic Melange and Denizgoren Ophiolite. Cetmi Ophiolitic Melange is exposed in the southern Biga Peninsula, west of the Kazdag Group and north of the town of Kucukkuyu, and in the northern Biga Peninsula, northwest of the town of Biga (Figs. 2, 3 and 4).

Cetmi Ophiolitic Melange has a tectonic contact with the Camlica Metamorphics in the northern part of the Biga Peninsula, and it also has a faulted contact with underlying high-grade metamorphic rocks of the Kazdag Group and is unconformably overlain by various

sedimentary and volcano-sedimentary rocks of Neogene age in the southern part of the Peninsula. Recent biostratigraphic studies suggest that geodynamic evolution of the melange was completed in the Mid-Cretaceous (Beccaletto et al., 2005), not in the Paleogene (Okay et al., 1990). Cetmi Ophiolitic Melange does not have many common characteristics with other melanges in northwestern Turkey, i.e., in the Izmir-Ankara and Intra-Pontide sutures; and therefore there is no direct correlation between them. However, it has several similarities to melanges in Rhodope Zone of Bulgaria and Greece.

Thus, it is suggested that Cetmi Ophiolitic Melange in the Biga Peninsula may represent an isolated fragment of the Rhodope Zone (Beccaletto et al., 2005).

Denizgoren Ophiolite, forming a northeast-trending belt starting from north of the town of Ezine, consists of partly serpentized harzburgite (Okay et al., 1990). Denizgoren Ophiolite tectonically overlies the Permo-Triassic sedimentary rocks of the Ezine Group in the west, along the Camkoy Thrust, and the Camlica Metamorphics in the east, along the Ovacak Thrust (Fig. 3). Amphibolites taken from the base of the Denizgoren Ophiolite give Ar/Ar radiometric ages of 117 ± 1.5 Ma and 118.3 ± 3.1 Ma (Okay et al., 1996) and 125 ± 2 Ma (Beccaletto and Jenny, 2004). These radiometric ages most probably indicate the initiation of the obduction process. There is a 100 Ma time-gap between Lower Cretaceous (Barremiyen) age metamorphosed base of the Denizgoren Ophiolite and the underlying Triassic (Carnian) Camkoy Formation

2.3. Sedimentary rocks

Mainly carbonate and clastic rocks of Permian and Triassic age in the Karakaya Complex are the oldest non-metamorphosed sedimentary rocks in the Biga Peninsula. Mid-Triassic to Jurassic neritic limestones of the Cetmi Ophiolitic Melange are the other Pre-Cenozoic sedimentary rocks (Fig. 4). Most of the non-metamorphosed and non-deformed Jurassic and younger sedimentary rock series are relatively well studied in the east of the Biga Peninsula, Bursa-Bilecik area, and therefore the sedimentary rocks in the Biga Peninsula are correlated with them and the same nomenclature is used, i.e., Bayirkoy Formation, Bilecik Limestone and Vezirhan Formation (Fig. 2) (Okay et al., 1990). Bayirkoy Formation in the Biga Peninsula, also named the Kirazli Conglomerate, though it is not well recognized due to pervasive silicification in places.

Cenozoic sedimentary rocks have extensive exposures in the west and northwest of the Biga Peninsula, generally northeast-trending exposures on both sides of the strait of the Dardanelles (Fig. 4). Eocene carbonate and clastic rocks, trending northeast, are concentrated in the Gallipoli Peninsula and Gokceada Island. Miocene continental clastic rocks and neritic limestone have exposures along the Dardanelles strait and southwest of the Bayramic Graben (Fig. 4). Cenozoic sedimentary rocks in the Biga Peninsula can be evaluated in four time-intervals, separated by disconformities: Maastrichtian–Early Eocene, Middle Eocene–Oligocene, Miocene and Pliocene–Holocene (Siyako et al., 1989). Early-Middle Miocene times are characterized by coeval volcanism and sedimentation. Lacustrine sediments like shale, siltstone and tuffs were deposited in small basins including economic coal deposits, such as Can lignite. Furthermore, other energy raw materials such as uranium deposits were formed associated with continental clastic rocks of the Miocene Kucukkuyu Formation (Figs. 2 and 4).

2.4. Magmatic rocks

Cenozoic volcano-plutonic rocks dominate the geology of the Biga Peninsula and therefore disguise older lithologies (Fig. 5). Though they cover very extensive areas and host many economical metallic mineral deposits as well as industrial raw materials, volcanic successions in the Biga Peninsula are not well studied or correlated in terms of volcanic stratigraphy and thus are poorly understood. One of the main reasons is a lack of reliable radiometric age dates as well as strong and extensive hydrothermal alteration causing problems with recognition and differentiation of the protoliths in many areas. Magmatic rocks in the Biga Peninsula can be evaluated in two broad categories; Pre-Cenozoic and Cenozoic.

2.4.1. Plutonic rocks

Mainly stock size plutons are exposed in the Biga Peninsula. Most of these intrusions trend either northeast, following the major tectonic grain of the peninsula, or eastnortheast, cutting the major tectonic grain

(Fig. 5). Sevketiye Pluton, the only known example of a Pre-Cenozoic granitoid in the Biga Peninsula, is located east of the town of Sevketiye (Fig. 5). A K/Ar age date from muscovite gives a Late Cretaceous age of 71.9 ± 1.8 Ma (Delaloye and Bingol, 2000). The main Cenozoic intrusions in the Biga Peninsula show calc-alkaline character and are represented by, from east to west, Kestanbol, Kuscaiyir, Evciler, Dikmen, Yenice, Eybek and Sarioluk Plutons in the south and center of the peninsula and Karabiga and Kapidag Plutons in the north (Fig. 5). Well-studied plutons indicate compositions ranging from granite to quartz diorite, for example Kestanbol Pluton is mainly granite and quartz monzonite and Evciler (Karakoy) Pluton is granite, quartz monzonite and quartz monzodiorite (Birkle and Satir, 1995; Yilmaz et al., 2001). Young granitoids in the Biga Peninsula generally are the products of Eocene to Oligo-Miocene plutonism. Compilation of the radiometric ages in the Biga Peninsula indicates that Dikmen, Karabiga, Kapidag and Kuscaiyir Plutons are Eocene in age. Evciler is a product of Oligocene plutonism and Eybek, Kestanbol and Yenice are the products of Oligo-Miocene age magmatic activity (Fig. 6), only one outlier from the Yenice Pluton gives an Eocene age. The oldest radiometric age from Cenozoic intrusions of 52.7 ± 1.9 Ma comes from Karabiga Pluton and the youngest radiometric age of 18.8 ± 1.3 Ma comes from Yenice Pluton (Fig. 6 and references therein). All dated samples from plutonic rocks suggest a younging age from north to south for plutonism in the Biga Peninsula, from Late Cretaceous to Early Miocene (Fig. 5).

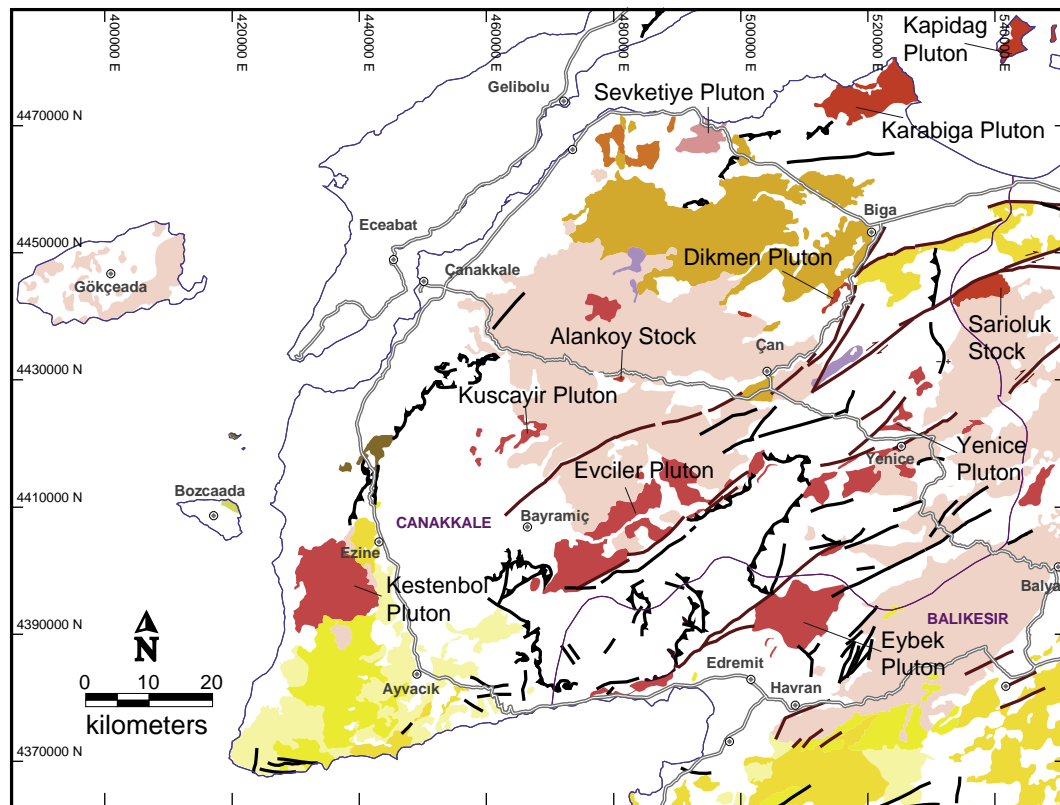
2.4.2. Volcanic rocks

Volcanic rocks of the Biga Peninsula were mainly formed by Cenozoic volcanism and are evaluated in two broad categories, Pre-Cenozoic and Cenozoic (Fig. 5). Basic volcanic rocks, i.e., basalts and spilites, associated with the Karakaya Complex or ophiolitic melanges characterize Pre-Cenozoic volcanic rocks in the Biga Peninsula (Fig. 5). Volcanic rocks related to Karakaya Complex are most probably Triassic in age.

In western Anatolia, origin of the Cenozoic volcanic rocks as well as initiation and mechanism of the extensional tectonic regime are subjects of an ongoing debate (for a brief overview in relation to metallogeny see Yigit, 2006). Some of the models include: tectonic escape (Dewey and Sengor, 1979; Sengor, 1979, 1982, 1987; Sengor et al., 1985), back-arc extension (Jackson and McKenzie, 1988; Kissel and Laj, 1988; Le Pichon and Angelier, 1979, 1981; McKenzie, 1978; Meulenkamp et al., 1988, 1994; Okay and Satir, 2000a), orogenic collapse (Dewey, 1988; Seyitoglu and Scott, 1991, 1992, 1996), slab break-off (Aldanmaz et al., 2000; Altunkaynak and Dilek, 2006; Dilek and Altunkaynak, 2007), and single-subduction model (Jolivet and Brun, 2010).

Cenozoic volcanism in the Biga Peninsula started in the Eocene in extensive areas with mainly andesitic and dacitic, calc-alkaline character and continued to basaltic alkaline volcanism through Late Miocene (Yilmaz, 1990). *Sensu lato* volcanism in the Biga Peninsula initiates with Middle Eocene medium-K calc-alkaline and continues through Oligocene with high-K calc-alkaline character. Early Miocene volcanism is characterized by high-K to shoshonitic lavas. In the Middle Miocene to Late Miocene, volcanism shifted to mildly-alkaline and alkaline characters respectively. Geochemistry of the volcanic rocks suggests increasing amounts of crustal contamination with decreasing subduction signature during the evolution of magmas from the Eocene through the Early Miocene. Middle to Late Miocene volcanism gives geochemical signatures indicating decreasing crustal component with an enriched asthenospheric mantle-derived melt (Altunkaynak and Genc, 2008).

Cenozoic calc-alkaline volcanism hosts many important economic deposits of metallic and industrial minerals. Though volcanic rocks dominate the geology of the Biga Peninsula, they are not well correlated, and therefore the same volcanic rocks are called by different names, i.e., Ezine Volcanics, Ezine Basalt, Tastepe Basalt and Ayvacik Volcanics refer to the same lithology. Furthermore, lack of sufficient radiometric age dates makes differentiation of the many phases of volcanism difficult. For example, radiometric age for Can Volcanics (Ercan et al., 1995) comes



EXPLANATION

Volcanic Rocks

Upper Miocene

Middle Miocene

Lower-Middle Miocene

Lower-Middle Miocene

Middle Miocene
(Lower Miocene in general)

Oligocene

Eocene

Eocene

Triassic

	Basalt
	Andesite
	Pyroclastic rocks
	Undifferentiated volcanic rocks
	Dacite, rhyolite, rhyodacite
	Undifferentiated volcanic rocks
	Andesite
	Undifferentiated volcanic rocks (sedimentary rocks in places)
	Basalt, spilite [Karakaya Complex]

Intrusive Rocks

Oligo-Miocene

Eocene

Upper Cretaceous

Granitoid

Granitoid

Granitoid

Active faults

Faults

Thrust faults

Roads

Major towns

Fig. 5. Distribution of the plutonic and volcanic rocks in the Biga Peninsula. Modified from MTA (2001).

from a sample taken either from Umurbey or Gokceada, and there is no age dated sample from the type location in Can.

Attempts at correlation of the volcanic rocks as well as volcanic facies (Ercan et al., 1990, 1995, 1998) did not create detailed maps for volcanic rocks, not even at a scale of 1:25,000. Compilation of the radiometric ages (Fig. 6 and references therein) with mainly K/Ar and some Ar/Ar suggests that calc-alkaline volcanism in the Biga Peninsula started in Late Eocene with Balıklıcesme Volcanics and continued extensively in Oligocene with Can Volcanics (named as Balcılar, Sapci and Kirazlı Volcanics in some areas), and ceased in Early Miocene with Behram Volcanics (named as Doyran Volcanics in some areas). It is assumed that alkaline volcanism in the Biga Peninsula started in Late Miocene, as in western Anatolia, with basaltic alkaline Ezine Volcanics (Yilmaz, 1990; Yilmaz et al., 2001). However, trachyandesitic and basaltic Oligocene Kirazlı and Early Miocene Huseyinfaki Volcanics show alkaline character in some areas (Ercan et al., 1995) and they might be precursors of the alkaline volcanism in the peninsula (Fig. 6).

3. Structural setting

Structural geology of the Biga Peninsula is intricate; there are no available palinspastic reconstruction maps of any scale. Pre-Cenozoic structures are dominated by thrust faults associated with ophiolite obductions. The oldest thrust faults are related to metaophiolites in the Kazdag Group and melanges in Hodul unit of the Karakaya Complex. Emplacement of the Denizgoren and Cetmi Ophiolites are mainly Late Cretaceous in age, and formed NE- and N-trending thrust zones respectively (Fig. 3). Cenozoic structural features are characterized by detachment-faulting related to exhumation and core-complex development of Kazdag Massif in Oligo-Miocene, and strike-slip faulting started in Early Miocene related to development of the North Anatolian Fault Zone (NAFZ).

Neotectonics of the area are subject to dextral-strike slip faulting as well as N-trending continental extension with rotations, causing challenging kinematic analysis of faults with not only strike-slip but also oblique and dip-slip components. E-trending principal

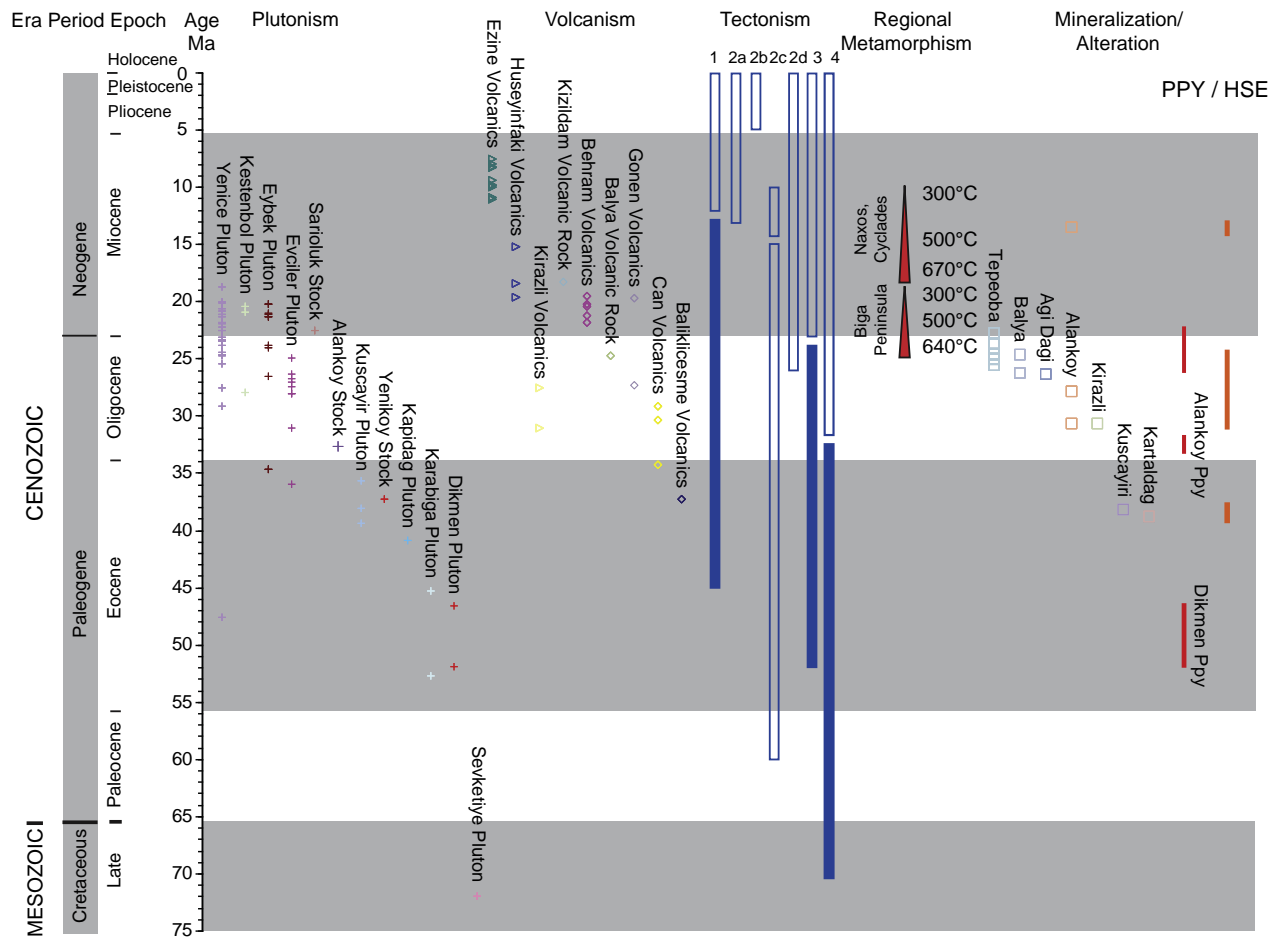


Fig. 6. Relationship between Cenozoic magmatism, tectonism, metamorphism and porphyry and epithermal mineralization in the Biga Peninsula. Total of 105 radiometric age data; 3 Re/Os, 28 Ar/Ar, 71 K/Ar, 2 Rb/Sr, 1 U/Pb (Aldanmaz et al., 2000; Beccalotto et al., 2007; Birkle and Satir, 1995; Delaloye and Bingol, 2000; Ercan et al., 1995; Fytikas et al., 1976; Karacik et al., 2008; Kaymakci et al., 2007; Murakami et al., 2005; other sources, and this study), rectangles: mainly alkaline, diamonds: calc-alkaline, pluses: granitoid, red bar showing porphyry (PPY) and orange bar showing HS epithermal (HSE) mineralization phases, continuous ore deposition of any particular deposit type is not implied. Tectonic models: 1. Tectonic escape (Dewey and Sengor, 1979; Sengor, 1979, 1982, 1987; Sengor et al., 1985), 2. Back-arc extension (a: Le Pichon and Angelier, 1979, 1981, b: Jackson and McKenzie, 1988; McKenzie, 1978, c: Kissel and Laj, 1988, d: Meulenkaemp et al., 1988, 1994), 3. Orogenic collapse (Dewey, 1988; Seyitoglu and Scott, 1991, 1992, 1996), 4. Single subduction model (Jolivet and Brun, 2010). Solid bars indicate compression and blank bars indicate extension. Regional metamorphism from Okay and Satir (2000a), Geologic time scale from Gradstein et al. (2004). (For interpretation of the references to color in this figure legend, the reader is referred to the web version of this article.)

deformation zone of the NAFZ bends to the SW in the Biga Peninsula and is the main control on the formation of the transtensional and transpressional fault jogs, which are favorable loci for magmatism as well as mineralization.

Based on the interpretation of the geological maps, LANDSAT and ASTER images incorporated with field observations, NE-, E- and NW-trending faults form three major groups in the Biga Peninsula. The NE- and NW-trending faults are conjugate Riedel shears. The most prominent faults are NE-trending dextral-strike slip systems (~060) (Fig. 5), related to the western extension of the NAFZ, which create pull-apart basins that control Oligo-Miocene sedimentation and volcanic activity. This current tectonic regime forms NE-trending basins and ranges, and forms the NW-boundary of the volcanic rocks in the Biga Peninsula (Figs. 4 and 5). Some of the NE-trending strike-slip faults are seismically active (Fig. 5), and also control the distribution of current hot-spring activity. The same relationship may be true for paleo-hot springs related to epithermal systems in the Biga Peninsula. NW-trending faults, possibly antithetic Riedel shears of the NAFZ, are less prominent structures, and are mostly distinct in satellite image interpretations. Other conspicuous structures are E-trending normal faults and fractures (tension fractures), forming loci for magmatism, mineralization and alteration. Inferred E-trending normal faults form the southern boundary of the Biga Peninsula along the northern edge of the Gulf of Edremit.

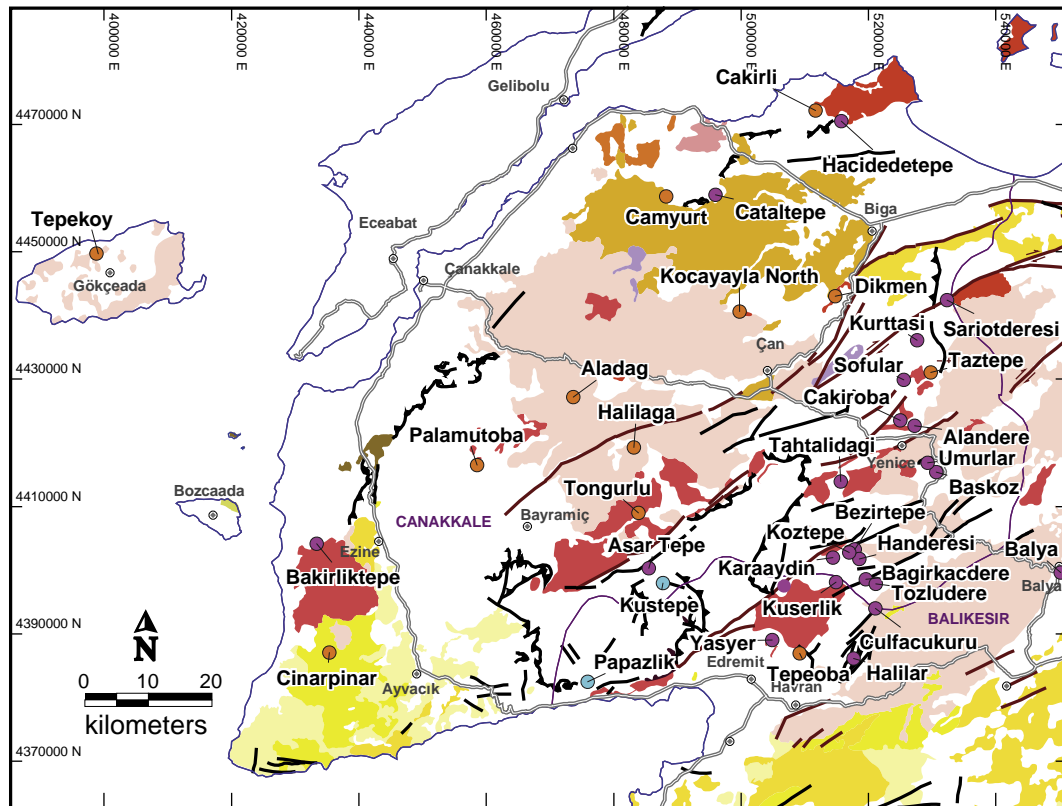
The LANDSAT and ASTER data overlain with DEM images indicates the presence of many circular volcanic structures, e.g., calderas and nested-calderas, associated with Cenozoic volcanic landforms. Most of these circular structures are spatially and temporally related to epithermal mineralization, such as Kirazli Caldera. However, true nature and volcanic facies of these circular structures need further clarification.

4. Mineral deposits and prospects

Mineral deposits of the Biga Peninsula are dominated by volcanic- and intrusion-related hydrothermal systems, which is a natural corollary of the preeminent geology. The database compilation extracted from the TMDD indicated that 67 deposits and prospects are epithermal type, out of a known 128 mineral deposits and prospects in the Biga Peninsula. Porphyry and skarns have 12 and 24 known deposits and prospects respectively.

4.1. Porphyry/skarn/carbonate replacement deposits

Known porphyry, skarn and CR deposits of the Biga Peninsula are associated with volcano-plutonic complexes of ages ranging from Eocene to Early Miocene (Fig. 7). Regional distribution of the intrusion related deposits is controlled by two NE-trending, parallel linear belts, reflecting major tectonic grain of the Biga Peninsula, which is



EXPLANATION

Deposits or Prospects

● Porphyry Cu/Au/Mo

● Skarn

● Carbonate Replacement

Fig. 7. Distribution of the porphyry, skarn and carbonate replacement deposits and prospects in the Biga Peninsula with emphasis on host-rock lithology, lithological explanation same as Fig. 5.

not consistent with the ENE-trend of the causative intrusive rocks across the whole country (Yigit, 2006, 2009). With the exception of Balya and a few others, skarn deposits and prospects such as Yenice district are located SE of the NE-trending porphyry–epithermal belt (Fig. 7). Lack of predominant coeval volcanic rocks in the Yenice skarn belt with the existence of surrounding Upper Paleozoic to Triassic metamorphic rocks may indicate deeper erosional levels, and thus, higher uplifting rates that could be related to the Oligo-Miocene core complex formation that resulted in exhumation of Kazdag Massif. Within Triassic assemblages carbonate rocks are especially favorable loci for younger skarn mineralization (Figs. 3 and 7).

4.1.1. Porphyry

Though a limited number of porphyry prospects have been discovered in the Biga Peninsula, their economical importance makes them appealing exploration targets, i.e., recently discovered Halilaga prospect. Tepeoba is the only porphyry Cu–Mo–Au prospect with calculated reserve data albeit it is not compliant to international reserve/resource reporting codes. Recent work on the porphyry prospects proved the predisposition of the geology for the formation of this type of deposit in the Biga Peninsula. Some of the porphyry prospects in the Biga Peninsula have spatial, temporal and genetic relations to known HS epithermal prospects, i.e., Aladag, Halilaga. Furthermore, porphyry potential of the many known skarn deposits and prospects remains untested along with that of some CR deposits with possible indication of porphyry environment.

Halilaga, discovered in 2007 with ongoing feasibility studies, consists of a main Kestane porphyry Cu–Au zone, Bakirlik skarn Au–Ag +/-base metal zone and related Kunk Hill and Kumlugedik HS epithermal zone forming lithocaps. The main Cu–Au porphyry mineralization, hosted by quartz, feldspar-hornblende porphyries, andesitic flows and tuffs of probably Oligocene age, contains pyrite, magnetite, chalcopyrite with minor chalcocite and molybdenite with visible disseminated Cu in drill holes (Grieve, 2009). Porphyry related alteration covers an area of more than 4 km long and 2 km wide, though the mineralized central zone of the porphyry system exposes over an area of 0.4 km long and 0.3 km wide. Majority of the stockwork and disseminated mineralization is related to potassic alteration assemblages overprinted by phyllic alteration. Density of the stockwork quartz veins can reach up to 35 to 50% in drill holes. Secondary Cu enrichment zones can contain up to 2.15% Cu and 0.93 g/t Au over a thickness of 25.8 m (e.g., discovery drill hole HD-01). HD-01 penetrated 298.2 m of mineralization grading at 0.50 g/t Au, 0.53% Cu, including over 105.4 m at 1.03 g/t Au and 1.03% Cu. Other important intervals include 267.3 m mineralization grading at 0.50 g/t Au, 0.26% Cu in drill hole HD-08, and 241.2 m of mineralization grading at 0.30 g/t Au, 0.22% Cu in drill hole HD-07A. The copper-bearing garnet skarn mineralization at Bakirlik is associated with granodiorite intruded into gray limestone, recrystallized marble and schists. Whether this spatially related skarn mineralization is genetically and temporally related to main porphyry system at Kestane remains to be determined.

Tepeoba porphyry Cu–Mo–Au deposit was discovered by Turkish Geological Survey (MTA) in 2001, though long time known W and

Mo mineralization exist in the district. Porphyry mineralization is related to Late Oligocene granodioritic and granitic porphyries intruded into metabasic and metasedimentary rocks. Porphyritic intrusions form 4 km long and 0.5 to 1 km wide contact metasomatic zone with breccia. A skarn zone with hornfels developed at the contact between granodiorite and schist is located approximately 0.5 km NW of the mineralized breccia zone. In the breccia-centered mineralization with surrounding veins and veinlets, pyrite, chalcopyrite, molybdenite, gold, bornite, malachite, magnetite, hematite and Fe-oxides are common minerals in drill cores, but rare on outcrops. Minerals in the alteration assemblages are controlled by host lithologies, potassic alteration is mainly related to granitic intrusions and phyllic alteration is mainly in the Pre-Jurassic metabasic rocks and schists. Potassic alteration zone with biotite and quartz is mainly concentrated on the breccia zone at the center, which is surrounded by an alteration zone containing sericite, tourmaline, epidote, chlorite and calcite. Though gold content is not included in ore reserve estimation, some of the mineralized zones in drill cores contain average 1 g/t gold with average 1% Cu and 0.05% Mo, up to 10 g/t gold values in some zones.

Dikmen porphyry Au–Mo–Cu mineralization, discovered by a joint venture between MTA and Mining Metal Agency of Japan (MMAJ) as a result of a 1988–91 exploration campaign in the Biga Peninsula, is associated with quartz–feldspar porphyry, granodiorite and aplitic dikes of Eocene age intruded into metasedimentary and metavolcanic rocks including marble of Triassic age. Two mineralized zones, namely Sigiregrek Stream in the SW and Domuzdami Stream in the NE, are located within approximately 3 km long and up to 0.5 km wide, NE-trending mineralized and altered zones. The porphyry system has associated skarn mineralization in the Sigiregrek Stream area at the contact between quartz–feldspar porphyry and marbles, forming a NE-trending zone of approximately 1.5 km long and 0.15 km wide, parallel to the trend of the main mineralized system. Porphyry mineralization occurs as stockworks, sheeted veins (Fig. 8A, B), veinlets and disseminations. Pyrite, molybdenite (Fig. 8C), chalcopyrite and supergene Cu minerals including brochantite are mainly associated with quartz–sericite–pyrite (QSP) alteration zones as well as advanced argillic and argillic alteration zones with kaolinite and dickite. Early geochemical work in the prospect indicated high-grade gold values compared to other porphyry deposits with > 10 g/t Au in rock-chip samples. A total of 9 grab and rock-chip samples in this study have values up 4.230 g/t Au, 2.44 g/t Ag, 1380 ppm Ba, 574 ppm Cu, 1260 ppm Mo, 1720 ppm Pb and 2330 ppm Zn.

Palamutoba is one of the most well-exposed porphyry prospects in the Biga Peninsula. Multiple phases of granodiorite, quartz–feldspar porphyry and feldspar porphyry of probably Late Eocene age are intruded into schists of Paleozoic age. Causative granodiorite intrusive contains common zoned plagioclase, but unusually primary biotite locally contains plagioclase inclusions (Fig. 8D and E). Prospect consists of two mineralized and altered zones, namely Magara Tepe and Maden Tepe (Fig. 8F), each of which is approximately 2 km long and 0.7–0.8 km wide. The prospect has well developed sheeted veins and stockworks in the QSP alteration zone (Fig. 8G), especially in the Magara Tepe Zone. Iron-oxide filled fractures, dominantly goethite and jarosite, are dominant in the Maden Tepe Zone. Leach cap of the system has goethite and jarosite with minor hematite in Magara Tepe Zone and goethite and hematite with minor jarosite in Maden Tepe Zone. NE-trending alteration zone in Magara Tepe and NW-trending alteration zone in Maden Tepe contain predominantly NE- and ENE-trending sheeted veins in stockworks. Reconnaissance rock-chip samples have values up to 0.215 g/t Au, 1.02 g/t Ag, 240 ppm Ba, 291 ppm Cu, 106.5 ppm Mo and 114.5 ppm Pb. Gold has positive correlation with Cu and Fe. Porphyry mineralization in the prospect is disguised by post-mineral porphyries in many areas, and therefore, makes exploration targeting difficult.

Tongurlu porphyry prospect is associated with granitic intrusions cut by aplite dikes. Fracture-controlled stockwork zones in the prospect

contain up to 13.60% Mo (Erdem, 1976). Andesitic lavas and pyroclastic rocks in a flow-dome setting have HS epithermal potential.

Reconnaissance sampling of the porphyry systems, generated in this study, of Cinarpinar, Aladag, Kocayayla North and Cakirli prospects indicated that geology and geochemistry of the mineralized systems are promising for porphyry type ore formation. Cinarpinar prospect has showings of porphyry-style stockworks in the oxidized outcrops (Fig. 8H). Unlike other prospects, Cinarpinar shows enrichment of REE and Th. Whole-rock analysis from the prospect indicated high concentration of Ce, La, P, Th and Y, suggesting existence of the REE mineral monazite. Porphyry style stockwork zones at the Aladag prospect (Fig. 8I) are contemplated to be related to Kirazli HS system. A total of 10 geochemical rock-chip samples collected in this study give up to 0.129 g/t Au, 2.68 g/t Ag, 1680 ppm As, 2020 ppm Ba, 712 ppm Cu, 105 ppm Mo, 247 ppm Pb and 19.8 ppm Sn values. Kocayayla district with known base metal deposits contains anomalous stockwork zones indicative of porphyry systems (Fig. 8J). Cakirli prospect in the northernmost Biga Peninsula is a candidate to form a new district for porphyry and related mineralization. At Cakirli, conspicuous high erosional rates with low-relief regional surfaces form a peneplane on the granitic rocks. Absence of the shallow features of the porphyry environment, e.g., preservation of the lithocap as well as lack of coeval volcanic rocks, indicates that a deeper part of the porphyry systems is exposed without known related epithermal systems. Taztepe and Tepekoy are examples of other porphyry prospects. Copper-moly mineralization at the Camyurt prospect in the northern Biga Peninsula with ancient workings, associated with quartz diorite intrusives of probably Eocene age, could be another potential porphyry/skarn prospect.

4.1.2. Skarn

Skarn deposits and prospects, dominated by base metals with a few notable exceptions which include Au–Cu and W–Mo rich systems, are clustered in the SE part of the peninsula, mainly in Yenice district. The only outliers are Cataltepe and Hacededetepe in the N and Bakirliktepe in the W of the Biga Peninsula (Fig. 7). Asar Tepe with high gold grades is the only authenticated Au–Cu skarn in the Biga Peninsula. Cakiroba, Tahtalidagi and Sofular are examples of the W–Mo rich systems and could be related to porphyry systems. Balya is historically classified as a skarn, but contains carbonate replacement and epithermal zones, indicating multiple hydrothermal events and related mineralization. Though classically called a skarn with inferred causative intrusion, Papazlik, with intermittent past production has similarities to carbonate replacement deposits. Yasyer skarn deposit also contains carbonate replacement zones.

Ancient and historical Balya mining district with past production of 4 Mt ore containing 400 kt Pb, 400 kt Zn, 3 t Au and 1 kt Ag has the largest base-metal reserve and resources in the Biga Peninsula. Historical underground mining concentrated in Sarisu, Ari and Orta orebodies, and the other mineralized zones are Hastane Tepe, Koca and Karaca located to the north. Modern underground mining started in 2009 where the historical workings are, and there is an ongoing feasibility study in the Hastane Tepe zone which is planned for production. Triassic age Karakaya Complex consisting of conglomerate, sandstone and shale as well as blocks of limestones of Permian age and dacite and andesitic lava, and subvolcanic intrusions are the predominant lithologies in the district. Known orebodies are preferentially located at the limestone contact with dacite or andesite as irregular bodies, within dacite as disseminations, and within limestone and dacite as irregular veins (Akyol, 1977). Galena, sphalerite, pyrite and chalcopyrite are major minerals with minor amounts of pyrrotite, marcasite, bismuth, sulfosalts, arsenopyrite, tetrahedrite-tennantite, bornite, argentite, heyrovskyite, magnetite, hematite, pyrolusite, orpiment/realgar and native tellurium. Garnet, tremolite and actinolite are common in the skarn zone. Argillic and phyllic alteration at the central part of the system is overprinted locally by advanced argillic alteration with hypogene colorless, tabular crystals of alunite,

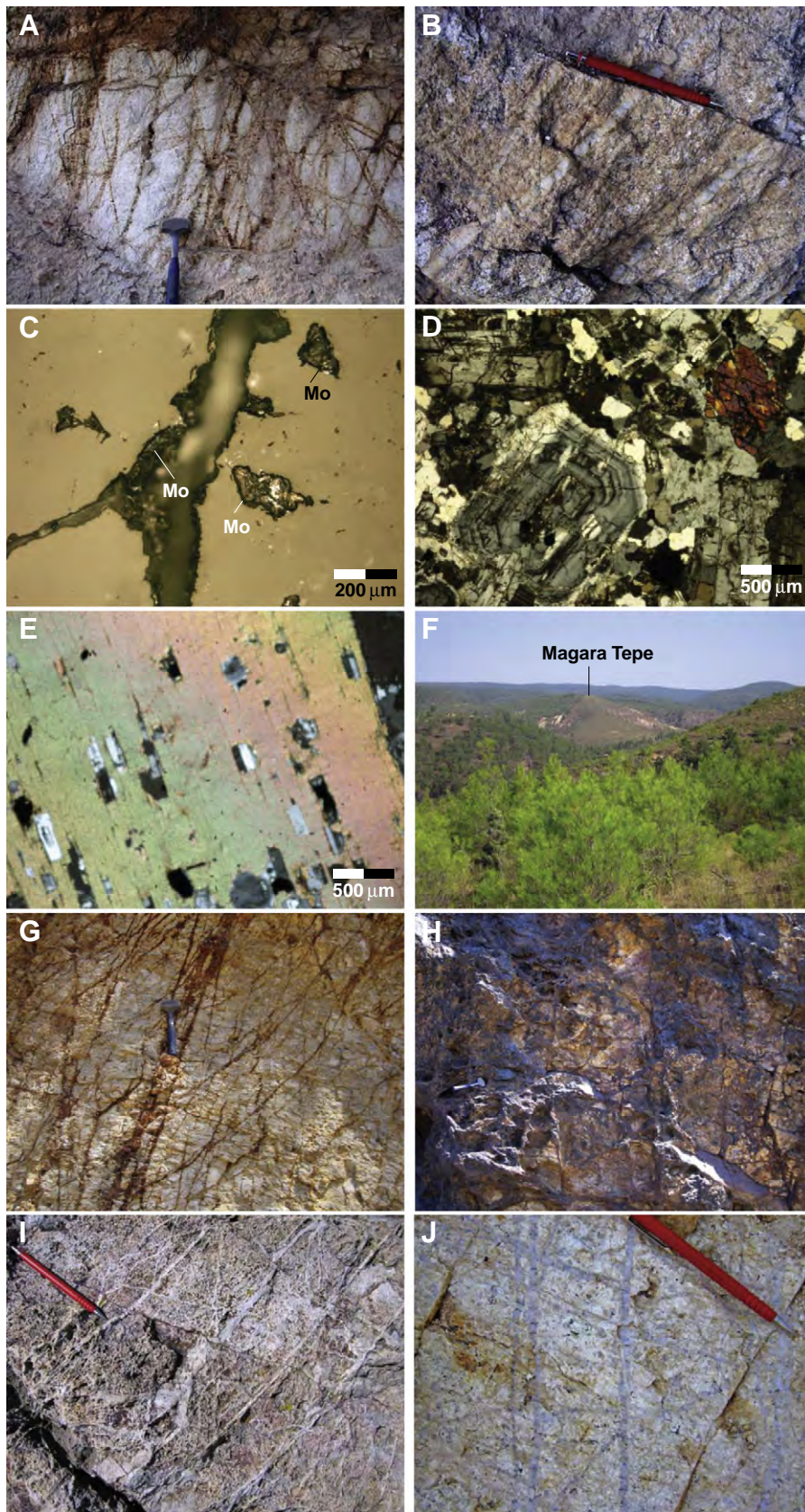


Fig. 8. A and B. Stockwork quartz veinlets in altered granodiorite in the Dikmen porphyry prospect [514841E, 4443098N], C. Photomicrograph of disseminated and vein molybdenite in quartz, Dikmen porphyry prospect [sample no BPGP-1180] [RL], D. Photomicrograph of zoned plagioclase and amphibole crystals in host-rock granodiorite in the Palamutoba porphyry prospect [sample no BPGP-1357] [XP], E. Photomicrograph of biotite with plagioclase inclusions in granodiorite, same sample as D., F. Alteration and oxidation of the leached cap at Magara Tepe Zone of the Palamutoba porphyry prospect [from 459341E, 4414993N looking NE], G. Sheeted and stockwork quartz veins in QSP altered schists at Magara Tepe Zone of the Palamutoba porphyry prospect [458541E, 4416576N], H. Siliceous stockwork veinlets with goethite and Mn-oxides at Cinarpinar prospect, I. Porphyry style quartz stockwork veinlets at Aladag prospect with anomalous Cu–Mo–Au–Ag, J. Porphyry-style quartz stockwork veinlets with sericitic alteration in mineralized porphyry at the Kocayayla prospect, containing anomalous Cu–Mo. Abbreviations used in this and all subsequent figures; PPL: Plain Polarized Light, XP: Crossed Polars, RL: Reflected Light.

halloysite, jarosite, kaolinite and quartz (Agdemir et al., 1994). Strong oxidation near surface with gossans consists of anglesite, cerussite, Fe- and Mn-oxides/hydroxides with galena relics. Average age of alteration and host-rock andesite are Late Oligocene. Multiple mineralizing events such as skarn, carbonate replacement and epithermal events in the Balya deposit need further work to elucidate the spatially related different events. In the literature there are no available geochemical studies on which to base genetic connotations.

Asar Tepe Fe–Cu–Au calcic skarn mineralization is associated with Late Eocene to Oligocene age Evciler pluton intruded into marbles and biotite–amphibolite gneiss of Paleozoic age. Gold and associated pyrite–pyrrhotite mineralization is probably controlled by a NE-trending structure dipping moderately NW. Massive sulfide mineralization contains pyrite, marcasite, pyrrhotite and chalcopyrite with quartz and calcite gangue. High-grade gold mineralization is associated with 200 m long central core zone (Yilmaz, 2007). Exoskarn mineralization consists of predominantly prograde garnet and diopside with minor retrograde tremolite, epidote, chlorite, scapolite and sericite. Rock-chip sampling in this study from the prospect shows values up to 1.5 m at 13.8 g/t Au, 3.21 g/t Ag, 297 ppm Bi, 110.5 ppm Co, 7570 ppm Cu and 29.6% Fe.

Yenice district contains several base-metal skarn deposits (Fig. 7) and prospects mainly associated with Oligo–Miocene age granitic intrusions, i.e., Eybek Granodiorite. Economically important orebodies with several Mt ore (Table 1), regardless of grade, are Bagirkacderesi, Handeresi and Culfacakuru, though no recent work has been done in the district. At Bagirkacdere, the skarn zone formed at the contact between Eybek Granodiorite and marble lenses within schists of Paleozoic age. Calc-silicates, garnet, epidote, actinolite and quartz are common gangue minerals in the skarn zone. Precious metal content of most of the base metal ore in the district is not reported, however, some of the deposits contain gold especially in gossan zones, e.g., Culfacakuru. In the district other skarn prospects include Sariotderesi [0.445 Mt at 0.7% Cu, 2.6% Pb, 7% Zn], Kurttasi, Alandere, Umurlar, Baskoz, Bezirtepe, Koztepe, Karaaydin, Kuserlik, Tozludere, and Halilar (Fig. 7).

4.1.3. Carbonate replacement

Papazlik is the only example of a CR deposit and is probably associated with Oligo–Miocene intrusives, exposed immediately to the SE. Papazlik base- and precious-metal deposit, with intermittent ancient and historical production from an underground mine, is hosted at the contact between quartz–chlorite–amphibolite schist and marble of Paleozoic age. Deposit contains an unclassified resource of 0.242 Mt grading at 5 g/t Au, 25 g/t Ag, 8.21% Pb and 6.72% Zn based on limited drilling, 2 surface and 8 underground drill holes (MTA, 1993b). Most of the mineralization occurs as open space fill with galena, Fe-poor sphalerite, pyrite, and minor chalcopyrite. Supergene minerals include malachite, azurite, cerussite and iron-oxides. Common silicification with comb and drusy quartz crystals as well as chalcedony, carbonate and argillic alteration is closely associated with mineralization. Argillic alteration is prominent especially at the sheared contact between vein and wall rocks. The northeast-trending vein with average thickness of 1 m is parallel to bedding plane cleavage. Though there is no skarn zone or causative intrusions exposed in the mine area, the deposit historically was classified as a skarn (e.g., Gumus, 1970). In the area, the only other known prospect with similar geological setting to Papazlik is Kustepe prospect located to the NE with intermittent past production and remaining small resource of Zn–Pb–Cu.

4.2. Epithermal deposits and prospects

Majority of the epithermal systems are HS style, though economical IS and LS deposits and prospects are present. Only a few epithermal deposits have affinities with IS style systems, their base metal and silver credentials are proven. More detailed studies in the epithermal deposits

of the Biga Peninsula will help recognition of more prospects of this style.

Known epithermal deposits and prospects are concentrated in the Oligocene volcanic and subvolcanic rocks (Fig. 9). Nevertheless, epithermal systems hosted in Late Eocene and Miocene volcanic rocks should not be neglected. In spite of the fact that number and size of the LS style epithermal deposits and prospects are dwarfed by HS style, LS deposits are important because of their bonanza grade [>30 gpt or 1 opt] zones, i.e., Kucukdere deposit. Majority of the HS epithermal deposits are clustered in the central Biga Peninsula with several of them in the SE Biga Peninsula. LS and IS deposits are mainly located in the northern and eastern Biga Peninsula (Fig. 9). Agi Dagi and Kirazli are the largest classical examples of HS epithermal systems in the Biga Peninsula. Agi Dagi has 1.4 Moz gold resources, compliant with international reporting codes. Updated gold resources in Kirazli are approximately 0.5 Moz gold. Ongoing feasibility work on both projects expects to expand gold resources and reserves.

Kisacik with approximately 1 Moz gold resources is the largest LS style epithermal deposit in the Biga Peninsula, though resources are not compliant with international reporting codes. Kucukdere is the classical example of a LS system. Koru, Arapucandere, Tesbihdere and Sahinli could be examples of the IS style epithermal systems in the peninsula.

Some of the HS epithermal systems show transition to porphyry environment as in Kirazli and Alankoy. Some of the epithermal systems are not well enough characterized to determine the styles of the mineralization, e.g., newly discovered epithermal prospects on Gokceada Island. Other deposits with Sb \pm Au and Hg endowment in epithermal class include Buyukyenic and Kucukyenic deposits with small resources in Ivrindi Sb district and Hodul Hg deposit.

4.2.1. HS deposits and prospects

Biga Peninsula has world class HS alteration zones, in which the volume of silica is only comparable to districts such as Yanacocha in Peru. Most of the chalcedonic quartz zones have been mined for industrial use, commercially called silex (mill balls, mill lining bricks etc.), and argillic and advanced argillic zones have been mined as industrial clays. Unfortunately, epithermal gold potential of these alteration zones has just started to be appreciated, especially after the discovery of Agi Dagi and Kirazli systems.

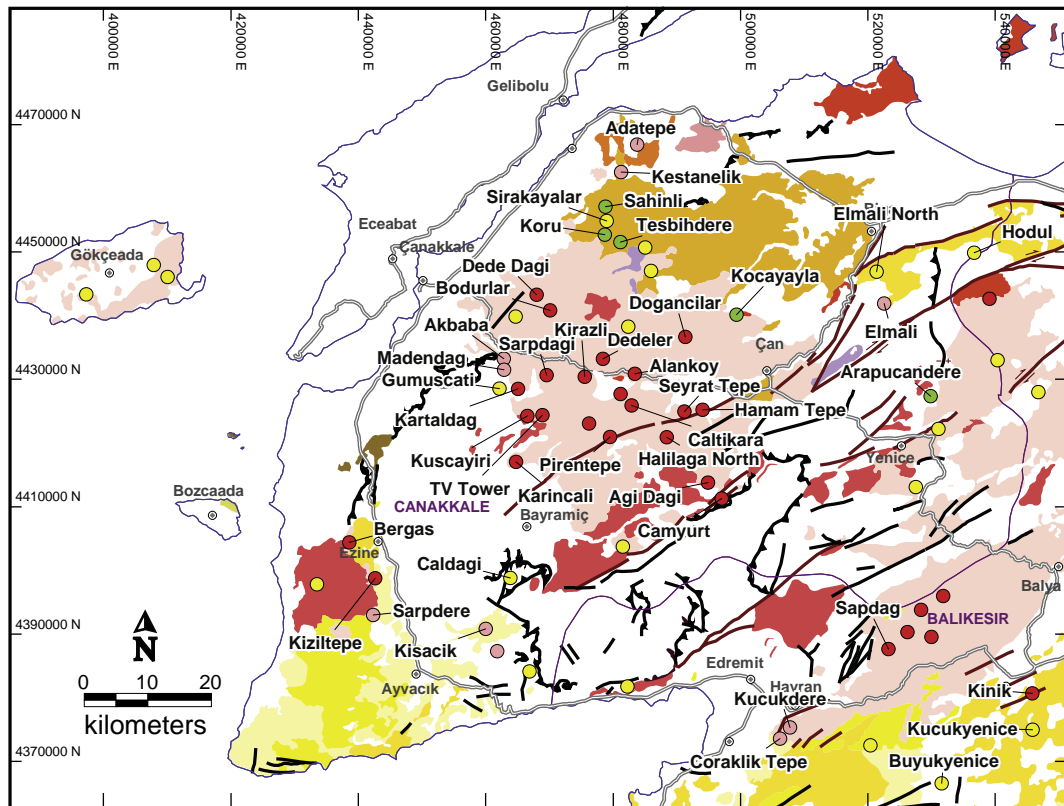
Agi Dagi prospect is an Oligocene flow-dome complex forming a prominent topographic high (Fig. 10A) and lies within a NE-trending mineralized and altered zone, which is approximately 5 km long and 2 km wide. The prospect consists of two defined orebodies, namely Baba Dagi with historical resources, and Deli Dagi located approximately 2.5 km NE, and many other mineralized zones including Ayitepe, Fire Tower, Tavsan Tepe and Ihlamur. Felsic to intermediate volcanic and sub-volcanic rocks including dacite, rhyolite, andesite and post-mineral quartz–feldspar porphyries are the main host rocks in the prospect. Primary textures of these lithologies have been destroyed by strong hydrothermal alteration over extensive areas. Pyrite is the most abundant primary sulfide mineral related to Au in the prospect, and trace to minor amounts of enargite, covellite, galena, molybdenite (particularly in Baba Dagi zone) are locally present. Gold–silver mineralization occurs as disseminations and breccias including phreatic, phreatomagmatic and tectonic. Phreatic (meteoric-hydrothermal) breccias include both heterolithic, rock-flour matrix supported, and hydrothermal mineral (e.g. quartz, chalcedony, pyrite, alunite and pyrophyllite) cemented. In many areas, distinction of lithic tuffs from other breccias could be difficult due to texture obliteration as a result of pervasive hydrothermal alteration. Hydrothermal mineral cemented breccias including crackle and jigsaw are associated with gold mineralization, higher grades commensurate with amount of pyrite (or Fe-oxide) in the matrix. E-trending phreatic breccias are important at Deli Zone (Cunningham-Dunlop and Lee, 2007a). Silicification with massive, vuggy residual quartz, late-stage blanket-like

Table 1

Mineral deposits with total Au reserve and/or resources >0.2 Moz or >0.5 Mt ore regardless of metal or grade in the Biga Peninsula, NW Turkey.

Deposit name	State	Commodity	Deposit type	Principal host rocks	Age of host rocks	Orebody/structure	Mineral reserves and/or resources/or grade	Status	Relevant references
Halilaga	Canakkale	Au, Cu	Porphyry Cu–Au	Quartz porphyry, feldspar-hornblende-quartz porphyry, andesitic flows and tuffs; granodiorite, gray limestone, recrystallized marble and schists at Bakirlik Hill	Oligocene?	Stockwork quartz veins and disseminations	Unclassified potential resource using Leapfrog grade shell: 250–350 Mt at 0.57 g/t Au and 0.45% Cu, (2 m composites at 0.3 g/t Au and 0.2% Cu cut-offs) based on 43 DHs, totaling 10,398.70 m	F	Grieve, 2009
Tepeoba	Balikesir	Cu, Mo, Au	Porphyry Cu–Mo–Au	Granodiorite, granite and granite porphyry (1) intruded into metabasic and metasedimentary rocks (2)	Oligo-Miocene (1), Pre-Triassic (2)	Breccia, disseminated, vein and veinlets	Resource: 19.24 Mt at 0.33% Cu, 0.041% Mo plus 4.86 Mt at 0.32% Cu, 0.046% Mo	P	Kucukefe et al., 2003; Murakami et al., 2005
Agi Dagi	Canakkale	Au, Ag	Epithermal HS	Felsic to intermediate volcanic rocks and porphyries	Oligocene	Disseminations, breccias/NE-trending mineralized and altered zone	Resource: Baba Zone: 26.601 Mt at 0.52 g/t Au, 0.60 g/t Ag (Indicated), 9.898 Mt at 0.48 g/t Au, 0.50 g/t Ag (Inferred) Deli Zone: 25.362 Mt at 0.67 g/t Au, 5.96 g/t Ag (Indicated), 7.970 Mt at 1.17 g/t Au, 11.18 g/t Ag (Inferred)(0.2 g/t Au cutoff)	F	Cunningham-Dunlop and Lee, 2007a; Keane et al., 2010
Kirazli	Canakkale	Au, Ag	Epithermal HS	Andesitic and dacitic lavas and pyroclastics	Oligocene	Stockworks, breccia, disseminated and replacement/NNE-trending mineralized zone, sub-horizontal ore zones	Resource: 11.831 Mt at 0.83 g/t Au, 13.92 g/t Ag (Indicated), 8.574 Mt at 0.65 g/t Au, 15.93 g/t Ag (Inferred)(0.2 g/t Au cutoff)	F	Pirajno, 1995; Cunningham-Dunlop and Lee, 2007b; Keane et al., 2010 Kilic et al., 2004
Kisacik	Canakkale	Au	Epithermal LS	Dacitic, rhyodacitic and andesitic volcanic rocks	Upper Miocene	Multi-phase hydrothermal breccias and stockworks/NE-trending mineralized and altered zone	Resource: 56.537 Mt at 0.55 g/t Au (Unclassified)	P	
Sahinli	Canakkale	Au, Ag	Epithermal	Andesitic and dacitic volcanic rocks (1), schists (2)	Eocene (1), Paleozoic (2)	Veins/mainly NE-trending veins with some E- and N-trends	Reserve: 2.778 Mt at 5.76 g/t Au (Unclassified)Resource: 7.5 Mt at 8.5 g/t Au (Unclassified)	P	Yildirim and Cengiz, 2004
Akbaba (=Madendag)	Canakkale	Au, Ag	Epithermal LS	Andesite porphyry (1), Schists (2)	Lower Miocene (1), Pre-Triassic (2)	Veins, breccia, stockworks/NE-trending silicified main zone	Resource: 8 Mt at 1.25 g/t Au (Unclassified)	P	MTA, 1993a
Kucukdere	Balikesir	Au, Ag	Epithermal LS	Andesite porphyry	Miocene	Banded-quartz–carbonate veins/NE-trending veins	Resource: 1.276 Mt at 6.43 g/t Au (Measured + Indicated), 0.138 Mt and 6.45 g/t Au (Inferred) or 1.406 Mt at 4.92 g/t Au, Most ore mined out Remaining Reserve: 0.923 Mt at 1.39% Cu, 7.38% Pb, 2.85% Zn, 1.5–2 g/t Au, 55–60 g/t Ag (Unclassified)	M	Colakoglu, 2000
Arapucan	Canakkale	Pb, Zn, Cu plus Ag–Au	Epithermal IS	Metasandstone and metadiabase (1), nearby dacitic rocks (2), and granitic intrusions (3)	Permian to Triassic (1), Oligocene (2), Miocene (3)	5 Major veins/E- and NE-trending veins	Remaining Reserve: 0.923 Mt at 1.39% Cu, 7.38% Pb, 2.85% Zn, 1.5–2 g/t Au, 55–60 g/t Ag (Unclassified)	M	Bozkaya, 2011
Koru	Canakkale	Pb, Zn plus Ag–Au	Epithermal IS	Andesite lava and pyroclastics, spherulitic rhyolite domes	Eocene	Veins, stockworks, breccias/NW-trending veins	Reserve: 0.5 Mt at 8% Pb, 2% Zn, 300 g/t Ag (Unclassified), plus past production; 9.4 Mt at 31% BaSO ₄	M	Bozkaya and Gokce, 2009
Balya	Balikesir	Pb, Zn, Cu plus Ag–Au	Skarn/CR/Epithermal	Dacite, andesite(1), limestone (2), Conglomerate, sandstone and shale (3)	Late Oligocene (1), Permian (2), Triassic (3)	Veins, replacements, disseminations	Remaining Reserve: 2.3 Mt at 8% Pb–Zn, average 1.5 g/t Au, 200 g/t Ag in concentrate; Significant past production	M	Agdemir et al., 1994;
Handeresi	Canakkale	Pb, Zn, Cu	Skarn	Schist, phyllite, metasandstone, marble (1), granodiorite (2), dacite (3)	Paleozoic (1), Oligo-Miocene (2), Oligocene (3)	NE-trending fold axis, N-trending post-mineral faults	Reserve: 3.100 Mt at 5.24% Pb, 2.05% Zn, plus Cu (Unclassified)	M	MTA, 1993b
Bagirkacdere	Canakkale	Pb, Zn, Cu	Skarn	Metasiltstone, phyllite, marble (1), Metagranodiorite (2), Granodiorite (3)	Paleozoic (1), Carboniferous (2), Miocene (3)	Disseminations, rarely massive/mineralized schistosity striking WNW, dipping NE	Reserve: 5.224 Mt at 3.8% Pb, 2.18% Zn, 0.45% Cu (Unclassified)	M	MTA, 1993b
Culfacukuru	Canakkale	Pb, Zn, Au	Skarn	Arkose (1), limestone (2), volcanic rocks (3)	Triassic (1), Upper Jurassic–Cretaceous (2), Oligocene (3)	Massive replacements/N-trending mineralized zone	Reserve: Zone I: 1.147 Mt at 1.74% Pb, 2.21% Zn, Zone II: 47.806 kt at 1.38% Pb, 1.90% Zn (Unclassified)	M	Akyol et al., 1977
Egmir	Balikesir	Fe	Lateritic Fe	Andesite porphyry, andesite tuffs and agglomerates	Upper Miocene–Pliocene	Ferricrete formation, hematite matrix talus breccia with locally stratiform, massive zones/NE-trending orebody	Remaining Reserve: 9 Mt at 53% Fe ₂ O ₃ , Total resources: 17.538 Mt at 46.5% Fe	M	Cihnioglu et al., 1994

Status: M: Mine, F: Feasibility, P: Prospect.



EXPLANATION

Deposits or Prospects

- Epithermal HS
- Epithermal IS
- Epithermal LS
- Epithermal/Style not known

Fig. 9. Distribution of the epithermal deposits and prospects in the Biga Peninsula with emphasis on host-rock lithology, lithological explanation same as Fig. 5.

chalcedonic quartz, and advanced-argillic/argillic alteration are associated with gold mineralization. Quartz crystals in the pervasive silicic alteration zones have fine-grained interlocking jigsaw mosaic textures in thin sections (Fig. 10B). Quartz, alunite, dickite and kaolinite dominate at high levels of the epithermal system, and pyrophyllite (Fig. 10C), halloysite, illite and sericite are dominant at depth. Oxide ore extending to a depth of 100 m at Baba Zone and both oxide and sulfide ore are present at Deli Zone. Agi Dagı prospect shows Mo enrichments in oxide zone, up to 500 ppm, relative to sulfide zone, 50 ppm, indicating the transition to porphyry Au–Mo systems, especially in Baba Dagı and Ayitepe zones (Cunningham-Dunlop and Lee, 2007a).

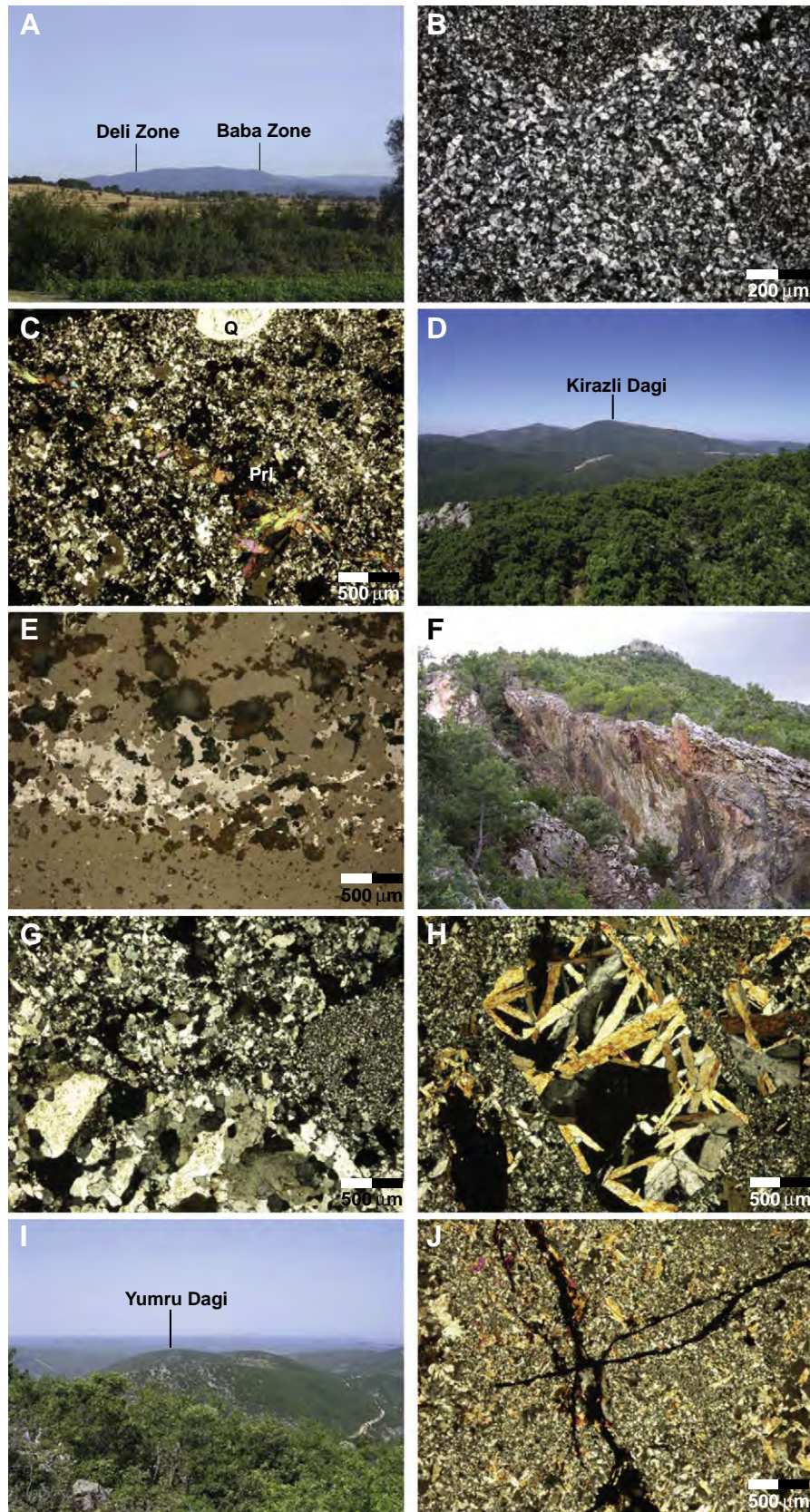
Camyurt is a newly discovered HS epithermal prospect, located approximately 4 km SE of the Agi Dagı HS system, and is hosted by felsic volcanic rocks. Approximately 1.5 km long, NE-trending discontinuous quartz vein system contains up to 70.4 m at 0.92 g/t Au including 11.7 m at 2.44 g/t Au in drill holes (Fronteer annual information form, 03.30.2008). Prospect has ongoing exploration work to test the potential of the whole vein system and promises significant resources.

Kirazlı prospect forms another prominent topographic high (Fig. 10D) in a flow-dome setting of Oligocene age in the Biga Peninsula. North-trending main orebody along Kirazlı Mountain below silica cap is approximately 1.2 km long and up to 0.35 km wide, and is intersected by ENE-trending, discontinuous ore zone in the SW, which is approximately 0.7 km long and up to 0.4 km wide, forming a reverse L-shaped orebody. Other target zones in the prospect include newly discovered Rock Pile Zone, Iri Zone, located approximately 1 km W and E of the

main zone respectively, and Kale Zone, located approximately 1.5 km S. Rock Pile Zone contains bonanza-grade gold values, up to 1080 g/t (31.50 opt) Au in rock samples. Gold–silver mineralization is hosted by andesitic and dacitic porphyritic lavas, intrusives and volcanoclastic rocks as well as tuffaceous lacustrine sedimentary rocks, which are cut by olivine phyric diabase dikes. Primary textures are largely obscured by strong hydrothermal alteration. Heterolithic and monolithic breccias of phreatic and phreatomagmatic origin, veins and disseminations are the main controls on mineralization. Gold mineralization is associated with late stage As-poor spheroidal pyrite, As-rich euhedral pyrite is usually gold poor. SEM study of mineralized samples shows clusters of sub-micron size gold grains in a rim of hematite (probably after pyrite) along the edge of a vugg in quartz (Keane et al., 2010). At least 4 stages of silicification have been differentiated in the prospect, which include widespread silicification with vuggy residual quartz (I), flat-lying chalcedonic quartz (forming aquitard) (II), gray quartz veins (III) and crystalline quartz in fractures and vuggs (IV) (Cunningham-Dunlop and Lee, 2007b). Advanced argillic alteration with alunite, dickite and kaolinite and argillic alteration are ubiquitous in the prospect. Low-grade Au mineralization is at the base of phase II silicification, and high-grade Au–Ag mineralization is associated with phase III silicification; containing up to 9.10 m grading 44.01 g/t Au in drill hole KD-01 and 9.30 m grading 1213 g/t Ag in drill hole KD-97. The prospect generally contains high-grade gold mineralization in the oxide zone, and low grade in the sulfide zones. On the silicified surface outcrops gold is associated with oxide, which is mainly specular hematite and hematite (Fig. 10E).

Kartaldag with ancient and historical gold mining is speculated to be Astyra, together with the Madendag prospect, both of which were operated by Astyra Gold Mining Company during WWI. Classical HS style epithermal gold and silver mineralization is hosted by Eocene

age quartz–feldspar porphyry andesite with up to 3% quartz eyes, based on TAS plot of the whole-rock analyses of only propylitically altered host rock. The prospect contains two mineralized zones, one of which with old surface and underground workings (Fig. 10F) is a



NE-trending zone, approximately 100 m long and up to 10 m thick with a lenticular orebody dipping steeply NW. Another is an unexplored E-trending, mineralized silicified ledge, approximately 500 m long and 50 m wide. Multi-stage silicification with vuggy residual quartz and chalcedony, and advanced argillic and argillic alteration with alunite, dickite, diaspore and kaolinite are the common alteration minerals associated with gold–silver mineralization (Fig. 10G and H). Replacement, vein and breccia related mineralization contains up to 10.7 g/t Au, and 73.4 g/t Ag in a total of 11 rock-chip samples in this study. Significant amount of pyrite in gold-rich zones is related to kaolinite. The epithermal system is only partly oxidized with jarosite, goethite and hematite, in order of abundance.

Pirentepe prospect was discovered in the early 90s as a result of an exploration campaign conducted by a JV between MTA and MMAJ. The prospect had known massive chalcedonic quartz and clay zones mined for silex and kaolinite by a local Turkish mining company. HS mineralization is hosted by andesitic lava and pyroclastics intruded by quartz porphyries, and is associated with resurgent domes of Oligocene age. The E-trending mineralized and altered zone in the prospect is approximately 3.5 km long and 1 km wide. Main mineralized zones are at Davulgali Tepe in the W and Pirentepe (Celdiren) in the E. Silicification is characterized by acid leached vuggy to massive quartz, which gently dips to the north. Advanced argillic alteration with alunite and kaolinite, and argillic alteration surround the silicified zones. A total of 15 rock and rock-chip samples from the prospect in this study contain up to 2.19 g/t gold, associated with disseminated and breccia zones. Oxidized zone contains common hematite and specular hematite. Best drill results from the prospect include 46.90 m grading 1.79 g/t Au, and 38.0 m grading 1.83 g/t Au, mineralization in both drill holes starting at 17 m depth (Fronteer News Release, 11.09.2006).

Halilaga North, another prospect discovered by MTA and MMAJ JV, is the original HS prospect of Halilaga, called Halilaga North after the discovery of Halilaga porphyry Au–Cu, to avoid confusion. Epithermal Au–Ag mineralization in the prospect, hosted by andesitic lava and pyroclastic rocks, is located in two zones, main Saguluk Tepe zone, approximately 1 km long and 0.2 km wide ENE-trending zone to the NE of Halilaga village, and Taskesilen-Kocatas zone, approximately 1 km long and 0.3 km wide NNE-trending zone to the SE of Halilaga village. It has characteristic alteration assemblages of HS epithermal deposits with massive and vuggy residual quartz, advanced argillic and argillic zones. Breccias, veins, and veinlets of mineralization contain up to 2.38 g/t Au and 60 g/t Ag in rock samples.

Kuscayiri prospect, renamed as Karaayi, is located W of the TV Tower prospect and was discovered using BLEG stream sediment sampling in the early 90s. Eocene andesitic lava and flow domes, andesitic and dacitic volcanoclastic rocks and quartz–feldspar porphyry intrusive at the contact with hornblende granodiorite are the main host rocks in the prospect. The prospect consists of two E-trending mineralized and altered zones, an oxide-rich zone in the E, SE of Ardic Tepe, and a sulfide zone at Yumru Dagı (Fig. 10I) in the W. These E-trending structures open E to Kayalidag (namely TV Tower prospect). Pyrite, up to 12%, minor chalcopyrite, specular hematite, hematite, malachite, magnetite, arsenopyrite and realgar are

observed minerals. Copper-rich zones lie through the SW of Yumru Dagı. An early QSP alteration is overprinted by late advanced argillic alteration with vuggy residual quartz. Advanced argillic alteration assemblages contain mostly alunite (Fig. 10J), pyrophyllite, and kaolinite. Copper mineralization is mainly related to the early QSP event (Yilmaz, 2003). Gold–copper mineralization is associated with disseminations, stockworks (Fig. 11A) and breccias. Oxidized zone with conspicuous specular hematite and hematite stockworks (Fig. 11B and C) in the prospect is relatively shallow, average 20 m thick but locally up to 40 m. Drilling intersected up to 78 m at 0.45 g/t Au, and 250 m at 0.3 g/t Au in the sulfide zones (Yilmaz, 2003). Average copper content is 0.23% in the sulfide zone. Best results from 21 RC and 7 DDH indicate 115.5 m at 0.52 g/t Au and 87.1 m at 0.62 g/t Au (Cheser Resources News Release, 03.01.2009). Part of the TV Tower prospect is an eastern extension of the Kuscayiri prospect, and rock-saw channel sampling at Kayalidag gives over 113 m grading at 1.1 g/t Au (FronteerGold News Release, 09.02.2010). Kuscayiri prospect may form a superjacent lithocap on the antipathy system, and therefore porphyry Au–Cu mineralization is anticipated at depth.

Sarpdagı prospect, recently included in the TV Tower prospect portfolio, is composed of NE-trending mineralized and altered zone, approximately 4 km long and 3 km wide. Main zones in the prospect are located at Bakirlik Tepe, Sarp Dagı and Oren Dagı. Andesitic lava and pyroclastic rocks of Oligocene age and schists of Pre-Triassic age are the main host rocks in the prospect. Disseminated, breccia and stockwork mineralization is associated with widespread silicification with chalcedonic quartz, advanced argillic alteration with kaolinite and dickite, and argillic alteration. Massive silicification forms well-developed flat-lying quartz zones over large areas. Pyrite, specular hematite and hematite are ubiquitous. Total of 21 rock-chip samples in this study from the prospect have values up to 0.502 g/t Au, 3.15 g/t Ag, 2610 ppm Ba, and 158.5 ppm Sb.

Alankoy (Arlik Dere) was also discovered by MTA and MMAJ JV in the early 90s, though ancient surface and underground workings are present. It has classical HS epithermal signatures with well-developed alteration assemblages (Fig. 11D). Prospect has very close spatial association to a small discrete granodioritic intrusion (named as Alankoy stock) with well developed skarn zones as well as quartz stockworks. Andesitic lavas and pyroclastic rocks and granodiorite of Oligocene age, and crystalline limestone, metavolcanic and sedimentary rocks of Triassic age form the host lithologies in the prospect. Main mineralized zones of HS epithermal mineralization are located at Kocatas Tepe, Saritas Tepe and Guvemalani Tepe. NE-trending silicified zone, approximately 2 km long and 1.7 km wide, contains shallow part of the epithermal system with steam-heated zone, which is exposed at Saritas Tepe with native sulfur in vuggy residual quartz. Some of the chalcedonic quartz zones were mined as silex, i.e., Akmacakil Tepe. Prospect contains abundant specular hematite and hematite in oxidized zones (Fig. 11E). Total of 22 rock and rock-chip samples in this study have values up to 0.705 g/t Au. A garnet-rich skarn zone with gossans located approximately 1 km E of the epithermal system is developed where crystalline limestones abut Alankoy granodiorite stock. Skarn zone is up to 1 km long and 0.5 km wide. Zinc gossans contain up to 0.104 g/t Au, 1.86 g/t Ag, 146 ppm Cu,

Fig. 10. A. General view of the prominent Agı Dagı flow-dome complex forming a topographic high with location of the major resource areas, Deli and Baba Zones [from 491990E, 4429413N, looking SSE], B. Photomicrograph of pervasive silicification, quartz crystals showing jigsaw mosaic textures [sample no BPGP-1100] [XP], C. Late stage pyrophyllite (Pr1) vein, at the center of the photomicrograph, with high-order interference colors in pervasively silicified host-rock with Fe-oxides, mainly hematite, note preserved but corroded primary quartz eye (Q), Agı Dagı HS epithermal prospect [sample no BPGP-1083b] [XP], D. General view of the main zone of the Kirazlı resource area, flow dome forming erosion resistant prominent hill [from 479465E, 4432023N looking SW], E. Photomicrograph of specular hematite and hematite in saccharoidal quartz, containing 0.993 g/t Au, Kirazlı prospect [sample no BPGP-1082] [RL], F. Historical workings at Kartaldag prospect with open pit, looking SW, G. Photomicrograph of multi-phase silic alteration, at least three-phases of silicification, early fine-grained quartz, medium-grained quartz and late-stage fracture and open space fill coarse-grained quartz, local chalcedonic quartz, Kartaldag prospect [sample no BPGP-1003] [XP], H. Hypogene alunite crystals, replaced plagioclase, note well-developed ghost crystal shape, in advanced argillic alteration zone with fine-grained quartz [sample no BPGP-1007a] [XP], I. General view of the prominent topography in the Kuscayiri prospect, showing E-trending mineralized zone at Yumru Dagı [Looking W from Kayalidag Mountain], J. Disseminated and fracture-fill alunite crystals in pervasively silicified host-rock, advanced argillic alteration zone, Kuscayiri prospect [sample no BPGP-1045] [XP].

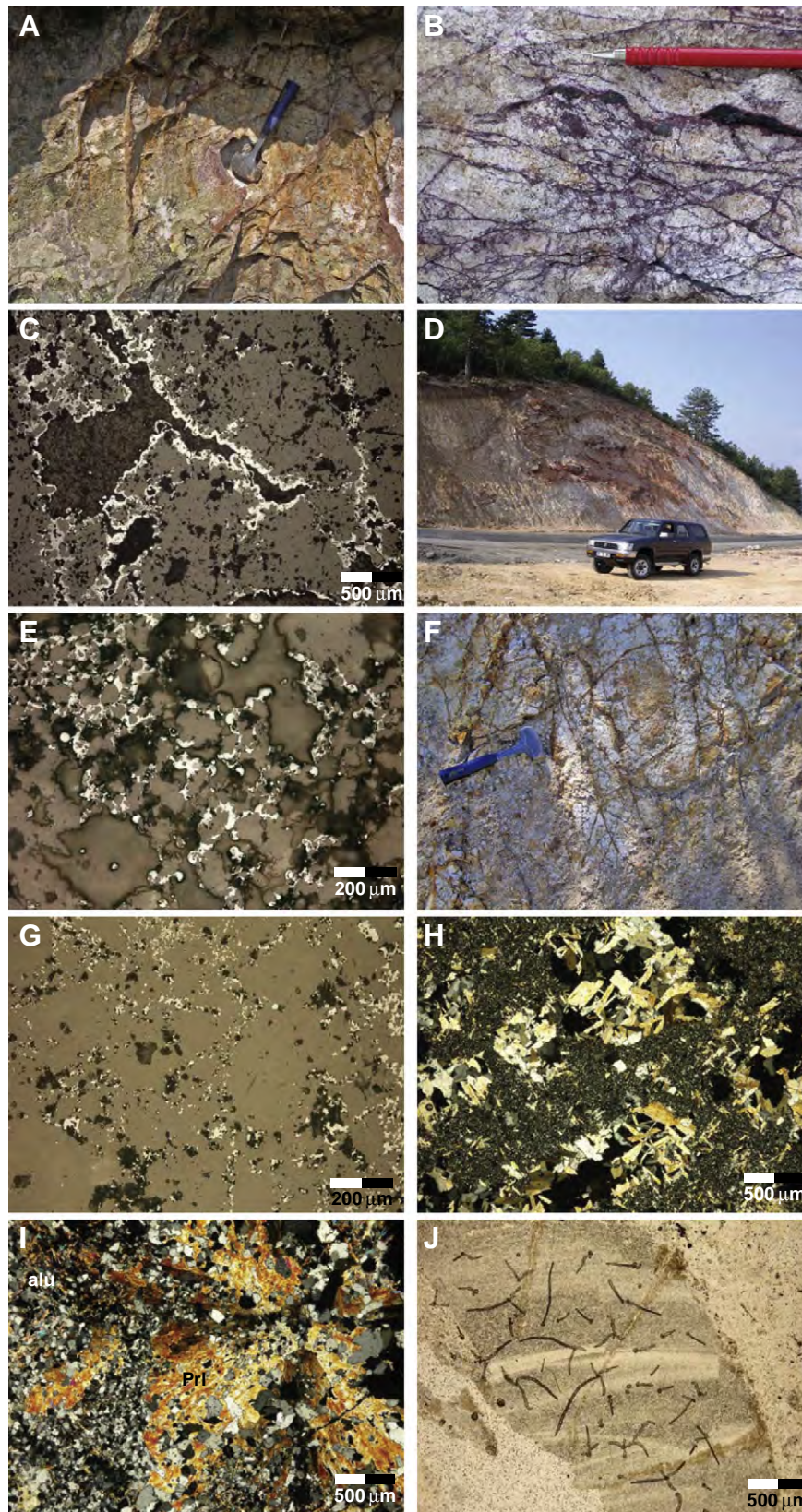


Fig. 11. A. Intense quartz stockwork veinlets with hematite, oxide zone at Kuscayiri prospect [467483E, 4424280N], B. Hematite and specular hematite bearing stockwork veinlets in feldspar-porphphy andesite showing moderate silicic and sericitic alteration [467983E, 4424144N], C. Photomicrograph of botryoidal specular hematite (light cream color), locally forming matrix or overgrown broken drusy quartz crystals, in acid-leached silicified breccia, Kuscayiri prospect [sample no BPGP-1053] [RL], D. Advanced argillic and argillic alteration zones with silic alteration, N slope of Saritas Hill, along Canakkale-Can road, Alankoy epithermal prospect, [482753E, 4431180N], E. Botryoidal specular hematite associated with vuggy silica, Alankoy prospect [sample no BPGP-1136] [XP], F. Porphyry-style quartz stockwork veinlets in QSP altered granodiorite, Alankoy prospect, G. Photomicrograph of hematite matrix mineralized breccia, containing 0.643 g/t Au and 69.8 g/t Ag, Dede Dagi prospect [sample no BPGP-1297] [RL], H. Photomicrograph of the alunite crystals replacing feldspar crystals in vuggy silica, advanced argillic alteration zone, Bodurlar prospect [sample no BPGP-1290] [XP], I. Radiating pyrophyllite crystals (PrI) and fine-grained alunite (alu) crystals, advanced argillic alteration zone, Bodurlar prospect [sample no BPGP-1296] [XP], J. Preserved sponge spicules in pervasively silicified rock, Tepekoy silex mine [sample no BPGP-1106] [PPL].

63.8 ppm In, 434 ppm Pb, 109 ppm Sb, 2590 ppm Mn, and 2480 ppm Zn. Porphyry-style stockwork zones in the Alankoy stock have anomalous gold values up to 0.236 g/t (Fig. 11F). Alankoy prospect may form a lithocap and thus a subjacent porphyry Au–Cu mineralization is anticipated at depth.

Dogancilar HS epithermal Au–Cu prospect consists of mainly veins that are related to a flow-dome complex of Oligocene age, forming a prominent hill called Karadag. All of the known mineralized zones are clustered around the rim of this flow dome, which are Bakirlik Tepe and Kucukbakirlik Tepe 2.5 km S, Magara Tepe 2 km NNE and Tombek Tepe 2.7 km NW, relative to flow-dome structure. Andesitic and dacitic pyroclastic rocks including lithic lapilli tuff, and pumice breccia are the main host rocks in the prospect. Gold mineralization is closely associated with Cu and barite in the Bakirlik vein and stockworks (Pirajno, 1995). Veins, stockworks, and breccias are associated with silicified zones, locally including flat-lying chaledonic quartz, and advanced argillic and argillic alteration including kaolinite, dickite and pyrophyllite. E-trending veins at Bakirlik Tepe, Kucukbakirlik Tepe and Tombek Tepe and ESE-trending veins at Magara Tepe control Au–Cu mineralization. Silicified zones are mined as silex in the E of Karadag. Oxidized zones in the prospect form gossan. Specular hematite and barite are abundant locally. A total of 11 rock-chip samples from the prospect in this study give values up to 4.8 g/t Au, 2630 ppm Ba, 231 ppm Cu, 474 ppm Pb, and 1665 ppm Zn.

Dede Dagi prospect has the typical signature of a HS epithermal system. Reconnaissance sampling of NE-trending silicified ledges with residual vuggy quartz and opaline quartz in the feldspar porphyry andesite host gives values up to 0.643 g/t Au, 92.8 g/t Ag, 706 ppm As, 1560 ppm Ba, 96.2 ppm Bi, 172 ppm Cu, 37.4 ppm Mo, 2470 ppm Pb, 137.5 Sb, and 153 ppm Zn in rock-chip samples. Oxidation zones with mineralized breccia contain common specular hematite with iron-oxides (Fig. 11G). Prospect is associated with Dede Dagi flow-dome complex.

Bodurlar prospect, located a couple km SE of the Dede Dagi prospect, has a well-developed, large, HS epithermal alteration system. Unlike most of the other HS systems, remnants of the shallow-level features of the epithermal system have been preserved, e.g., native sulfur in vuggy residual quartz. Lithic lapilli tuff, fine-grained tuff, and andesite porphyry, intruded by unaltered basaltic dikes, are the main host rocks in the prospect. Prospect has well developed alunite and pyrophyllite crystals in the advanced argillic alteration zones, the latter can reach up to cm in size (Fig. 11H and I). Common specular hematite is conspicuous in the prospect. Reconnaissance rock-chip sampling [15 samples] of the silicified ledges trending NE in the prospect contains up to 0.225 g/t Au, 1.24 g/t Ag, 830 ppm As, 3340 ppm Ba and 42.9 ppm Mo values. The prospect has a typical flow-dome setting.

Hamam Tepe and Seyrat Tepe HS prospects with pronounced E-trending mineralized and altered zones are related to resurgent domes. Massive chaledonic quartz zones are mined as silex in some of the prospects. Caltikara is the other industrial mineral prospect with HS epithermal gold potential. Resurgent domes in Caltikara are associated with HS style alteration. Massive chaledonic quartz zones are mined for silex in Tepekoy mine at Hamam Tepe prospect, and kaolinite is mined for industrial clay, as in some of the other epithermal prospects. At Tepekoy silex mine chaledonic silica zones have preserved micro fossils, sponge spicules (Fig. 11J).

Other potential HS epithermal prospects include Karincali, Dedeler with active silex mine, in the central Biga Peninsula. Sapdag district with several prospects and Kinik with known Sb workings are the examples of HS epithermal prospects in SE Biga Peninsula. In the western Biga Peninsula, HS prospects include Bergas and Kiziltepe. Bergas prospect with ancient and historical base-metal workings was reported as skarn (Gumus, 1970). However, large silicified zones with vuggy residual quartz as well as advanced argillic alteration zones with alunite and kaolinite promises epithermal gold–silver mineralization. Feldspar porphyry andesite and andesitic lithic lapilli tuff are the main host-

rocks in the prospect. Approximately 1.8 km long and 0.5 km wide, NE-trending mineralized and altered zone contains up to 0.182 g/t Au, 0.38 g/t Ag, 2060 ppm As, 3280 ppm Ba, 118.5 ppm Cu, 70.5 ppm Mo, and 732 ppm Pb values in 11 rock-chip samples in this study. Prospect may have subjacent porphyry Au–Cu–Mo mineralization. Disseminated and breccia controlled mineralized zones contain common iron-oxides with specular hematite. Kiziltepe epithermal/porphyry prospect whole-rock samples in this study from skarn zones of Kestanol Pluton have up to 384 ppm U values.

4.2.2. LS deposits and prospects

Biga Peninsula has classical low-sulfidation systems, though limited numbers of deposits and prospects are scattered throughout the peninsula (Fig. 7). The discrete Kucukdere gold–silver deposit with bonanza grade ore in the SE Biga Peninsula is the only modern mine of this style. Some of the LS deposits and prospects are developed alongside and/or spatially associated with HS epithermal deposits, as in Madendag, and Akbaba. Madendag and Akbaba have close spatial association to Kartaldag HS system. This spatial association is not unusual, but it is less common. Kestanelik and Elmali prospects are examples of LS systems, located in the northern and northeastern Biga Peninsula respectively.

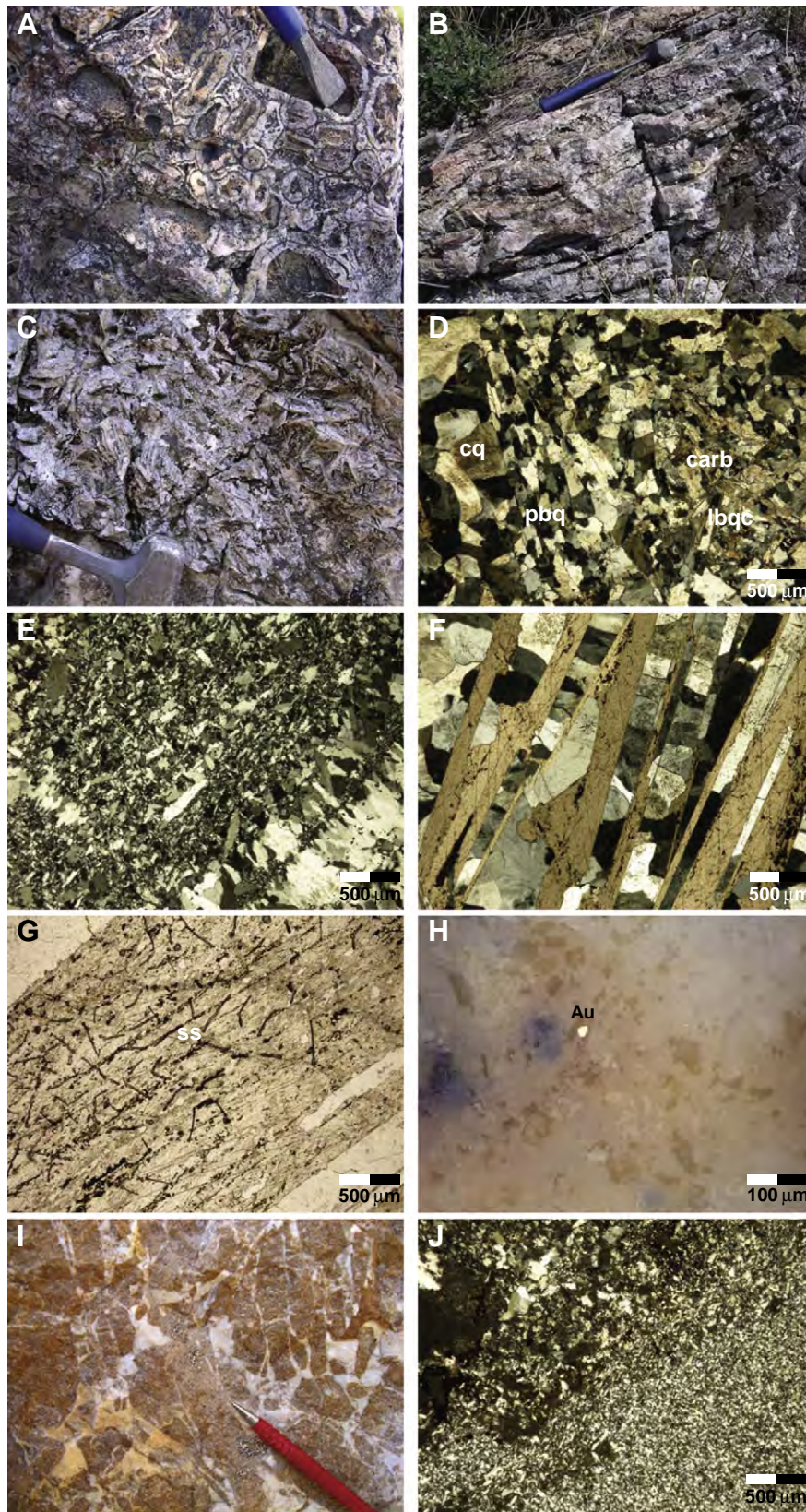
Kucukdere deposit, the classical LS system after Ovacik in Turkey, is hosted by feldspar-porphyry andesite of Miocene age. Discontinuous banded-quartz–carbonate vein system in Karayarik and Germe Tepe form a major NE-trending, 2 km long and up to 30 m thick zone dipping 60 to 90° SE. Related shallowly dipping (up to 30°) splay veins, up to 20 m thick, are located SE of this major vein system (Colakoglu, 2000). These splay veins may be precipitated from ore-forming fluids ascending along the high-angle feeders and bleeding out. Veins consist of common breccia, cockade, banded, and bladed quartz after calcite textures (Fig. 12A–F), and have Fe- and Mn-oxide rich zones. Silicification with chaledonic quartz, carbonate alteration with ankerite, and argillic alteration with kaolinite and illite occur associated with gold–silver mineralization. Preserved micro fossils, sponge spicules, have been observed on bladed quartz–calcite (Fig. 12G). A total of 12 rock-chip samples from the prospect in this study give up to 122 g/t Au, 121 g/t Ag, 150 ppm Ba, 446 ppm Cu, 2.9% Mn, 1270 ppm Pb, and 725 ppm Zn values. Microscopic gold has been observed in high-grade samples (Fig. 12H). Kucukdere Au–Ag deposit (ore shipped to Ovacik processing plant) open pit was mostly mined out between 2006 and 2009. A small discrete orebody called Coraklik Tepe, located a couple of kilometers SW, with 45 koz reserves is planned to be in production by 2013.

Kisacik (Baharlar) with 1 Moz gold resources is the largest LS epithermal deposit with calculated resources in the Biga Peninsula, though the resource is not compliant to international reporting codes. The prospect was discovered by MTA in early 2000s, but contains ancient mine workings. Lithic lapilli tuff with local ignimbrites and quartz–feldspar porphyries of Upper Miocene age are the main host rocks in the prospect. NE-trending mineralized and altered zone containing en-echelon NW-trending structures is approximately 1.5 km long and 0.5 km wide, and contains 4 to 5 mineralized zones. Multi-phase breccias, discontinuous stockwork quartz veinlets, beige opaline quartz occurring as veinlets and/or matrix in breccia (Fig. 12H and I), and fine-grained sulfides, mainly pyrite and marcasite, are closely associated with gold mineralization. Up to 14 ppm Au in soil, up to 3 ppm Au and 1 ppm Ag in rock samples have been reported from the prospect (Kilic et al., 2004). Drill cores contain up to 65 g/t Au. A total of 11 rock-chip samples from this study give values of up to 0.707 g/t Au.

Akbaba, also known as Madendag, Au–Ag mineralization occurs at the unconformity contact between Pre-Triassic schists and andesite porphyry. A NE-trending silicified ledge with white, cream to gray chaledonic quartz has mineralization in mostly massive breccia zones. Partly oxidized zones contain abundant disseminated pyrite locally. Gold–silver mineralization is concealed in the prospect due

to young volcanic cover rocks. Therefore, potential of finding hidden orebodies in the prospect is likely. Akbaba lacks banded-quartz-carbonate veins, unlike other LS epithermal systems. Up to 9.53 g/t Au and 6.23 g/t Ag values in rock-chip samples have been detected from a total of 8 samples in this study.

Madendag, located approximately 1.5 km S of Akbaba, is an ancient and historical mine, and is hosted by Pre-Triassic mica schists. Although porphyry andesites of probable Lower Miocene age are exposed in the prospect, they are post-mineral subvolcanic intrusives. No genetically related magmatic rocks crop out in the prospect. The



prospect consists of two mineralized zones, main zone with old workings containing 5 quartz veins, and unexplored Kaletas (Meydan) Tepe zone in the SW. Main gold mineralization is related to 110-striking vein dipping steeply SW with breccias (No:1 Vein; Higgs, 1962). ESE- and SSE-trending, locally banded and lenticular veins contain breccia and stockwork zones. Two vein sets at Kaletas, 145- and 110-striking and steeply dipping, occur as concordant and discordant to schistosity. Vein sets consist of milky and vitreous quartz with local breccias. No up to date resource data on the prospect, but historical data indicates a small orebody with 15 kt at 5.8 g/t Au (Higgs, 1962). Up to 11.1 g/t Au and 10.55 g/t Ag values were obtained in rock-chip samples in this study, total of 12 samples. There is extensive old surface and underground workings in the prospect, 2 adits totaling 900 m, 4 shafts and inclines totaling 400 m (Molly, 1961).

Emali prospect consists of NW-trending major quartz-veins intersected by a series of N-trending quartz veins, which are hosted by lapilli tuffs of Middle Miocene and limestones of Permian age at the contact with Paleozoic age schists. NW-trending zone of mineralization with anomalous Au (> 1 ppm in rock and > 10 ppb in soil) extends discontinuously for 3 km. LS quartz veins with chalcedonic quartz as well as local bladed quartz after calcite and brecciation have Au and Ag values up to 20 g/t and 25.8 g/t respectively in rock samples. Total of 4 core holes totaling 300.8 m were drilled in the prospect, of which best interception is 6.1 m at 6 g/t Au including a subinterval of 2.6 m at 13.2 g/t Au (Eurasian Minerals News Release, 02.17.2009).

Kestanelik LS epithermal prospect with ongoing exploration, a part of the Sahinli prospect, is located in the northern Biga Peninsula, and is hosted by volcanic and sedimentary rocks of probably Eocene age, and Paleozoic schists. NE- and E-trending vein system mainly at Kara Tepe and Kovanlik Tepe is exposed over an aggregate strike length of approximately 2.5 km. Major mineralized quartz veins with up to 15 m thickness include K3 with over 520 m strike length, K2 with over 100 m strike length, K1 with over 235 m strike length, and Karakovan-W. Mineralized zones contain bonanza grade gold values, especially in oxidized zones, for example up to 4.5 m at 31.48 g/t Au in rock-chip channel samples in K3 vein. However, most of the high-grade mineralization is limited to shallow level (extending to a depth of more than 50 m) oxidized zone, and therefore, could be nugget effect, which is more the norm than the exception throughout the upper parts of vein systems. There is a sharp decrease in the ore-grade after this depth. Best interception in the drill holes is 6 m at 15.44 g/t Au (Chesser News Release, 03.23.2010). A new zone called Meydan with bonanza-grade gold mineralization on the surface outcrops contains up to 419 g/t [12.2 opt] Au.

Adatepe prospect in the northern Biga Peninsula, one of the prospects generated during the course of this project, is hosted by lithic lapilli tuff with metamorphic quartz and schist clasts and ignimbritic andesite porphyry of Eocene, and schists of Paleozoic age. Prospect has a N-trending, main mineralized zone, bending NNW, approximately 0.6 km long and 0.2 km wide, forming a prominent ridge. Silicification with chalcedonic and opaline quartz surrounded by argillic alteration is closely associated with mineralization. Veins with polymict breccia zones have gold mineralization up to 1.26 g/t Au with anomalous As and Ba in rock-chip samples, 1860 ppm As and 340 ppm Ba respectively, total of 6 rock-chip samples.

4.2.3. IS deposits and prospects

Most of the known IS deposits and prospects, such as Sahinli, Tesbihdere and Koru, are associated with Eocene volcanic rocks in the northern Biga Peninsula, and a deposit, Arapucandere, is located in the eastern Biga Peninsula (Fig. 7). Some of the IS style epithermal deposits and prospects in the Biga Peninsula, as well as in Turkey, are not well recognized and characterized, and therefore are included in the epithermal clan.

Koru Pb–Zn–Ag–Au mine, started production in 1959, is associated with andesitic lava and pyroclastic rocks and spherulitic rhyolite domes of probably Eocene age. The deposit consists of a main orebody with two different producing zones called Eskikisla and Tahtalikuyu with many small mineralized zones. NW-trending veins dipping moderately SW (50–210, dip and dip direction), up to 5 m thick and 200 m long with at least 80 m downdip extension. These veins form a WNW-trending zone, and are cut and offset by NE-trending faults. Veins, stockworks, breccias and fracture-controlled orebody consists of mainly sphalerite, galena, pyrite and chalcocopyrite with accompanying quartz, barite and calcite gangue, barite rich zones can be potentially economical, e.g., 9.4 Mt at 31% BaSO₄. Up to 3.2 ppm gold-bearing zones associated with quartz-adularia were reported. Fluid inclusion studies from limited samples of Tahtalikuyu and Eskikisla orebodies show that primary inclusions in sphalerite have salinities ranging from 2.07 to 9.99 wt.% NaCl equivalent with homogenization temperatures ranging from 120 to 160 °C. Primary inclusions in barite have salinities ranging from 6.02 to 11.09 wt.% NaCl equivalent with homogenization temperatures up to 80 °C (Bozkaya and Gokce, 2001). Secondary fluid inclusions in barite have homogenization temperatures of up to 270 °C. Sulfur isotope studies (Bozkaya and Gokce, 2009) on limited samples (n = 6) from mainly vein ore from Tahtalikuyu and Eskikisla with one sample from stockwork zone indicate $\delta^{34}\text{S}$ values ranging from –4.0 to –0.1‰ in sphalerite and galena and 14.9 to 17.3‰ in barite, indicating different source for sulfur in sulfide and sulfate minerals, magmatic and sedimentary or Cenozoic sea water respectively. Lead-isotope compositions (²⁰⁶Pb/²⁰⁴Pb, ²⁰⁷Pb/²⁰⁴Pb and ²⁰⁸Pb/²⁰⁴Pb) of galena give model ages ranging from 70 to 1 Ma for the reservoir, compatible with the age of Cenozoic magmatic activity. The geochemical studies mentioned above failed to classify the Koru deposit genetically.

Sahinli precious and base metal system is hosted by andesitic and dacitic volcanic rocks including ignimbrites, basaltic volcanic rocks of probably Eocene age, which are intruded by andesite porphyry and rhyolitic lava domes and basaltic dikes. Approximately 3.4 km long NE-trending discontinuous vein zone with mainly NE-trending lenticular veins, dipping 50–80° SW, though some of the veins strike E and N. Quartz veins containing stockwork and breccia zones are up to 900 m long and 10 m thick with average thickness of 3 m, and have approximately 250 m down-dip extension (Yilmaz et al., 2010). Silicification and argillic alteration with illite/muscovite, mixed-layer illite/smectite are associated with base- and precious-metal mineralization. Barren probably post-ore advanced argillic alteration with alunite, dickite/nacrite and pyrophyllite is also present. Pyrite, galena, Fe-poor sphalerite with minor chalcocopyrite, Sb–Ag–tetrahedrite, and electrum are the main ore minerals with quartz, chalcedony and barite gangue. Supergene minerals include digenite, chalcocite, covellite,

Fig. 12. A. Cockade textures with central altered feldspar-porphyry andesite clasts and milky quartz matrix, Kucukdere LS epithermal gold deposit [507844E, 4375312N], B. Banded quartz-carbonate vein splays, dips much shallower compared to main vein system, Kucukdere gold deposit [507661E, 4374787N], C. Lattice-bladed pseudo-quartz crystals after calcite, Kucukdere gold deposit [508036E, 4375280N], D. Parallel bladed quartz (pbq) and lattice-bladed quartz (lbq) after calcite, note locally preserved carbonate minerals (carb), plumose texture chalcedonic quartz (cq), Kucukdere gold deposit [Sample no BPGP-1199] [XP], E. Reticulated quartz and late stage syntaxial quartz veinlets, Kucukdere gold deposit [BPGP-1200] [XP], F. Parallel-bladed chalcedonic quartz after calcite, and carbonate, Kucukdere gold deposit [Sample no BPGP-1209] [XP], G. Preserved micro fossils, sponge spicules (ss), in parallel-bladed quartz-carbonate, Kucukdere gold deposit, same sample as F [PPL], H. Gold grain in banded quartz-carbonate veins, high-grade gold sample location containing 122 g/t Au and 121 g/t Ag, Kucukdere gold deposit [sample no BPGP-1208] [RL], I. Beige color opaline silica injected (matrix), mineralized crackle breccia with Fe-oxides, mainly goethite, containing 0.517 g/t Au, Kisacik epithermal prospect [460047E, 4390753N], J. Late-stage quartz veinlet with reticulated texture in silicified tuff, note alignment of quartz crystals along the selvage of the veinlet, Kisacik epithermal prospect [sample no BPGP-1225] [XP]. (For interpretation of the references to color in this figure legend, the reader is referred to the web version of this article.)

and cerussite. In the prospect there is an unambiguous Au–quartz and Ag–base-metal (galena) association. Additional placer gold mineralization in Miocene–Pliocene conglomerates, agglomerates and tuffs as well as Plio–Quaternary terraces are reported from the prospect (Yildirim and Cengiz, 2004). Though the prospect is claimed to have multiple million ounces of unclassified gold resources, real gold reserve and/or resource estimate is unavailable for the prospect. Mean homogenization temperatures in fluid inclusions from main stage quartz at Sahinli vary from 241 to 280 °C, mainly concentrated between 250 and 300 °C, and salinity values are between 4.3 and 6.9 wt.% NaCl equivalent. Fluid inclusion and isotope studies ($\delta^{18}\text{O}$, $\delta^{34}\text{S}$ and δD) of the ore forming fluids indicate that two fluids mixing, meteoric and subordinate magmatic, are the main mechanism for metal precipitation, with no supportive evidence for boiling in the system (Yilmaz et al., 2010).

Tespirdere deposit, another example of the IS style–epithermal deposit, is located SE of the Koru mine. The relatively higher average homogenization temperatures (295 °C) in fluid inclusions measured at the Tespirdere deposit, may indicate a relatively deeper part of the epithermal system (Yilmaz et al., 2010).

Arapucandere (Kor Maden) underground Pb–Zn–Cu–Ag–Au mine, intermittent production since 1972, is hosted by metasandstone and metadiabase dikes and sills of Permian to Triassic age, near dacitic and granitic rocks of Oligocene and Miocene age respectively. In the Arapucandere mine there are a total of 5 major economical veins, namely Veins I to V, from NW to SE. Structurally controlled veins strike E and NE. However, E-striking veins are more economical, such as Veins IV and V, dipping 50° S, 2 m thick and 400 m long and 1.5 m thick and 110 m long respectively. Other important veins are located approximately 1.25 km SE of Arapucandere mine, Somas Maden area. Galena, sphalerite, chalcopyrite and pyrite with quartz, calcite and barite gangue are the main mineral assemblages in the veins with minor amounts of marcasite, covellite, and specular hematite. Silicification, sericitization and argillic alteration with local halloysite is closely associated with veins. Development of tremolite–actinolite, epidote and chlorite in metadiabase in some areas, such as Vein V, may indicate skarnified host-rocks. Geochemical analyses of 3 samples in this study from Vein V give values up to 10.5% Cu, 9.66% Pb, 7.47% Zn, 558 g/t Ag, 1.160 g/t Au, 2340 ppm Bi, 354 ppm Cd, 335 ppm Co, 374 ppm Mn, and 215 ppm W. Two-phase, liquid–vapor inclusions from main-stage sphalerite and quartz give an average 295 °C (ranging from 229 to 384 °C) and 303 °C (ranging from 242 to 438 °C) respectively with inferred salinity values ranging from 1.8 to 18.5 wt.% NaCl equivalent (Orgun et al., 2005). A later study (Bozkaya et al., 2008) with direct salinity measurements from samples indicated that primary fluid inclusions in sphalerite range from 14.0 to 34.0 wt.% NaCl equivalent with average value of 25.3% in 85 measurements, and primary inclusions in quartz range from 13.6 to 25.5 wt.% NaCl equivalent with average value of 22.7 wt.% NaCl equivalent in 57 measurements, which is slightly lower than mineralizing fluids. The same study indicated homogenization temperatures, without pressure correction, of 276.3 to 319.7 °C with 301.4 °C average value ($n=11$) in primary inclusions in sphalerite, 150.2 to 306.7 °C with 240.2 °C average value ($n=21$) in primary inclusions in quartz, and 206.1 to 321.9 °C with average value of 263.6 °C ($n=19$) in primary inclusions in calcite. Sulfur isotope studies from galena and pyrite in a total of 13 samples with 13 measurements give $\delta^{34}\text{S}$ values ranging from -5.2 to -1.2‰ , with average values of -3.95 and -2.24‰ respectively, and suggest a magmatic source (Orgun et al., 2005). A recent study (Bozkaya, 2011) with a total of 20 measurements from 12 samples gives similar sulfur isotope values with a wider range for galena, sphalerite and chalcopyrite from mainly Veins IV and V, ranging from -5.94 to -0.86‰ with average values of -3.86 , -4.22 and -2.56‰ respectively. Lead-isotope compositions ($^{206}\text{Pb}/^{204}\text{Pb}$, $^{207}\text{Pb}/^{204}\text{Pb}$ and $^{208}\text{Pb}/^{204}\text{Pb}$) of galena from the same veins in the same study give model ages of 114 to 63 Ma, which may indicate lead derivation from Triassic host rocks. The $\delta^{18}\text{O}$ from quartz crystal and δD from fluid inclusions, ranging

from 2.3 to 4.9‰ and -90 to -55 respectively, indicate that mineralizing fluids were slightly modified meteoric water (Bozkaya et al., 2008). None of the geochemical studies mentioned above classified the Arapucandere deposit genetically.

5. Other deposit types

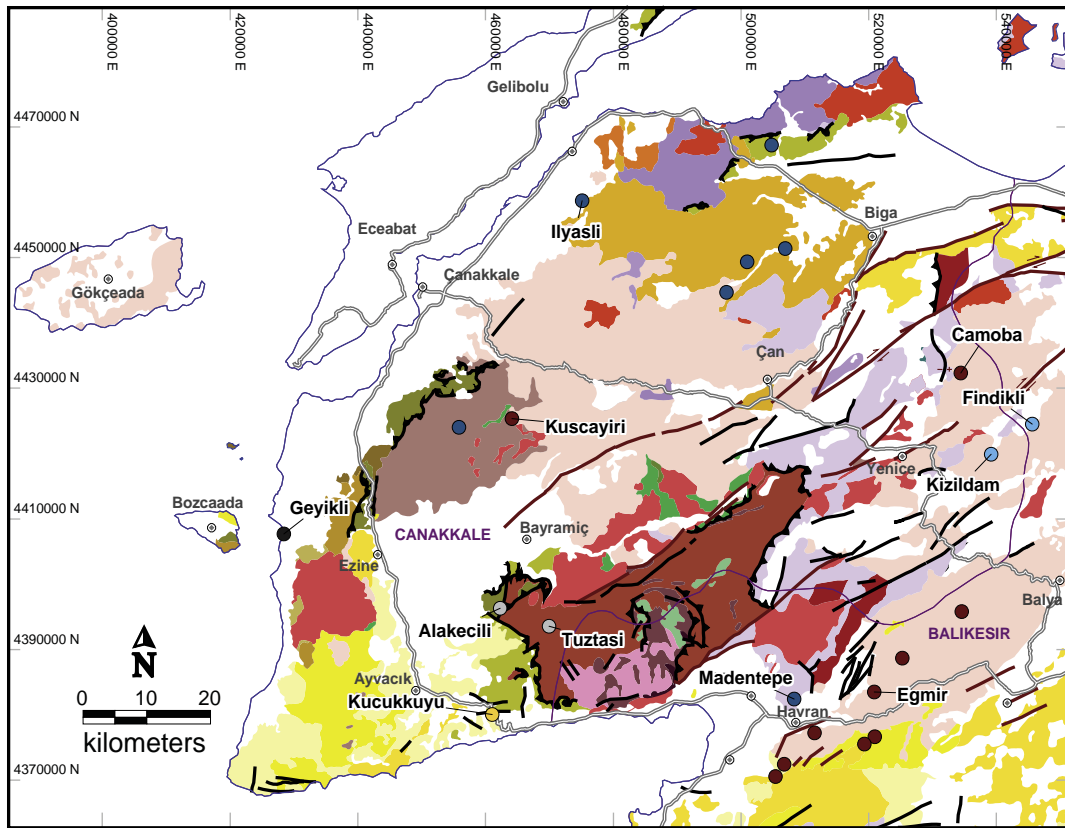
5.1. Distal-disseminated Au–Ag deposits

Carbonate-rock hosted Kizildam and Findikli Au–Ag prospects, with many affinities to Carlin-type gold deposits, in the eastern Biga Peninsula (Fig. 13) can be classified as sedimentary-rock hosted distal disseminated Au–Ag deposits. Antimony Au–Ag mineralization at Kizildam occurs at the contact between limestones, containing slump breccias, and andesitic porphyry, Upper Jurassic to Lower Cretaceous and Oligocene age respectively. A nearby granitic intrusion is located approximately 1.6 km NW. Prospect is long-time known for old Sb workings (Yuce, 1978), but Au–Ag potential has only been considered recently. NE-trending mineralized zone with an E-trending vein is approximately 1.5 km long, containing reported Sb showings in 4 different areas. Veins, veinlets and breccias, containing locally banded and drusy quartz and cockade texture, contain stibnite and arsenian? pyrite. Silicification, characterized by jasperoid formation, decalcification and argillic alteration are closely associated with Au–Ag–As–Sb mineralization. Argillically altered zones with fine-grained disseminated arsenian? pyrite contain gold mineralization up to 1.8 g/t Au and 1.24 g/t Ag. A total of 9 rock-chip samples taken from the prospect in this study give values up to 4.25 g/t Au, 4.52 g/t Ag, 9190 ppm As, 170 ppm Ba, 30.9 ppm Mo, 123 ppm Sb, and 11.15 ppm Te. Gold is probably associated with fine-grained disseminated arsenian? pyrite. Findikli, located to the NE, is another sedimentary-rock hosted gold prospect, similar to Kizildam. Findikli also contains anomalous Mo values up to 46.1 ppm.

5.2. Orogenic Au deposits

Biga Peninsula contains examples of two subcategories of the orogenic gold deposits in Turkey; mesothermal and listwanite-hosted. Mesothermal gold deposits and prospects in Turkey are mainly associated with pre-Mesozoic massifs, especially the Mendere Massif containing many prospects with small discontinuous quartz veins. Listwanite-hosted deposits are hosted by ophiolitic ultramafic rocks, mainly serpentinites, and are related to thrust faults, normal faults, and shear zones. These structures are favorable loci for high-fluid flow, and related mineralization accompanied with silica-carbonate alteration (listwanitization) and typically postdates the serpentinization process (Yigit, 2006, 2009). Tuztasi prospect, hosted by metamorphic rocks of the Kazdag Massif, and Alakecili hosted by listwanitized ophiolitic rocks could be examples of these subcategories respectively (Fig. 13).

Tuztasi Au–Ag prospect is located at the NE end of approximately 8 km long NE-trending shear-zone of Au–quartz veins, and consists of 3 major NE-trending veins dipping 20 to 40° NW, 6 to 12 m thick and up to 1.2 km long. Gold–silver mineralization is hosted by Paleozoic gneiss and schist of Kazdag Massif and is closely associated with silicic and argillic alteration. Mineralized veins with drusy to saccharoidal quartz and breccias with cockade textures contain Au–Ag mineralization associated with pyrite and arsenopyrite. The prospect contains >1600 ppb Au in soil samples (Yilmaz, 2007). Total of 8 rock-chip samples from the prospect in this study show up to 2.68 g/t Au, 145 g/t Ag, $>10,000$ ppm As, and 176 ppm Sb values. Though the prospect is classified as epithermal based on mainly silica textures, it is deduced that orogenic gold mineralization in the prospect could be remobilized during the Latest Oligocene Kazdag metamorphic core complex formation, causing epithermal signatures. Listwanite hosted gold at Alakecili is associated with ophiolitic ultramafic rocks



EXPLANATION

Deposits or Prospects

- Lateritic Fe [Ferricrete]
- Volcanogenic Mn
- Distal-Disseminated Au
- Orogenic Au
- Volcanogenic U
- Placer U-Th

Fig. 13. Distribution of the other deposits and prospects in the Biga Peninsula with emphasis on host-rock lithology, lithological explanation same as Figs. 3 and 5.

of Upper Cretaceous age. Anomalous Au–Ag as well as Co–Ni–Cr values are present in the silicified and listwanitized ultramafic rocks.

5.3. Volcanogenic Mn deposits

Most of the volcanogenic Mn deposits and prospects are related to mainly Eocene volcanic activity in the northern Biga Peninsula (Fig. 13). Most of them contain small resources (<0.1 Mt ore regardless of grade) and some of them were worked during, before and after WWI, i.e., Ilyasli and Medentepe (Temasalik). There is no recent mining activity in any of the prospects.

5.4. Volcanogenic U deposits

Kucukkuyu is the only known volcanogenic uranium mineralization in the Biga Peninsula, and is hosted by tuffs and tuffites of Middle-Upper Miocene Arikli Member of the Kucukkuyu Formation (Figs. 2 and 13). Uranium mineralization is associated with the phosphate mineral dahllite. Total of 250 t of U_3O_8 was defined in the prospect in the 1970s with average grade of 0.08% U_3O_8 or 0.8% U_3O_8 (depending on the data source), no recent work has been done in the prospect.

5.5. Lateritic Fe deposits

Iron deposits and prospects in the Biga Peninsula, spatially related to Miocene andesitic subaerial volcanic rocks, are reported as sedimentary exhalative (SEDEX) or volcanogenic sedimentary (Cihnioglu et al., 1994), or transported laterite deposits (Gumus, 1999). However, the majority of these should be properly classified more accurately as ferricrete formations. Lateritic deposits are mainly residual or in-situ formations by definition, unlike ferricrete formations which mainly contain somewhat transported clasts and Fe-oxide cement materials (relatively short distance). These unique economical iron deposits of epicontinental setting are common in the Biga Peninsula (Fig. 13), and are mostly associated with talus breccias as in Kuzcayiri, or small fault-controlled basins over the altered or unaltered Miocene volcanic rocks as in Egmir deposits. Some of the deposits contain siliceous sinters along the faults, but they are thought not to be related to iron deposition. Egmir and Kuzcayiri deposits are the typical examples of this type.

Egmir open pit deposits, consisting of Buyukegmir and Kucukegmir orebodies, lie over the altered andesite porphyry, andesite tuffs and agglomerates of Upper Miocene to Pliocene age. The district was discovered in 1951 and there has been intermittent production since 1953. NE-trending orebody in Buyukegmir deposit is 1.4 km long, 60–300 m wide and average 18 m thick, up to 45 m. The deposit

contains hematite matrix volcanic clast breccias with local stratiform and massive hematite with minor amounts of pyrite, traces of rutile and barite. A layer of kaolinite is formed at the base of the orebody, and silicic alteration in the volcanic rocks is probably not related to iron deposition. The deposits contain hematitized fossil plants. Buyukegmir ore has high As content and Kucukegmir orebody, located 400 m S of Buyukegmir, is mined out.

Kuscayiri [0.369 Mt at 39.62% Fe and 39.69% SiO₂] is another ferricrete formation with andesite porphyry clasts and andesitic agglomerates cemented by hematite and goethite. NW-trending discontinuous orebody with past production is stratiform and approximately 1 km long. Hematite–goethite matrix talus breccia is most probably associated with extension-related regional uplifting during Upper Miocene to Pliocene. Due to low grades and high SiO₂ content, there is no current production. Camoba [0.202 Mt ore grading 52.17% Fe and 12.86% SiO₂] is another example of this type of deposit. Past production came from 3 open pits in the mine.

5.6. Placer deposits

Beach sands of Holocene age in the Geyikli prospect host the only known placer in the Biga Peninsula (Fig. 13), and contain U and Th with high-radiation values. Heavy mineral concentrates in the beach sands, ranging 7 to 50%, have non-magnetic minerals like uranothorianite (containing 25% UO₂), thorianite, uraninite, titanite, zircon, apatite, corundum, anatase and thorite (Andac, 1971; Andac and Mucke, 1975). Source for the radioactive minerals is most probably the Kestanbol Pluton to the east.

6. Mineral reserves and resources

Gold, Ag, Pb, Zn, Fe and Sb are the preeminent metals in most of the producing metal mines in the Biga Peninsula (Table 1) excepting historical Cu, U, Mn and Mo production. Table 1 shows geological characteristics and reserve and/or resource data for significant deposits and prospects with more than 0.2 Moz gold or >0.5 Mt ore regardless of grade. Majority of current exploration and development efforts are concentrated on the Au (Ag) and Cu deposits and prospects as well as Pb–Zn (Au–Ag).

Total gold endowment of the Biga Peninsula is 9.18 Moz gold [284.2 t] contained in twelve different deposits and prospects including unclassified resources as well as by-product gold. Six of which, Halilaga, Agi Dagı, Kirazlı, Sahinli, Kisacik, and Akbaba are epithermal and porphyry type gold deposits and contain significant gold [>0.3 Moz or 10 t] resources (Table 1).

7. Geochronology

7.1. Ar/Ar dating method

Radiometric dating of selected samples of mineralization, alteration and host-rock were carried out in Actlabs in Canada, using the following techniques. The samples wrapped in Al foil were loaded

in an evacuated and sealed quartz vial with K and Ca salts and packets of LP-6 biotite interspersed with the samples to be used as a flux monitor. The sample was irradiated in the nuclear reactor for 48 h. The flux monitors were placed between every two samples, thereby allowing precise determination of the flux gradients within the tube. After the flux monitors were run, J values were then calculated for each sample, using the measured flux gradient. LP-6 biotite has an assumed age of 128.1 Ma. The neutron gradient did not exceed 0.5% on sample size. The Ar isotope composition was measured in a Micro-mass 5400 static mass spectrometer. 1200 °C blank of ⁴⁰Ar did not exceed $n \cdot 10^{-10} \text{ cm}^3 \text{ STP}$ (Standard Temperature and Pressure).

7.2. Age of magmatism, mineralization and alteration

Though many radiometric age dates (mainly K/Ar and some Ar/Ar) are available for the magmatic rocks of the Biga Peninsula (Fig. 6, references therein), lack of age dating for mineralization and alteration makes metallogenic and geochronological studies difficult. In many instances age of the mineralized system is inferred from age of causative magmatic activity. In many areas the relationship between mineralization, and host and wall rocks is not clear due to pervasive hydrothermal alteration. Thus, inferred ages of mineralization are debatable in most cases.

⁴⁰Ar/³⁹Ar step-heating age dating was performed on suitable samples taken from Agi Dagı, Kartaldag, Kuscayiri and Alankoy prospects (Table 2). Priority was given to the samples from important prospects in terms of economics and exploration, e.g., HS epithermal and porphyry. All of the samples were taken from surface outcrops, except Agi Dagı. Core sample from Agi Dagı prospect came from 121 m depth of a diamond drill hole immediately northeast of Baba Dagı Zone. In many prospects, suitable mineral samples for age dates were not found. Four alunite samples were chosen from vuggy silica and advanced argillic alteration of the HS epithermal systems and one hornblende sample was taken from the causative granodiorite intrusive in Alankoy porphyry/epithermal prospect, which has weak propylitic alteration (Table 2). Using textural and paragenetic relationships hypogene alunite samples were chosen for analyses, and then samples were checked on transmitted light microscope and then on SEM. All of the samples yielded age spectrum with well-behaved plateaus, and gave precise weighted mean plateau ages (WMPA) (Figs. 14–18).

Interpretation of the ⁴⁰Ar/³⁹Ar step-heating age dates incorporated with other available age data indicates that at least two phases of HS epithermal gold mineralization and at least three phases of porphyry Cu–Au–Mo mineralization occurred in the Biga Peninsula (Fig. 6). Continuous mineralization in any of these phases of a particular deposit type is not implied. Late Eocene age early phase in HS epithermal systems is characterized by Kartaldag and Kuscayiri prospects. An alunite sample from Kartaldag prospect gives $38.8 \pm 0.7 \text{ Ma}$ WMPA and $38.8 \pm 1.1 \text{ Ma}$ inverse isochron age (IIA), while an alunite sample from Kuscayiri prospect gives $38.2 \pm 0.5 \text{ Ma}$ WMPA, and $39.4 \pm 0.6 \text{ Ma}$ IIA. This early phase is probably related to emplacement of the Kuscayiri Pluton, K/Ar ages in hornblendes ranging 35.7 to 39.4 Ma (Fig. 6). Secondary

Table 2
Summary table of ⁴⁰Ar/³⁹Ar age dating results.

Prospect	Sample no	Mineral separation	IIA (Ma) ± 1σ	TFA ± 1σ	WMPA (Ma) ± 1σ	Ca/K	Comments
Kartaldag	BPGP-1007	Alunite, trace of quartz	38.8 ± 1.1	39.4 ± 0.6	38.8 ± 0.7	0.03–4.6	3 steps plateau
Kuscayiri	BPGP-1045	~50% alunite, ~50% quartz + goethite	39.4 ± 0.6	36.6 ± 0.6	38.2 ± 0.5	0.04–0.6	3 steps plateau
Alankoy	BPGP-1146	~50% alunite, ~50% quartz	27.5 ± 0.3	27.1 ± 0.3	27.9 ± 0.2	0.01–1.3	3 steps plateau
Agi Dagı	BPGP-1083a	~70% alunite, ~30% quartz	25.8 ± 1.4	27.1 ± 0.9	26.4 ± 0.9	0.02–1.1	3 steps plateau
Alankoy	BPGP-1245	Hornblende	28.3 ± 2.6	35.7 ± 0.5	32.7 ± 0.7	0.08–0.2	4 steps plateau

Explanation: 1σ = estimated uncertainty (1 sigma); IIA = inverse isochron age; TFA = total fusion age; WMPA = weighted mean plateau age; Ca/K = apparent Ca/K ratios; IPWMA = Intermediate Plateau Weighted mean age.

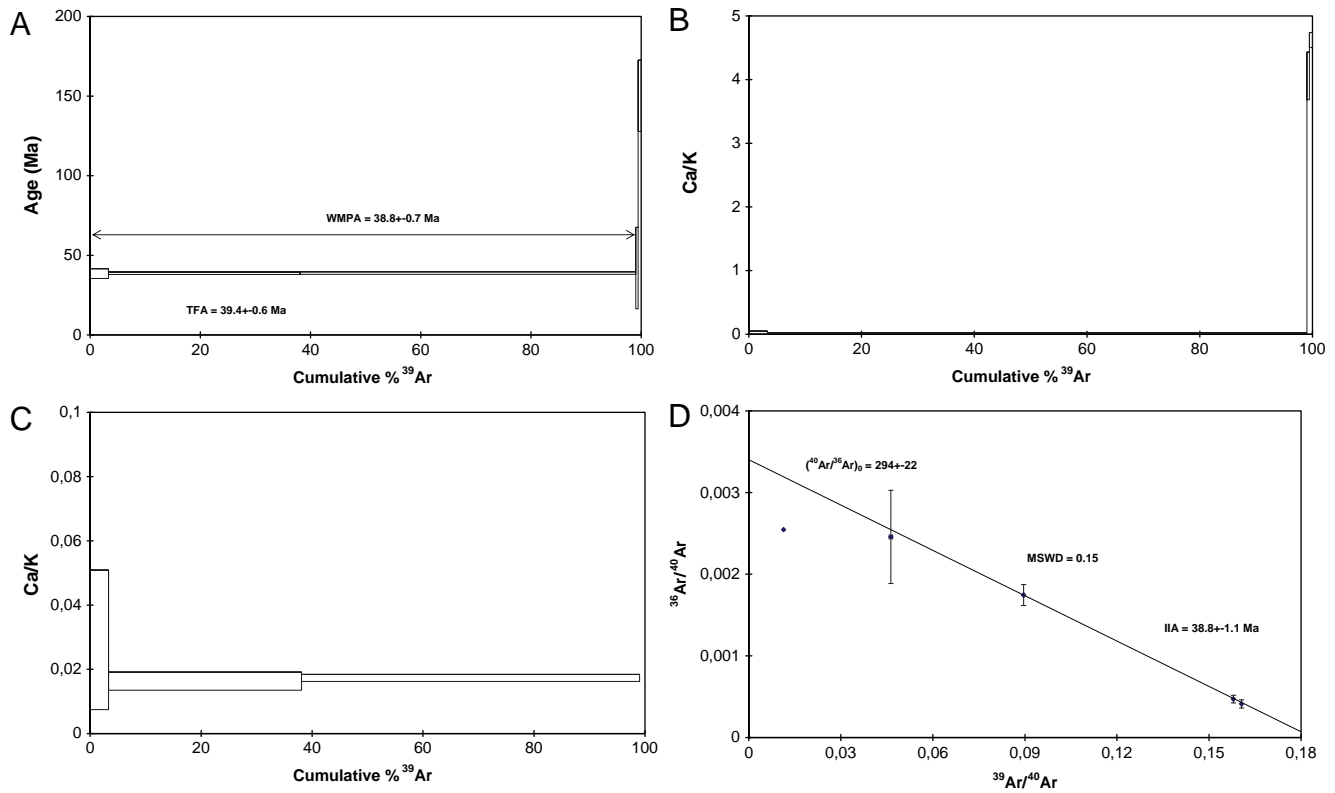


Fig. 14. Alunite sample [BPGP-1007] from Kartaldag prospect, A. Age spectrum, B and C. Ca/K spectrum, D. Isochron diagram.

younger phase of the HS epithermal mineralization and alteration occurred in Early Oligocene, and dominates the early phase. This phase formed the largest HS systems, such as Agi Dagi, not only in Biga Peninsula, but also in Turkey. An alunite sample from Agi Dagi gives 26.4 ± 0.9 Ma WMPA, and 25.8 ± 1.4 Ma IIA, while an alunite sample from Alankoy HS system gives 27.9 ± 0.2 Ma WMPA, and 27.5 ± 0.3 Ma IIA. Previous K/Ar ages from whole-rock quartz-alunite at Alankoy prospect are 30.7 ± 1.5 and 13.6 ± 1.7 Ma, which may indicate a much younger phase of HS or supergene alteration. Kirazli prospect and Balya deposit also correspond to this phase of mineralization in the Biga Peninsula. At Kirazli whole-rock age of quartz-alunite alteration, though it may not be reliable, gives 30.7 ± 1.5 Ma. At Balya, whole-rock age from unaltered host-rock hornblende andesite gives 24.8 ± 1.2 Ma while argillic-phyllic alteration zone, and argillic-phyllic alteration overprinted by advanced argillic alteration give 24.7 ± 1.2 Ma and 26.3 ± 1.3 Ma respectively (Agdemir et al., 1994).

The oldest phase of the three-phased porphyry Cu–Au–Mo mineralization in the Biga Peninsula is characterized by Dikmen and Cakirli prospects related to Dikmen and Karabiga stocks (Fig. 6 and references therein). Though age of the mineralization is not known in Dikmen prospect, radiometric age dating of the Dikmen granodiorite gives 46.6 ± 2.3 Ma to 51.9 ± 2.6 Ma, K/Ar whole-rock. Middle phase is characterized by Early Oligocene Alankoy granodioritic stock. Hornblende separates from Alankoy granodiorite gives 32.7 ± 0.7 Ma WMPA, and 28.3 ± 2.6 Ma IIA, though the large errors and very high $^{40}\text{Ar}/^{39}\text{Ar}$ ratio should be noted. It is believed that porphyry mineralization associated with Alankoy stock is most probably closely related to Alankoy HS epithermal prospect. In other words, vuggy silica and advanced argillic alteration zones in the Alankoy HS system form a lithocap on the subjacent porphyry system. If such a genetic relationship exists, IIA of hornblende from Alankoy granodiorite stock is more accurate, 28.3 ± 2.6 Ma IIA cooling age vs. 27.9 ± 0.2 Ma WMPA advanced argillic alteration age. The youngest Late Oligocene porphyry phase is

characterized by Tepeoba prospect and related plutonism. Direct age dating of the molybdenite in Tepeoba using Re/Os method indicated Late Oligocene age with 25.03 ± 0.14 Ma and 25.11 ± 0.14 Ma for veins surrounding breccia and 25.62 ± 0.09 Ma for breccia (Murakami et al., 2005). In the same study, K/Ar ages indicated 23.8 ± 1.2 and 23.8 ± 1.4 Ma for phlogopite in breccia, and 22.8 ± 1.4 Ma and 24.6 ± 1.4 Ma for muscovite surrounding the breccia. K/Ar ages in the causative intrusions indicated that biotite from granodiorite gives 20.3 ± 1.0 and 21.4 ± 1.2 Ma while K-feldspar in granite gives older ages, 34.7 ± 2.0 Ma.

8. Metallogenic considerations

Metallogenic correlations of Turkish mineral deposits within the TMB were discussed in some detail by Yigit (2006, 2007a, 2007b, 2009). Metallogeny of the Biga Peninsula has been mainly shaped by Cenozoic magmatic-related mineral deposits and prospects. Biga Peninsula metallogeny, a part of the Anatolide porphyry–skarn–epithermal belt (Yigit, 2006, 2009), extends westwards to the Oligo-Miocene Serbomacedonian-Rhodope metallogenic belt (Heinrich and Neubauer, 2002; Marchev et al., 2005a) of Balkan Peninsula of SE Europe (Fig. 1, inset). Serbomacedonian-Rhodope belt contains porphyry (e.g., Skouries, Buchim, Maronia), epithermal (e.g., Perama Hill, Madjarova), CR (e.g., Olympias), and detachment-fault related (e.g., Ada Tepe) deposits and prospects. Maronia porphyry mineralization with 29.8–28.7 Ma (Melfos et al., 2002), Perama Hill epithermal deposit related to 35–25 Ma volcanic rocks, and HS and IS epithermal mineralization and alteration in Madjarova district have temporal relations to the similar phases of mineralization and alteration as exist in the Biga Peninsula (Marchev et al., 2005a, Rice et al., 2007). Carbonate-hosted Olympias (Kiliias et al., 1996) deposit could be an analogy to Papazlik Pb–Zn (Au–Ag) deposit in the Biga Peninsula.

Age of the main precious and base metal epithermal deposits in the Rhodope Massif is clustered in mostly Early Oligocene rocks, 30

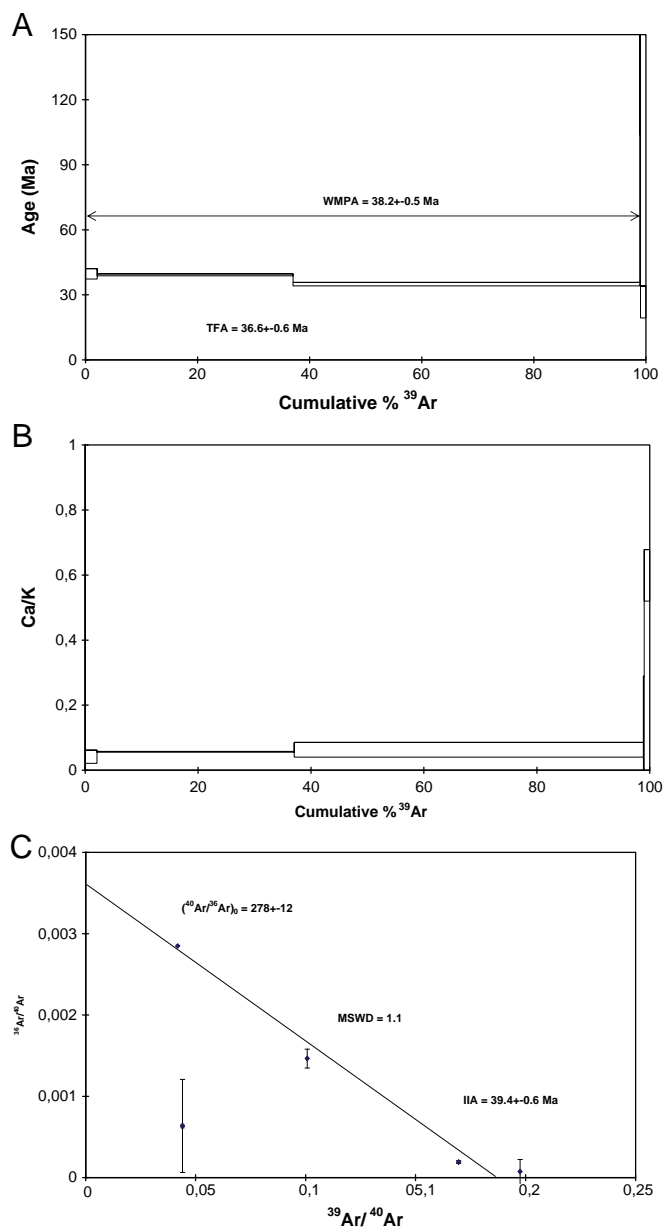


Fig. 15. Alunitic sample [BPGP-1045] from Kuscayiri prospect, A. Age spectrum, B. Ca/K spectrum, C. Isochron diagram.

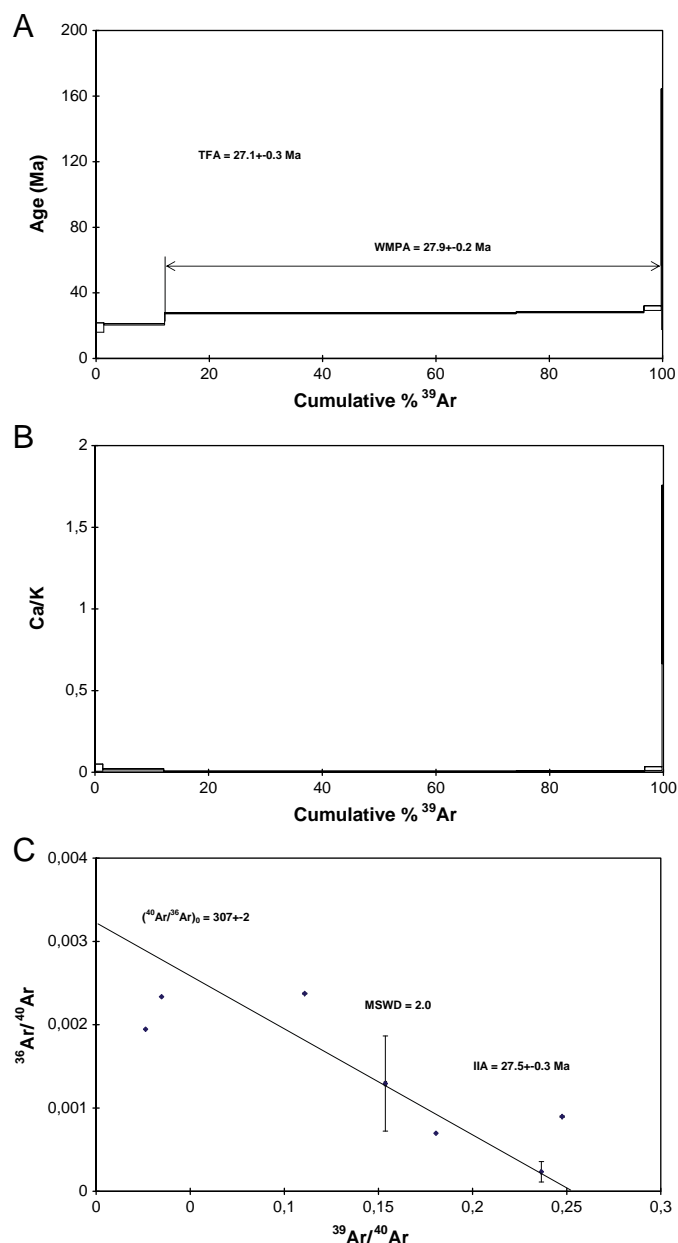


Fig. 16. Alunitic sample [BPGP-1146] from Alankoy prospect, A. Age spectrum, B. Ca/K spectrum, C. Isochron diagram.

to 33 Ma (Marchev et al., 2005a; Moritz et al., 2010). The oldest volcanic rocks in the Eastern Rhodope Massif have 34.62 Ma Ar/Ar ages, which is very similar to initiation of the volcanism in the Biga Peninsula with Can Volcanics, 34.3 Ma K/Ar ages, except one K/Ar age from Balıkkıesme Volcanics which is 37.3 Ma (Fig. 6 and the references therein). Recent Ar/Ar age data (Moritz et al., 2010) indicated that IS and HS epithermal systems in the eastern Rhodopes formed within a very short time frame, 31.2 to 32.13 Ma Ar/Ar. This mineralizing event may be characterized by Kirazlı and Alankoy HS epithermal systems in the Biga Peninsula, 27.9 to 30.7 Ma (Fig. 6).

The earlier, Late Eocene phase, of HS epithermal gold systems in the Biga Peninsula (Kuscayiri: 38.2, Kartaldag: 38.8 Ma) appears to be missing in the Rhodopes. However, Late Eocene (34.71–37.55 Ma Ar/Ar) mineralizing event is characterized by sedimentary-rock hosted LS epithermal systems in the Rhodope Massif (e.g., Ada Tepe) (Moritz et al., 2010). However, Ada Tepe is related to detachment-faults formed as a result of core-complex development, rather than magmatism (Marchev et al., 2005b). In the Biga Peninsula, existence of similar

systems is not reported, but detachment-fault related gold deposits are known in western Turkey (Yigit, 2006; 2009).

Base-metal skarns in the Yenice district could be comparable to polymetallic Pb–Zn–Ag deposits in the Rhodope Massif (e.g., Madan; Marchev et al., 2005a). Though there are no available radiometric ages for correlations, age of the intrusions in the district is mainly Oligo–Miocene (29.2 ± 1.6 to 18.8 ± 1.3 Ma). At Madan Paleozoic metamorphic-rock hosted mineralization is related to Early Oligocene dike swarms and ignimbrites (Vassileva et al., 2005).

Neogene Inner Carpathian Metallogenic belt of Apuseni and Metaliferi Mountains of Transylvania, Romania, containing the Golden Quadrilateral (e.g., Rosia Montana) (Heinrich and Neubauer, 2002), could correlate with Miocene epithermal systems in the Biga Peninsula. Ophiolite and ophiolitic melanges of Jurassic to Cretaceous, potentially important especially for listwanite-hosted gold, and lateritic Ni–Co deposits in the Biga Peninsula, extend westwards to Greece, Albania, Serbia, Montenegro, and Bosnia-Herzegovina in SE Europe.

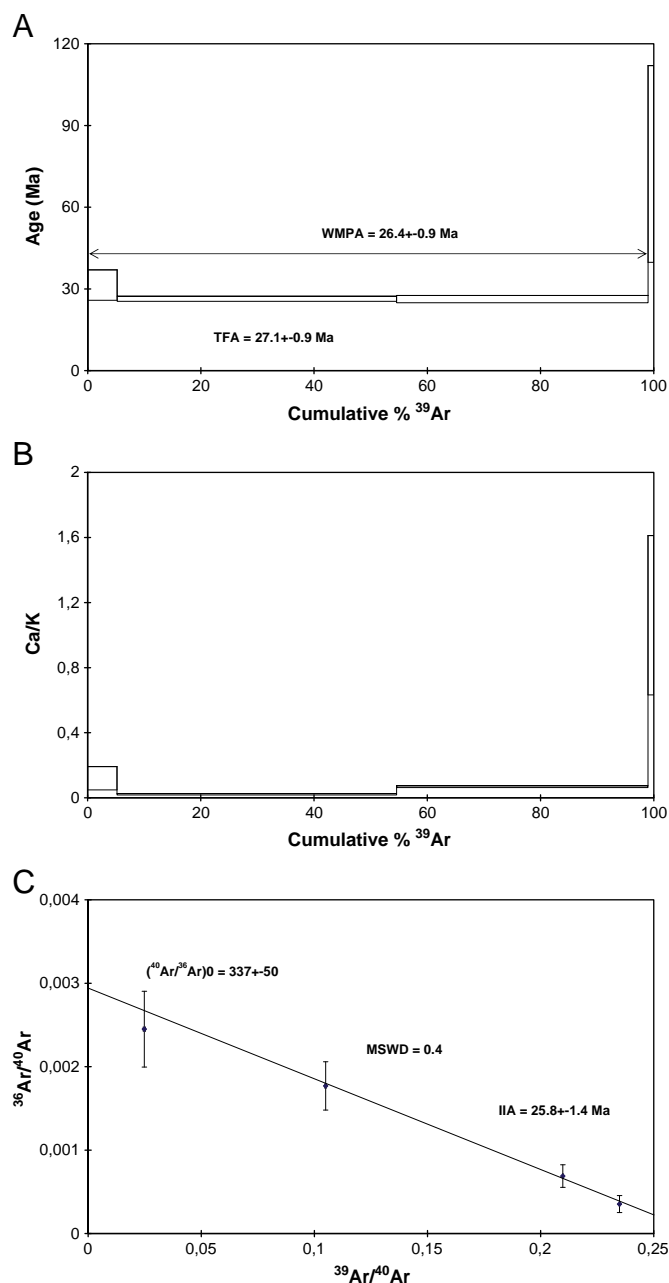


Fig. 17. Alunite sample [BPGP-1083a] from Agi Dagi prospect, A. Age spectrum, B. Ca/K spectrum, C. Isochron diagram.

Yigit (2006 and 2009) emphasized a close relationship between intrusive and related mineralization, and the Aegean Trench rollback. The Aegean Trench in the south appears to control the dominantly east-trending porphyry and/or metallogenic belts in Turkey, a fact that is overlooked in many studies. A conspicuous west-northwest trending intrusive and related porphyry deposit belt, called the Anatolides Metallogenic Belt, overprints the general tectonic fabric of Turkey, and cuts across the Sakarya Zone, the Izmir–Ankara–Erzincan Suture and Central Anatolian Crystalline complex. Furthermore, both magmatic and volcanic rocks have younging ages from north to south since Cretaceous, supporting a single subduction model with a south migrating arc. Porphyry deposits as well as causative intrusions have a younging age from north to south in the Biga Peninsula. If this single subduction model is the case (Jolivet and Brun, 2010), angle of the subduction may control the composition of the magmatic

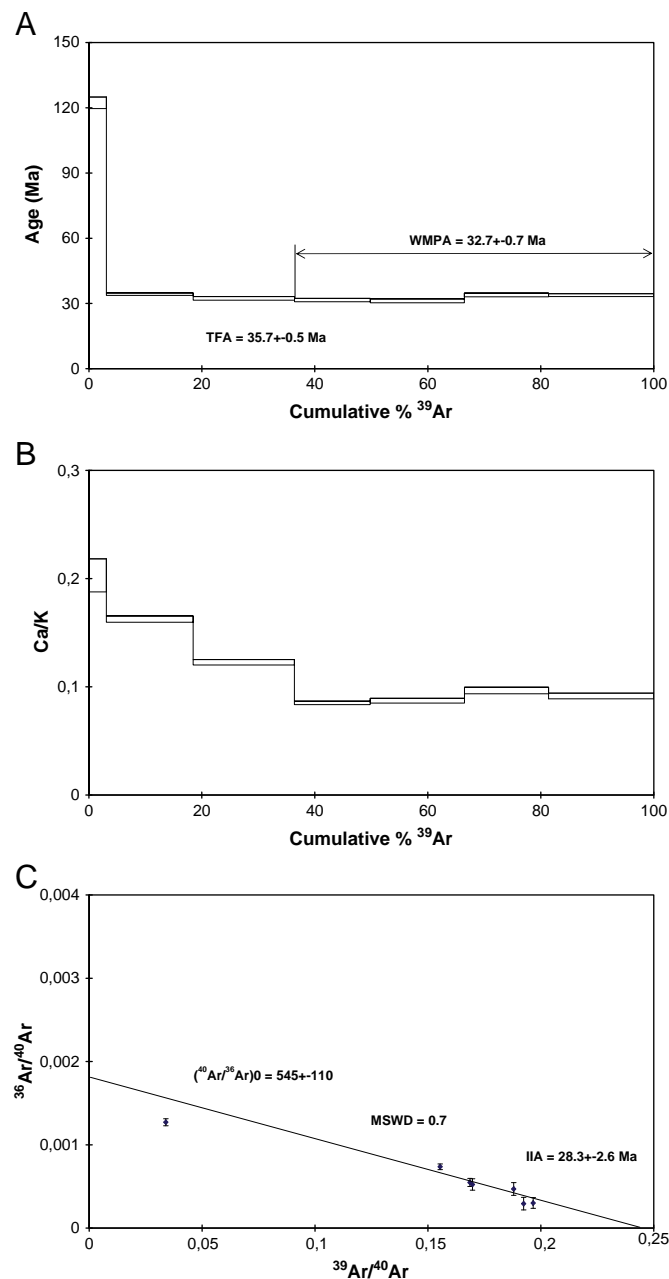


Fig. 18. Hornblende sample [BPGP-1245] from Alankoy prospect, A. Age spectrum, B. Ca/K spectrum, C. Isochron diagram.

rocks and distribution of the deposits, in contrast to other models (e.g., tectonic escape, back-arc extension or orogenic collapse models; discussed in Yigit, 2006).

When compared to the Mo rich porphyry deposits of the world, with the exception of Bingham and Ok Tedi, Dikmen porphyry prospect has unusually high Au values as is usual in Turkish porphyries (i.e., Kisladag) or other porphyry deposits in the TMB (i.e., Skouries) (Yigit, 2006; 2009).

9. Implications for mineral exploration

9.1. Regional to district scale

Though numbers of producing mines are limited in the Biga Peninsula, types of the deposits as well as size of the new HS epithermal

and porphyry Cu–Au discoveries can be compared to major mineral belts in other parts of the world. Studies on the prime metallogenic belts indicate that orogenic belts with proven metallogenic credentials or new domains of the orogenic belt predisposed to exceptional metal endowment have high-potential for mineral exploration (e.g., for gold, Sillitoe, 2008). Therefore, Biga Peninsula with proven metal endowment forms a prolific sector for future mineral exploration within TMB. Based on the current discoveries and metallogenic analyses, gold and copper are the primary targets for mineral exploration. However, base-metal as well as iron endowment of the district should not be underestimated.

Amount of silica in the Biga Peninsula can only be comparable to systems like the Late Miocene Yanacocha district of Peru. However, Biga Peninsula contains much larger silicic alteration cells compared to Yanacocha, which is roughly 15×20 km (Bell et al., 2005). In the Biga Peninsula, surface geochemical sampling of these large silicic alteration zones substantiated that in many areas they are barren in terms of gold mineralization. It should be kept in mind that the leached caps of the buried gold deposits in Yanacocha district also do not have any surface gold geochemical signatures. At the surface, gold is depleted, and Hg, Sb, and As are enriched. In exposing gold deposits, gold positively correlated with Ag, As, Ba, Bi and Hg (Bell et al., 2005). Therefore, many prospects with extensive silica zones, e.g. flat-lying silica zones at Sarpdag prospect, or many industrial mineral prospects containing silex and kaolinite deposits in many areas, should be evaluated for their epithermal gold potential. Furthermore, these flat-lying massive silica zones could form an aquitard for later mineralized fluids, as in Kirazli and Agi Dagi.

Caldera structures in many areas spatially control distribution of epithermal mineralization, e.g., Kirazli and Kartaldag calderas. Caldera bounding ring fractures are the main loci of the flow domes, which, in turn, control the gold mineralization at the margins. Though there are no detailed geological studies on the volcanic successions and facies of the caldera formations in many areas, low erosional rates enable recognition of distinct morphological circular patterns (based on GIS geospatial analyses using LANDSAT and ASTER images draped over high-resolution DEM's, and field checks) that control loci of the prospects. Most of the important HS epithermal prospects are associated with flow-dome complexes, forming prominent topographic highs that can be recognized easily, e.g., Agi Dagi, Kirazli, Kusayiri, TV Tower prospects.

Porphyry prospects, e.g., Tepeoba and Halilaga, are also associated with Oligocene magmatism. HS epithermal prospects, e.g., Kartaldag and Kusayiri, are however related to Late Eocene magmatism. LS epithermal deposits and prospects, e.g., Kucukdere and Kisacik, are related to Miocene volcanic rocks. Therefore, priority target for Au–Cu exploration is the Eocene to Oligocene age volcano-plutonic rocks, especially of ages 38 Ma to 25 Ma.

The unusual nature of the Mo rich porphyry Au deposits is exemplified by Dikmen prospect in the Biga Peninsula. In the early days of exploration by multi-national companies in Turkey this caused some major handicaps as they did not show much interest in porphyry Mo prospects and deposits and thus underestimated their gold endowment.

Northernmost Biga Peninsula is a candidate to form a new district for porphyry and related mineralization, though only a few prospects were generated in this study, e.g., Cakirli. At Cakirli, conspicuous high erosional rates and lack of coeval volcanic rocks indicate that a deeper part of the porphyry system is exposed without preserved lithocaps or known related epithermal systems. Furthermore, a few examples of HS epithermal prospects in the volcanic rocks to the north of the Canakkale–Can road, e.g., Dede Dagi and Bodurlar, are associated with flow-dome complexes, and promise a high potential for this type of mineralization.

A close spatial relationship between some of the epithermal systems and Pre-Triassic metamorphic basement rocks exists in the Biga

Peninsula, e.g., Madendag, Akbaba, Kartaldag, Kestanelik, prospects. It appears that volcanic structures, e.g., calderas, cutting the metamorphic basement rocks are somewhat more prospective. Studies in epithermal systems such as the Kushikino and Hishikari deposits in Japan suggest that the role of basement metamorphic rocks may be important in the formation of mineralizing systems (Morishita and Nakano, 2008).

Duration of the hydrothermal systems can also be comparable to Yanacocha district of Peru. Available ⁴⁰Ar/³⁹Ar radiometric age data indicate long-lived, multiple mineralizing and alteration systems in the Biga Peninsula. Differentiated mineralization and alteration phases in the Biga Peninsula based on the limited radiometric age data indicate that causative porphyry intrusions have coeval volcanic and subvolcanic rocks that host HS epithermal systems. This is especially unambiguous for Oligocene systems. Though there are no available radiometric ages in many other epithermal and porphyry prospects, geologically inferred host-rock ages have a similar relationship with the exception of some LS epithermal systems (e.g., Miocene age Kucukdere).

Silicified rocks in the Biga Peninsula with high-resistivity can be identified using geophysical techniques, e.g., induced polarization (IP) with resistivity and chargeability, time-domain electromagnetic (TDEM) and controlled-source audio magnetotelluric (CSAMT), as in other epithermal districts. Flat-lying silica zones can be efficiently determined by CSAMT survey, while IP chargeability can be useful to recognize the oxide-sulfide boundary.

Widespread ash flows with large-volume of ignimbrites of Lower to Middle Miocene age in the Biga Peninsula are not permissive for porphyry and superjacent epithermal gold deposits. Ash-flows, indicative of caldera formation, are the product of explosive volcanism which is not conducive to ore formation due to absence of retained volatiles during pyroclastic eruptions (Sillitoe, 2010). However, these ash flows may host LS style epithermal veins, therefore, should not be ignored in regional exploration programs. In the Can–Etili area ash flows may disrupt the earlier mineralization, as is the case in Chala deposit in the large Borovitsa caldera of the Rhodope Massif (Singer and Marchev, 2000).

Skarn deposits are clustered in the Yenice district, mainly associated with Oligo-Miocene intrusions. These intrusives lack coeval volcanic rocks in the district, indicating high-erosional rates that might be a cogent control on the distribution of skarn deposits in the district. In the district existence of metamorphic rocks containing abundant carbonate levels are the other favorable factor for formation of skarn deposits.

Yenice district skarn deposits may have genetically related porphyry potential, though they are mainly explored for their base-metal content. Thus Cu–Au–Mo potential of the district should be evaluated. It should be kept in mind that many proximal skarn deposits with absence of hydrous, retrograde overprints, which commonly contains magnetite, actinolite, epidote, chlorite, smectite, quartz, carbonate and iron sulfides, are unlikely to host significant Cu–Au deposits (Meinert et al., 2003; Sillitoe, 2010).

Ophiolitic rocks, locally listwanitized, have great potential for lateritic Ni–Co deposits, as in Caldag in western Turkey. In the Biga Peninsula most of the exploration efforts are concentrated on magmatic rocks, however, potential ore deposits and prospects related to ophiolitic as well as metamorphic complexes covering extensive areas in the Biga Peninsula should not be underrated. Deficiency of mineral deposits and prospects in these rocks is mainly due to lack of exploration.

Ferricrete iron deposits in the Biga Peninsula were formed by easily available iron, such as from widespread specular hematite. Leached iron forms a matrix between angular volcanic clasts, in some areas containing clay-rich zones at the base. These epicontinental lateritic formations are thought to be related to a major regional uplifting event during Upper Miocene to Pliocene in the Biga Peninsula.

Volcanogenic Mn deposits and prospects of the Biga Peninsula do not have much recent exploration activity. Most of them are associated with silicified rocks and epithermal in origin, and thus they should be

evaluated for their epithermal gold potential. Cyprus-type Mn deposits may exist associated with widespread ophiolitic rocks in the Biga Peninsula.

Conceptual Cu–Au exploration is not popular for blind orebodies in Turkey in contrast to other parts of the world, e.g., Great Basin of the US or in the Chilean Andes of S America. Though the country is underexplored and there are plenty of deposits and prospects with surface exposures, potential of the Neogene basins should be evaluated, especially in Biga Peninsula as well as W Turkey. Extensional, thin-skin tectonic regime in W Turkey caused many horst and graben structures to form with infill of varying thickness. In many areas known favorable host-lithologies, especially for porphyry Au–Cu systems, are not projected to graben-fills or pediments. At this stage of exploration in the Biga Peninsula as well as W Turkey, there is a great opportunity to acquire mineral exploration licenses easily over these Neogene sedimentary basins, e.g., Bayramic Graben, unlike in the mountain ranges. Then reconnaissance Au–Cu exploration could be employed using geochemical exploration with partial/selective leach techniques for analyses. This method can also be used to find the extension of LS veins under basin fill, for example Miocene age LS epithermal systems like Kucukdere in Biga Peninsula and Ovacik district in W Turkey.

9.2. Deposit scale

In deposit scale exploration, E-trending discontinuous extensional structural zones containing mineralized and altered zones with silica ledges, are locally important in controlling gold mineralization, i.e., Kusayiri, Pirentepe, Kartaldag and Hamam Tepe prospects. Origin of these E-trending structures should be elaborated on to further decipher metallogeny of the Biga Peninsula. The incidence of these silica ledges in mineralizing systems should be examined in a geochronological framework.

Silica textures like jigsaw mosaic to feathery (plumose) chalcedonic quartz, e.g., Agi Dagi, indicate a formation temperature between 100 and 180 °C. Reticulate and saccharoidal or reticulate saccharoidal e.g., Kucukdere, Arapucandere, Kisacik and Findikli, indicate a formation temperature above 180 °C (Yigit et al., 2006 and references therein). Common bladed calcite in Kucukdere, commonly replaced by quartz pseudomorphs, may help to locate high-grade zones, because they show concomitant rapid cooling in LS epithermal systems in the boiling zones, which in turn causes loss of CO and thus ore deposition. However, some of them may be barren due to marginal water influx late in the life of the epithermal system (Hedenquist et al., 2000).

Pyroclastic rocks with intrinsic permeability favorably control mineralization and alteration, especially silicification. Subhorizontal, tabular massive opaline or chalcedonic silica is the site of paleo-water tables, the characteristic base of steam-heated environment. Preserved minor erosional remnants of steam-heated horizons and their chalcedonic bases are normally barren and devoid of precious and base metals as well as As and Sb, unless telescoped onto the underlying mineralization due to water-table descent, though elevated vapor element (e.g., Hg, F) contents are commonly present. Existence of these zones may indicate mineralized porphyry at depth (Sillitoe, 1999; 2010). Therefore, prospects with preserved steam-heated zones in the Biga Peninsula may indicate subjacent porphyry Cu–Au mineralization, e.g., native-sulfur bearing steam-heated vuggy silica zones at Alankoy prospect.

Conspicuous specular hematite as stockwork veinlets or dissemination or fracture-fill is a good exploration tool in many HS epithermal prospects, e.g. Kirazli, Agi Dagi, Kusayiri, Sarpdag, and Piren Tepe. Specular hematite probably forms as a result of magnetite transformation. Abundant magnetite indicating high oxygen fugacities (f_{O_2}) is favorable for the formation of gold-rich porphyry deposits (Sillitoe, 1979). Thus, some of these HS epithermal deposits with abundant specular hematite may form a lithocap, and may

suggest subjacent blind porphyry Cu–Au mineralization, as in Kusayiri. Abundant specular hematite may indicate epithermal-porphry transitional environments as in Maricunga Belt, northern Chile (Muntean and Einaudi, 2001).

HS lithocaps drill tested in many prospects end at barren sericitic or chlorite/sericite alteration zones, however, potential of subjacent blind porphyry mineralization that may exist below has not been tested (Sillitoe, 2010). Many HS epithermal prospects may form superjacent to porphyry deposits or may be telescoped, therefore, A- and B-type veinlets in sericitic and/or advanced argillic zones may still be recognized due to their refractory nature, if they developed in the potassic alteration zone. Porphyry style stockwork zones at the Aladag prospect are considered to be related to Kirazli HS system. Kocayayla district with known base metal deposits contains anomalous stockwork zones indicative of porphyry systems. Therefore, many long-known epithermal prospects should be reevaluated.

Gokceada Island with several newly discovered prospects may form a new district for epithermal and/or porphyry deposits. Known prospects are associated with Oligocene volcano-plutonic rocks, which are most probably equivalent to the mineralized rocks on the mainland or similar to the porphyry systems on Limnos and Lesvos islands (e.g. Voudouris and Alfieris, 2005).

Some of the high-temperature values in fluid inclusions in Arapucandere as well as high salinities may indicate a transition to subepithermal veins in the porphyry environment. High-salinities may also indicate high base-metal and Ag/Au values as in other IS deposits with mainly Zn–Pb-dominated mineralization (Sillitoe and Hedenquist, 2003). However the fluid responsible for quartz and carbonate gangue deposition in IS vein deposits is commonly much lower in salinity than the episodic pulses of saline fluid that deposit the ore and related sulfide minerals.

Though host rock is interpreted as lithic-lapilli tuff at the Kisacik epithermal prospect, centimeter-size clasts and rock-flour matrix containing tuffaceous components are reminiscent of diatreme breccias, e.g. Cripple Creek Breccia in Colorado. The low-grade gold mineralization could be diatreme-hosted gold, which implies much higher tonnage gold potential in the prospect though grades may be low.

Kizildam and Findikli prospects in the eastern Biga Peninsula have many affinities to Carlin-type gold deposits, in terms of host-rocks, mineralization and alteration, e.g. limestone host-rock, arsenian? pyrite, antimony gold association, jasperoid formation, and decalcification (Yigit and Hofstra, 2003; Yigit et al., 2003, 2006). However, they are related to magmatism with higher grade Ag values, and they can be classified as distal-disseminated gold deposits (cf. Carlin-type, Cline et al., 2005) like Mesel in Indonesia, Jeronimo in Chile, and Zarshuran in Iran.

Existence of limited number of prospects in the Biga Peninsula should not discourage exploration for radioactive minerals, such as U and Th. High concentration of fissionable metals in beach placers at Geyikli prospect is probably derived from Kestanelik Pluton, because some of the epithermal/porphyry prospects in the source area contain high-concentration of U and Th, e.g., Kiziltepe and Cinarpinar.

Some of the prospects in the Biga Peninsula have unusual enrichment of indium, such as zinc gossans in Alankoy prospect. Indium, used to produce indium tin oxide (ITO) mainly used in flat-panel display devices and LCDs, has increasing demand in the world market. Therefore, indium potential as well as other minor metals could be an exploration interest in the Biga Peninsula.

Bonanza grade gold values in Rock Pile zone of the Kirazli prospect and Meydan Zone of Kestanelik prospect suggest that more than two decades of modern exploration is not sufficient to find even highly-mineralized surface outcrops. Therefore, relying heavily on the geochemistry without geology, mineralization, alteration and structural geology of the ore forming systems is inefficient to discover orebodies.

Acknowledgment

Catherine Yigit is thanked for her discussions of the ins and outs of the paper and detailed editing. TUBITAK is gratefully acknowledged for financial support as most of the data were generated from the author's project supported by the Turkish Science Foundation (TUBITAK Project 104Y062 "Gold Metallogeny of the Biga Peninsula, NW Turkey"). Eldorado Gold Turkey is thanked for supporting some geochemical and TerraSpec analyses. The manuscript benefited from constructive comments by Peter Marchev. Thorough reviews by an anonymous reviewer and editorial handling by Jaroslav Lexa improved the content.

References

- Agdemir, N., Kirikoglu, M.S., Lehmann, B., Tietze, J., 1994. Petrology and alteration geochemistry of the epithermal Balya Pb–Zn–Ag deposit, NW Turkey. *Miner. Deposita* 29, 366–371.
- Akyol, Z., 1977. Geology of the Balya Mine area. *Geol. Eng. J. Chamb. Geol. Eng. Turkey* 3, 10–27.
- Akyol, Z., Yucel, A., Sendil, T., 1977. Report summaries of metallic mineral studies in northwestern Anatolia: MTA report no.5787, 87p. (in Turkish).
- Akyurek, B., Soysal, Y., 1980. 1:100000 scale compilation of Biga Peninsula and its southern part: MTA report no. 7847, 16p. (in Turkish).
- Aldanmaz, E., Pearce, J.A., Thirlwall, M.F., Mitchell, J.G., 2000. Petrogenic evolution of late Cenozoic, post-collisional volcanism in western Anatolia, Turkey. *J. Volcanol. Geotherm. Res.* 102, 67–95.
- Allen, S.H., 1999. Finding the Walls of Troy, Frank Calvert and Heinrich Schliemann at Hisarlik. University of California Press, Berkeley and Los Angeles, California. (409pp.).
- Altunkaynak, S., Dilek, Y., 2006. Timing and nature of postcollisional volcanism in western Anatolia and geodynamic implications. In: Dilek, Y., Pavlides, S. (Eds.), *Postcollisional Tectonics and Magmatism in the Mediterranean region and Asia: Geological Society of America Special Paper*, 409, pp. 321–351.
- Altunkaynak, S., Genc, S.C., 2008. Petrogenesis and time-progressive evolution of the Cenozoic continental volcanism in the Biga Peninsula, NW Anatolia (Turkey). *Lithos* 102, 316–340.
- Andac, M., 1971. Mineralogy of radioactive beach sands and petrology of their source rocks in Biga Peninsula, south of historical Troy. *MTA Bull.* 76, 75–79 (in Turkish).
- Andac, M., Mücke, A., 1975. Heavy mineral paragenesis to the south of Troy. *MTA Bull.* 85, 183–185 (in Turkish).
- Beccaleto, L., 2004. Geology, correlations, and geodynamic evolution of the Biga Peninsula (NW Turkey). *Mem. Geol. Lausanne* 43, 146.
- Beccaleto, L., Jenny, C., 2004. Geology and correlation of the Ezine Zone: a Rhodope fragment in NW Turkey? *Turkish J. Earth Sci.* 13, 145–176.
- Beccaleto, L., Bartolini, A.C., Martini, R., Hochuli, P.A., Kozur, H., 2005. Biostratigraphic data from the Cetmi Melange, northwest Turkey: paleogeographic and tectonic implications. *Palaeogeogr. Palaeoclimatol. Palaeoecol.* 221, 215–244.
- Beccaleto, L., Bonev, N., Bosch, D., Bruguier, O., 2007. Record of a Paleogene syn-collisional extension in the north Aegean region: evidence from the Kemer micaschists (NW Turkey). *Geol. Mag.* 144 (2), 393–400.
- Bell, P.D., Gomez, J.G., Loaya, C.E., Pinto, R.M., 2005. Geology of the gold deposits of the Yanacocha district, northern Peru. XXVII Mining Convention, Arequipa, Peru, Technical Papers. *Geology* 1–20.
- Bingol, E., Akyurek, B., Korkmaz, B., 1975. Geology of the Biga Peninsula and some characteristics of the Karakaya Formation. Symposium Book of 50th anniversary of the Turkish Republic, MTA, Ankara, pp. 71–76 (in Turkish with English abstract).
- Birkle, P., Satir, M., 1995. Dating, geochemistry and geodynamic significance of the Tertiary magmatism of the Biga Peninsula, NW Turkey. In: Erler, A., Ercan, T., Bingol, E., Orcen, S. (Eds.), *Geology of the Black Sea Region*, General Directorate of Mineral Research and Exploration & Chamber of Geological Engineers, Ankara, pp. 171–180.
- Borsi, S., Ferrara, G., Innocenti, F., Mazzuoli, R., 1972. Geochronology and petrology of recent volcanics in the Eastern Aegean Sea (West Anatolia and Lesbos Island). *Bull. Volcanol.* 36, 473–496.
- Bozkaya, G., 2011. Sulfur- and lead-isotope geochemistry of the Arapucandere lead–zinc–copper deposit, Biga Peninsula, northwest Turkey. *Int. Geol. Rev.* 53 (1), 116–129.
- Bozkaya, G., Gokce, A., 2001. Geology, ore petrography and fluid inclusion characteristics of the Koru (Canakkale) Pb–Zn deposit. *Engineering Faculty Bulletin of Cumhuriyet University. Earth Sci.* 18 (1), 55–70 (in Turkish with English abstract).
- Bozkaya, G., Gokce, A., 2009. Lead and sulfur isotope studies of the Koru (Canakkale, Turkey) lead–zinc deposits. *Turkish J. Earth Sci.* 18, 127–137.
- Bozkaya, G., Gokce, A., Grassineau, N.V., 2008. Fluid inclusion and stable isotope characteristics of the Arapucandere Pb–Zn–Cu deposits, northwest Turkey. *Int. Geol. Rev.* 50, 848–862.
- Cavazza, W., Okay, A.I., Zattin, M., 2009. Rapid early-middle Miocene exhumation of the Kazdag Massif (western Anatolia). *Int. J. Earth Sci.* 98, 1935–1947.
- Cihnioglu, M., Isbasarir, O., Ceyhan, U., Adiguzel, O., 1994. Iron Inventory of Turkey: Ankara. MTA publication. 408pp.
- Cline, J.S., Hofstra, A.H., Muntean, J.L., Tosdal, R.M., Hickey, K.A., 2005. Carlin-type gold deposits in Nevada: critical geologic characteristics and viable models. In: Hedenquist, J.W., Thompson, J.F.H., Goldfarb, R.J., Richards, J.P. (Eds.), *Economic Geology 100th Anniversary Volume*, pp. 451–484.
- Colakoglu, A.R., 2000. The characteristics of Kucukdere epithermal (Havran-Balikesir) gold vein. *Geol. Bull. Turkey* 43, 99–110.
- Cunningham-Dunlop, I.R., Lee, C., 2007a. Agi Dag gold property, Canakkale Province, Turkey. Technical Report for Fronteer Development Group Inc (112pp.).
- Cunningham-Dunlop, I.R., Lee, C., 2007b. Kirazli gold property, Canakkale Province, Republic of Turkey. Technical Report for Fronteer Development Group Inc (78pp.).
- Delaloye, M., Bingol, E., 2000. Granitoids from Western and Northwestern Anatolia: geochemistry and modeling of geodynamic evolution. *Int. Geol. Rev.* 42, 241–268.
- Dewey, J.F., 1988. Extensional collapse of orogens. *Tectonics* 7, 1123–1139.
- Dewey, J.F., Sengor, A.M.C., 1979. Aegean and surrounding regions: complex multiplate and continuum tectonics in a convergent zone. *Geol. Soc. Am. Bull.* 90, 84–92.
- Dilek, Y., Altunkaynak, S., 2007. Cenozoic crustal evolution and mantle dynamics of post-collisional magmatism in western Anatolia. *Int. Geol. Rev.* 49, 431–453.
- Duru, M., Pehlivan, S., Senturk, Y., Yavas, F., Kar, H., 2004. New results on the lithostratigraphy of the Kazdag Massif in northwestern Turkey. *Turkish J. Earth Sci.* 13, 177–186.
- Ercan, T., Ergul, E., Akcoren, F., Cetin, A., Granit, S., Asutay, J., 1990. Geology of the Balikesir-Bandırma region, petrology of the Tertiary volcanism and its regional distribution. *MTA Bull.* 110, 113–130 (in Turkish).
- Ercan, T., Satir, M., Steinitz, G., Dora, A., Sarifakioglu, E., Adis, C., Walter, H.-J., Yildirim, T., 1995. Features of Tertiary volcanism observed at Biga Peninsula and Gokceada, Tavsan Islands, NW Anatolia. *MTA Bull.* 117, 55–86 (in Turkish).
- Ercan, T., Turkecan, A., Guillou, H., Satir, M., Sevin, D., Saroglu, F., 1998. Features of the Tertiary volcanism around the Sea of Marmara. *MTA Bull.* 120, 199–222 (in Turkish).
- Erdem, E., 1976. Mining geology molybdenum study of Tongurlu-Yesilkoy-Sariot (Bayramic-Canakkale). MTA Report (14p (in Turkish)).
- Fytikas, M., Giulini, O., Innocenti, F., Marinelli, G., Mazzuoli, R., 1976. Geochronological data on recent magmatism of the Aegean Sea. *Tectonophysics* 31, T29–T34.
- Gorur, N. (Ed.), 1998. Triassic to Miocene Paleogeographic Atlas of Turkey. MTA Publication, Ankara (43pp.).
- Gradstein, F.M., Ogg, J.G., Smith, A.G., Bleeker, W., Lourens, L.J., 2004. A new geologic time scale, with special reference to Precambrian and Neogene. *Episodes* 27 (2), 83–100.
- Grieve, P., 2009. Technical Report on the Halilaga Exploration Property, Canakkale, Western Turkey. Technical Report by Geology and Resources Solutions Ltd. for Fronteer Development Group Inc (157pp.).
- Gumus, A., 1970. Metallogeny of Turkey; Explanation of 1:2 500 000 scale metallogenic map of Turkey. MTA, publication, 144 (in Turkish).
- Gumus, A., 1999. Exogenic Ore Deposits. DEU Publication, Izmir. (210 p (in Turkish)).
- Hedenquist, J.W., Arribas, A.R., Gonzalez-Urien, E., 2000. Exploration for epithermal gold deposits. In: Hagemann, S.G., Brown, P.E. (Eds.), *Gold in 2000*, Reviews in Economic Geology, 13, pp. 245–277.
- Heinrich, C.A., Neubauer, F., 2002. Cu–Au–Pb–Zn–Ag metallogeny of the Alpine-Balkan-Carpathian-Dinaride geodynamic province. *Miner. Deposita* 37, 533–540.
- Higgs, R., 1962. Geology of the Madendag Gold Prospect, Canakkale. MTA Report, 3863 (60p (in Turkish)).
- Jackson, J.A., McKenzie, D., 1988. The relationship between plate motions and seismic moment tensors and rates of active deformation in the Mediterranean and Middle East. *Geophys. J.* 93, 45–73.
- Jolivet, L., Brun, J.-P., 2010. Cenozoic geodynamic evolution of the Aegean. *Int. J. Earth Sci.* 99, 109–138.
- Kalafatcioglu, A., 1963. Geology around Ezine and Bozcaada and the age of limestones and serpentines. *MTA Bull.* 60, 61–70.
- Karacik, Z., Yilmaz, Y., Pearce, J.A., Ece, O.I., 2008. Petrochemistry of the south Marmara granitoids, northwest Anatolia, Turkey. *Int. J. Earth Sci.* 97, 1181–1200.
- Kaymakci, N., Aldanmaz, E., Langereis, C., Spell, T.L., Gurer, O.F., Zanetti, K.A., 2007. Late Miocene transcurrent tectonics in NW Turkey: evidence from paleomagnetism and ⁴⁰Ar–³⁹Ar dating of alkaline volcanic rocks. *Geol. Mag.* 144 (2), 379–392.
- Keane, J., Jutras, M., Welhener, H., Browne, R., 2010. Technical report on the Agi Dag-Kirazli gold project, Canakkale province, Republic of Turkey. Prepared for Alamos Gold Inc, by K D Engineering, 451p.
- Ketin, I., 1966. Tectonic units of Anatolia (Asia Minor). *MTA Bull.* 66, 23–34.
- Kiliass, S.P., Kalogeropoulos, S.I., Konnerup-Madsen, J., 1996. Fluid inclusion evidence for the physicochemical conditions of sulfide deposition in the Olympias carbonate-hosted Pb–Zn (Au, Ag) sulfide ore deposit, E. Chalkidiki peninsula, N. Greece. *Miner. Deposita* 31, 394–406.
- Kilic, M., Kucukefe, S., Avsar, M., Sari, R., Vural, A., Pehlivan, N., 2004. Preliminary geological and geochemical data on Kisacik (Ayvacik-Canakkale) Au mineralization. 57th Geological Congress of Turkey, Extended Abstracts Book, 8–12 March, p. 101 (Abstract).
- Kissel, C., Laj, C., 1988. The Tertiary geodynamical evolution of the Aegean arc: a paleomagnetic reconstruction. *Tectonophysics* 146, 183–201.
- Kucukefe, S., Sari, R., Kilic, M., Tekin, Z., Avsar, M., 2003. Preliminary findings of the Tepeoba (Havran-Balikesir) breccia-hosted Cu–Mo–(Au) mineralization. 56th Geological Congress of Turkey, Ankara, April 14–20, 2003, MTA, Extended Abstracts, pp. 99–100.
- Le Pichon, X., Angelier, J., 1979. The Hellenic arc and trench system: a key to the neotectonic evolution of the eastern Mediterranean area. *Tectonophysics* 60, 1–42.
- Le Pichon, X., Angelier, J., 1981. The Aegean Sea. *Philos. Trans. R. Soc. Lond.* A300, 357–372.
- Marchev, P., Kaiser-Rohrmeier, M., Heinrich, C., Ovtcharova, M., von Quadt, A., Raicheva, R., 2005a. Hydrothermal ore deposits related to post-orogenic extensional magmatism and core complex formation: the Rhodope Massif of Bulgaria and Greece. *Ore Geol. Rev.* 27, 53–89.

- Marchev, P., Jeleu, D., Hasson, S., 2005b. Ada Tepe sedimentary hosted, low-sulfidation epithermal Au deposit, SE Bulgaria. *Ore Geol. Rev.* 27, 92–93.
- McKenzie, D., 1978. Active tectonics of the Alpine-Himalayan belt: the Aegean Sea and surrounding regions. *Geophys. J. R. Astron. Soc.* 55, 217–254.
- Meinert, L.D., Hedenquist, J.W., Satoh, H., Matsuhisa, Y., 2003. Formation of anhydrous and hydrous skarn in Cu–Au ore deposits by magmatic fluids. *Econ. Geol.* 98, 147–156.
- Melfos, V., Vavelidis, M., Christofides, G., Seidel, E., 2002. Origin and evolution of the Tertiary Maronia porphyry copper–molybdenum deposit, Thrace, Greece. *Miner. Deposita* 37, 648–668.
- Meulenkamp, J.E., Wortel, W.J.R., Van Wamel, W.A., Spakman, W., Hoogerduyn Strating, E., 1988. On the Hellenic subduction zone and the geodynamic evolution of Crete since the late Middle Miocene. *Tectonophysics* 146, 203–215.
- Meulenkamp, J.E., van der Zwaan, G.J., van Wamel, W.A., 1994. On Late Miocene to Recent vertical motions in the Cretan segment of the Hellenic Arc. *Tectonophysics* 234, 53–72.
- Moix, P., Beccaleto, L., Kozur, H.W., Hochard, C., Rosselet, F., Stampfli, G.M., 2008. A new classification of the Turkish terranes and sutures and its implication for the paleotectonic history of the region. *Tectonophysics* 451, 7–39.
- Molly, E.W., 1958. Gold mineralization in the west of Turkey (Aydin, Manisa and Canakkale provinces). MTA report no. 2789 (29pp. (in Turkish)).
- Molly, E.W., 1961. Western Turkey gold and platinum exploration. MTA report no. 2841 (53pp. (in Turkish)).
- Morishita, Y., Nakano, T., 2008. Role of basement in epithermal deposits: the Kushi-kino and Hishikari gold deposits, southwestern Japan. *Ore Geol. Rev.* 34 (4), 597–609.
- Moritz, R.I., Marton, I., Ortelli, M., Marchev, P., Voudouris, P., Bonev, N., Spikings, R., Cosca, M., 2010. A review of age constraints of epithermal precious and base metal deposits of the Tertiary Eastern Rhodopes: coincidence with late Eocene–early Oligocene tectonic plate reorganization along the Tethys. In: Chatzipetros, A., Melfos, V., Marchev, P., Lakova, I. (Eds.), XIX Congress of the Carpathian–Balkan Geological Associations, Thessaloniki, Greece, 23–26 September 2010, p. 262.
- MTA, 1993a. Gold and silver inventory of Turkey. MTA publication, no.198 (46pp. (in Turkish)).
- MTA, 1993b. Lead–zinc inventory of Turkey. MTA Publication, no.199 (94pp. (in Turkish)).
- MTA, 2001. Geological map of Turkey: Istanbul and Izmir sheets, scale 1:500000. MTA Publication, Ankara.
- Muntean, J.L., Einaudi, M.T., 2001. Porphyry–epithermal transition: Maricunga Belt, northern Chile. *Econ. Geol.* 96, 743–772.
- Murakami, H., Watanabe, Y., Stein, H., 2005. Re–Os ages for molybdenite from the Tepeoba breccia-centered Cu–Mo–Au deposit, western Turkey: Brecciation-triggered mineralization. In: Mao, J., Bierlein, F.P. (Eds.), Mineral Deposit Research: Meeting the Global Challenge, Proceedings of the Eight Biennial SGA Meeting, Beijing, China, 18–21 August, 2005, 1, pp. 805–808.
- Okay, A.I., Altiner, D., 2004. Uppermost Triassic limestone in the Karakaya Complex–stratigraphic and tectonic significance. *Turkish J. Earth Sci.* 13, 187–199.
- Okay, A.I., Goncuoglu, M.C., 2004. The Karakaya complex: a review of data and concepts. *Turkish J. Earth Sci.* 13, 77–95.
- Okay, A.I., Satir, M., 2000a. Coeval plutonism and metamorphism in a latest Oligocene metamorphic core complex in northwest Turkey. *Geol. Mag.* 137, 495–516.
- Okay, A.I., Satir, M., 2000b. Upper Cretaceous eclogite-facies metamorphic rocks from the Biga Peninsula, northwest Turkey. *Turkish J. Earth Sci.* 9, 47–56.
- Okay, A.I., Tuysuz, O., 1999. Tethyan sutures of northern Turkey. In: Durand, B., Jolivet, L., Horvath, L., Serranne, M. (Eds.), The Mediterranean Basins: Tertiary Extension within the Alpine Orogen. Geological Society, London, Special Publication no. 156, pp. 475–515.
- Okay, A.I., Siyako, M., Burkan, K.A., 1990. Geology and tectonic evolution of the Biga Peninsula. *TAPG Bull.* 2 (1), 83–121.
- Okay, A.I., Satir, M., Maluski, H., Siyako, M., Monie, P., Metzger, R., Akyuz, S., 1996. Paleo- and Neo-Tethyan events in northwestern Turkey: geologic and geochronologic constraints. In: Yin, A., Harrison, M. (Eds.), *Tectonics of Asia*. Cambridge University Press, pp. 420–441.
- Okay, A.I., Tansel, I., Tuysuz, O., 2001. Obduction, subduction and collision as reflected in the Upper Cretaceous–Lower Eocene sedimentary record of western Turkey. *Geol. Mag.* 138, 117–142.
- Okay, A.I., Satir, M., Siebel, W., 2006. Pre-Alpidic Paleozoic and Mesozoic orogenic events in the Eastern Mediterranean region. In: Gee, D.G., Stephenson, R.A. (Eds.), *European Lithosphere Dynamics*. Geological Society, London, Memoirs, 32, pp. 389–405.
- Orgun, Y., Gultekin, A.H., Onal, A., 2005. Geology, mineralogy and fluid inclusion data from the Arapucan Pb–Zn–Cu–Ag deposit, Canakkale, Turkey. *J. Asian Earth Sci.* 25, 629–642.
- Pirajno, F., 1995. Volcanic-hosted epithermal systems in northwest Turkey. *S. Afr. J. Geol.* 98, 13–24.
- Rice, C.M., McCoy, R.J., Boyce, A.J., Marchev, P., 2007. Stable isotope study of the mineralization and alteration in the Madjarovo Pb–Zn district, south-east Bulgaria. *Miner. Deposita* 42, 691–713.
- Sengor, A.M.C., 1979. The North Anatolian transform fault: its age, offset and tectonic significance. *J. Geol. Soc. Lond.* 136, 269–282.
- Sengor, A.M.C., 1982. Factors governing the neotectonic evolution of the Aegean. In: Erol, O., Oygur, V. (Eds.), Panel on Neotectonics of the Western Anatolia. Geological Society of Turkey, 1982 Meeting Proceedings, Ankara, pp. 59–71.
- Sengor, A.M.C., 1984. The Cimmeride orogenic system and the tectonics of Eurasia. Geological Society of America Special Paper, no.195. 82pp.
- Sengor, A.M.C., 1987. Cross-faults and differential stretching of hanging walls in regions of low-angle normal faults: examples from western Turkey. In: Coward, M.P., Dewey, J.F., Hancock, P.L. (Eds.), *Continental Extensional Tectonics*. Geological Society Special Publication no.28, pp. 575–689.
- Sengor, A.M.C., Yilmaz, Y., 1981. Tethyan evolution of Turkey: a plate tectonic approach. *Tectonophysics* 75, 181–241.
- Sengor, A.M.C., Yilmaz, Y., Ketin, I., 1980. Remnants of a pre-late Jurassic ocean in northern Turkey: fragments of Permian–Triassic Paleo-Tethys? *Geol. Soc. Am. Bull.* 91, 599–609.
- Sengor, A.M.C., Yilmaz, Y., Sungurlu, O., 1984. Tectonics of the Mediterranean Cimmerides: nature and evolution of the western termination of Paleo-Tethys. In: Dixon, J.E., Robertson, A.H.F. (Eds.), *The Geological Evolution of the Eastern Mediterranean*, Special Publication of Geological Society London, n.17, pp. 77–112.
- Sengor, A.M.C., Gorur, N., Saroglu, F., 1985. Strike-slip deformation basin formation and sedimentation: strike-slip faulting and related basin formation in zones of tectonic escape: Turkey as a case study. Society of Economic Paleontologists and Mineralogists, Special Publication, v.37, pp. 227–264.
- Seyitoglu, G., Scott, B.C., 1991. Late Cenozoic crustal extension and basin formation in west Turkey. *Geol. Mag.* 128, 155–166.
- Seyitoglu, G., Scott, B.C., 1992. Late Cenozoic volcanic evolution of the northeastern Aegean region. *J. Volcanol. Geotherm. Res.* 54, 157–176.
- Seyitoglu, G., Scott, B.C., 1996. The cause of N–S extensional tectonics in western Turkey: tectonic escape vs back-arc spreading vs orogenic collapse. *J. Geodyn.* 22, 145–153.
- Sillitoe, R.H., 1979. Some thoughts on gold-rich porphyry copper deposits. *Miner. Deposita* 14, 161–174.
- Sillitoe, R.H., 1999. Styles of high-sulfidation gold, silver and copper mineralization in porphyry and epithermal environments. Pacific Rim '99 Congress Proceedings, Bali, Indonesia, AIMM, Melbourne, pp. 29–44.
- Sillitoe, R.H., 2008. Major gold deposits and belts of the North and South American Cordillera: distribution, tectonomagmatic settings, and metallogenic considerations. *Econ. Geol.* 103, 663–687.
- Sillitoe, R.H., 2010. Porphyry copper systems. *Econ. Geol.* 105, 3–41.
- Sillitoe, R.H., Hedenquist, J.W., 2003. Linkages between volcanotectonic settings, ore-fluid compositions, and epithermal precious-metal deposits. In: Simmons, S.F., Graham, I.J. (Eds.), *Volcanic, Geothermal and Ore-forming Fluids: Rulers and Witnesses of Processes within the Earth*, Society of Economic Geologists Special Publication, 10, pp. 315–343.
- Singer, B., Marchev, P., 2000. Temporal evolution of arc magmatism and hydrothermal activity, including epithermal gold veins, Borovitsa caldera, southern Bulgaria. *Econ. Geol.* 95, 1155–1164.
- Siyako, M., Burkan, K.A., Okay, A.I., 1989. Tertiary geology and hydrocarbon potential of the Biga and Gelibolu Peninsulas. *TAPG Bull.* 1 (3), 183–199.
- Stampfli, G.M., 2000. Tethyan oceans. In: Bozkurt, E., Winchester, J.A., Piper, J.D.A. (Eds.), *Tectonics and Magmatism in Turkey and Surrounding Area*. Geological Society, London, Special Publication no. 173, pp. 1–23.
- Tekeli, O., 1981. Subduction complex of pre-Jurassic age, northern Anatolia, Turkey. *Geology* 9, 68–72.
- Vassileva, R.D., Bonev, I.K., Marchev, P., Atanassova, R., 2005. Pb–Zn deposits in the Madan ore field, south Bulgaria. *Ore Geol. Rev.* 27, 90–91.
- Voudouris, P., Alferis, D., 2005. New porphyry–Cu±Mo occurrences in the north-eastern Aegean, Greece: ore mineralogy and epithermal relationships. In: Mao, J., Bierlein, F.P. (Eds.), Proceedings of the 8th Biennial Meeting of the Society for Geology Applied to Mineral Deposits (SGA), Beijing, China, pp. 473–476–473–476.
- Yigit, O., 2006. Gold in Turkey—a missing link in Tethyan metallogeny. *Ore Geol. Rev.* 28, 147–179.
- Yigit, O., 2007a. “Gold in Turkey—a missing link in Tethyan metallogeny” (*Ore Geology Reviews* 28, 147–179)—Reply. *Ore Geol. Rev.* 30, 141–142.
- Yigit, O., 2007b. Recent discoveries and exploration trends in Turkey. In: Andrew, C.J., et al. (Ed.), Proceedings of the Ninth Biennial Meeting of the Society for Geology Applied to Mineral Deposits (SGA), Dublin, Ireland, August 20–23, 2007, pp. 109–112.
- Yigit, O., 2009. Mineral deposits of Turkey in relation to Tethyan Metallogeny: implications for future mineral exploration. *Econ. Geol.* 104, 19–51.
- Yigit, O., Hofstra, A.H., 2003. Lithochemistry of Carlin-type gold mineralization in the Gold Bar district, Battle Mountain–Eureka Trend, Nevada. *Ore Geol. Rev.* 22, 201–224.
- Yigit, O., Nelson, E.P., Hitzman, M.W., Hofstra, A.H., 2003. Structural controls on Carlin-type gold mineralization in the Gold Bar district, Eureka County, Nevada. *Econ. Geol.* 98, 1173–1188.
- Yigit, O., Hofstra, A.H., Hitzman, M.W., Nelson, E.P., 2006. Geology and geochemistry of jasperoids from the Gold Bar district, Nevada. *Miner. Deposita* 41, 527–547.
- Yildirim, S., Cengiz, I., 2004. Geological and geochemical characteristics of Sahinli (Lapseki–Canakkale) Au–Ag mineralization. MTA, 57th Geological Congress of Turkey, Ankara, March 8–12, 2004, pp. 87–88 (Extended Abstracts).
- Yilmaz, Y., 1990. Comparison of young volcanic associations of western and eastern Anatolia formed under a compressional regime: a review. *J. Volcanol. Geotherm. Res.* 44, 69–87.
- Yilmaz, H., 2003. Geochemical exploration for gold in western Turkey: success and failure. *J. Geochem. Explor.* 80, 117–135.
- Yilmaz, H., 2007. Stream sediment geochemical exploration for gold in the Kazdag Dome in the Biga Peninsula, western Turkey. *Turkish J. Earth Sci.* 16, 33–35.
- Yilmaz, Y., Genc, S.C., Karacik, Z., Altunkaynak, S., 2001. Two contrasting magmatic associations of NW Anatolia and their tectonic significance. *J. Geodyn.* 31, 243–271.
- Yilmaz, H., Oyman, T., Sonmez, F.N., Arehart, G.B., Billor, Z., 2010. Intermediate sulfidation epithermal gold–base metal deposits in Tertiary subaerial volcanic rocks, Sahinli/Tespil Dere (Lapseki/Western Turkey). *Ore Geol. Rev.* 37, 236–258.
- Yuce, N., 1978. Report on Yenice–Kabali–Gonen–Sebeli antimony mineralization. MTA report no.6571 (39pp. (in Turkish)).